Radiobiological Evaluation of New Boron Delivery Agents for Boron Neutron Capture Therapy

by

Yoonsun Chung

B.S., Nuclear Engineering (2000)
M.S., Nuclear and Quantum Engineering (2002)
Korea Advanced Institute of Science and Technology, Republic of Korea

Submitted to the Department of Nuclear Science and Engineering
in Partial Fulfillment of the Requirements for the Degree of

Doctor of Philosophy in Nuclear Science and Engineering
at the
Massachusetts Institute of Technology

February 2008

Signature of Author: _____
Department of Nuclear Science and Engineering
September 17, 2007

Certified by: _____
Jeffrey A. Coderre
Associate Professor of Nuclear Science and Engineering
Thesis Supervisor

Certified by: _____
Otto K. Harling
Professor of Nuclear Science and Engineering
Thesis Supervisor

Certified by: _____
Jacquelyn C. Yanch
Professor of Nuclear Science and Engineering
Thesis Reader

Accepted by: _____
Jacquelyn C. Yanch
Professor of Nuclear Science and Engineering
Chair, Department Committee on Graduate Students

Radiobiological Evaluation of New Boron Delivery Agents for Boron Neutron Capture Therapy

by

Yoonsun Chung

Submitted to the Department of Nuclear Science and Engineering on September 28, 2007
in Partial Fulfillment of the Requirements for the Degree of
Doctor of Philosophy in Nuclear Science and Engineering

ABSTRACT

This thesis evaluates the radiobiological effectiveness of three new boron compounds namely a boronated porphyrin (BOPP) and two liposome formulations for neutron capture therapy (BNCT). The methodology utilizes *in vitro* and *in vivo* comparisons that characterize compounds relative to boric acid and boronophenylalanine (BPA).

In vitro evaluations utilized a colorimetric assay and 96-well plates to minimize the quantities of compound required for testing. The assay was optimized for the murine SCCVII, squamous cell carcinoma to determine the chemical toxicity and relative cellular uptake of a compound. BOPP was toxic at low concentrations and comparisons between the different compounds for thermal neutron irradiations were performed with approximately 5 μg ^{10}B/ml in the culture medium to allow radiation induced effects to govern the observed response. Using less than 300 μg of compound and 250 kVp X-rays as control irradiations, a compound biological effectiveness (CBE) of 3.3 ± 0.7 was determined for BOPP that is comparable to the result for boric acid (3.5 ± 0.5) indicating a non-selective intracellular accumulation of ^{10}B. BPA has a significantly higher CBE of 6.1 ± 0.7.

Boronated liposomes (MAC-16 and MAC+TAC) were evaluated with the EMT-6 murine mammary carcinoma. Biodistribution studies showed high ^{10}B uptake in tumor (20-40 μg ^{10}B/g) 30 hours after a single i.v. injection (dose 6-20 μg ^{10}B per gram of body weight). Tumor control experiments were performed using thermal neutrons to study the efficacy of the boron delivered by liposomes and BPA. The MAC-16 produced a 16 % tumor control and BPA (dose 43 μg ^{10}B/gbw) 63 % for tumor boron concentrations of approximately 20 μg ^{10}B/g and the same neutron fluence. Liposome doses were limited by injection volume and so two injections were tried 2-hours apart that doubled the boron concentration in tumor compared to a single administration. This improved the therapeutic response to 67 % with less apparent skin damage than with BPA. Microscopic studies using fluorescent labeled liposomes revealed ^{10}B was non-uniformly distributed and concentrated at the edge of the tumor.

Based on these studies in the tumor cell lines chosen neither of the compounds appear superior to BPA.

Thesis Supervisor: Jeffrey A. Coderre, Ph.D.
Associate Professor of Nuclear Science and Engineering, Massachusetts Institute of Technology

Thesis Supervisor: Otto K. Harling, Ph.D.
Professor of Nuclear Science and Engineering, Massachusetts Institute of Technology

ACKNOWLEDGEMENTS

First of all, I would like to thank my Lord GOD, who is given me the way, the truth, and the life.

I would like to dedicate this thesis to my mother, Young-In Kim, who is always giving me unconditional love and support. I love you, mom! Also, I thank my sisters and brother-in-laws. Their love has always been my strength here miles away from home.

I would like to express my deep gratitude to my advisor Professor Jeffrey Coderre for his encouragement and guidance. I was able to conduct this research with his enthusiasm, inspiration, and understanding which was always there when I needed it.
I am grateful to Professor Otto Harling for providing motivating, enthusiastic and critical advice. It was a great opportunity to me to conduct this research under his supervision.
I am also thankful to Professor Jacquelyn Yanch for being my thesis reader and giving me valuable suggestions and insightful comments.
I am deeply grateful to Dr. Kent Riley and Dr. Peter Binns for the scientific and technical support to dosimetry, irradiations, and boron analysis as well as for their careful review of my thesis. Their guidance and advice were always considerate. Also I would like to thank Dr. Kent Riley for serving on my thesis committee and for providing the HRQAR images, along with Tom Harris, which could give us answer to a mysterious problem.
I am obliged to Professor M. Frederick Hawthorne and Richard Julius in University of Missouri, Columbia, for providing boronated liposomes.
I thank Dr. Hang Lee, a Professor in Harvard Medical School, for giving me the guidance for the uncertainty analysis.
Special thanks are due to the MIT reactor staff, especially Judy Maro, for her help to carry out experiments at the MITR.

I am grateful to Professor Soon-Heung Chang who was my supervisor during my master in KAIST for always being very supportive and encouraging.

I would like to thank my colleagues in the lab here at MIT for all their help, support, interest and valuable discussion. Especially I am obliged to Brad Schuller, Vered Anzenberg, Rebecca Raabe, and Tom Harris.
I also would like to thank Hyeongpil Ham, Jeongik Lee, Wesley Williams, and Lisa Treat for going through the NUKE qualifying exams together.

I've made beautiful friendships during five years in Boston. I will always remember them with precious and wonderful memories: especially Minsoo Jung, Eunmi Choi, Hyungjoon Cho, and all my friends from First Korean Church in Cambridge and MIT.

I would like to thank to my lovely friends in the USA and Korea who have been always supportive and encouraging to me: especially, Mihee Lim, Yoonkyong Lee, Juwon Ahn, Jeongeun Lee, Seil Nam, Kyong Kim.

This work was supported by the National Institute of Health under Grant CA97342 to MFH and the Innovations in Nuclear Infrastructure and Education program (DE-FG07-02ID14420) of the U.S. Department of Energy.

To,

My dear mother,

Young-In Kim

TABLE OF CONTENTS

TABLE OF FIGURES

CHAPTER ONE

CHAPTER TWO

CHAPTER THREE

CHAPTER FOUR

TABLE OF TABLES

CHAPTER TWO

CHAPTER THREE

CHAPTER FOUR

CHAPTER ONE

INTRODUCTION

1-1. Background of BNCT

Boron neutron capture therapy (BNCT) is an experimental type of binary radiation therapy which aims to treat some cancer types difficult to successfully treat with conventional therapies such as the malignant brain tumor, glioblastoma multiforme (GBM). The principle of BNCT was first introduced by G.L. Locher in 1936, only 4 years after the neutron was discovered [1]. BNCT is based on the capture interaction of a thermal neutron with boron-10 (^{10}B), which has a very high thermal neutron capture cross-section (3837 barns, 1 barn = 10^{-24} cm^2 [2]). BNCT is carried out in two steps: 1) the tumor must be selectively loaded with a ^{10}B-labeled compound and 2) the tumor region, usually including some surrounding normal tissues, is irradiated with low energy neutrons. The nontoxic stable isotope of natural boron, ^{10}B, and the low energy neutrons each have only minor effects on normal tissue. However, when these two components are combined, very localized and lethal radiation damage is produced in the tumor cells containing ^{10}B. This selective energy deposition from ^{10}B is based upon the following neutron capture reaction:

$$^{10}B + {}^{1}n \rightarrow [^{11}B] \rightarrow {}^{7}Li + {}^{4}He + 2.31\ MeV + \gamma\ (0.48\ MeV)\ (94\ \%)$$

$$^{10}B + {}^{1}n \rightarrow [^{11}B] \rightarrow {}^{7}Li + {}^{4}He + 2.79\ MeV\ (6\ \%)$$

that is more likely with neutrons in the thermal energy range (E_{th} < 0.4 eV) [2]. The secondary charged particles have very short ranges in tissue of approximately 9 μm for the α particle and 5 μm for the ^{7}Li ion [2]; these distances are comparable to the diameter of a mammalian cell [3]. Thus, these particles result in highly selective damage constrained mostly to tumor cells containing ^{10}B. Figure 1.1 illustrates the $^{10}B(n,\alpha)^{7}Li$ nuclear reaction in the cell. If a boron compound with satisfactory tumor selectivity and uptake is used with a neutron beam achieving a uniform and adequate neutron fluence in the treatment volume, then BNCT can potentially destroy not only the bulk tumor but also the associated

infiltrating tumor cells in the surrounding normal tissue [4]. Therefore, BNCT is a cellular targeting radiation therapy.

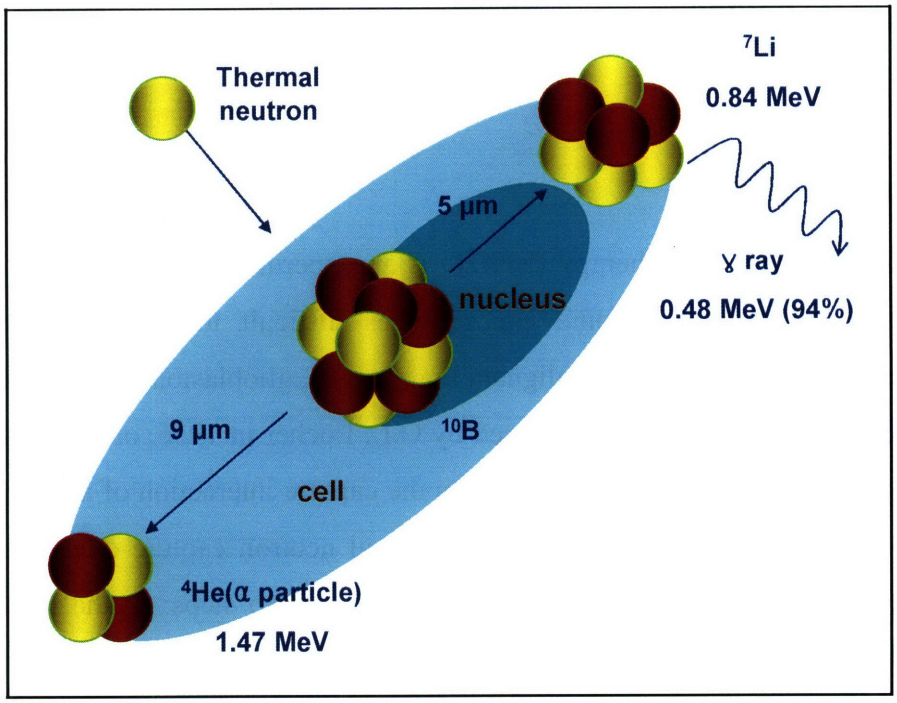

Figure 1.1. Schematic of the $^{10}B(n,\alpha)^{7}Li$ reaction in a cell. ^{10}B captures a thermal neutron and splits into two highly energetic particles, alpha and recoiling ^{7}Li ions, with energies of 1.47 and 0.84 MeV, respectively.

The first clinical studies of BNCT for GBM were initiated in the 1950s and early 1960s at Brookhaven National Laboratory (BNL) and Massachusetts General Hospital (MGH)/Massachusetts Institute of Technology (MIT) [5]. These efforts to prolong patient life were discouraging due to two major factors: 1) poor penetration of the thermal neutron beam at the depth of the tumor site and 2) inadequate selective accumulation of ^{10}B in tumor relative to blood and skin [4]. As boron delivery agents, inorganic salts such as borax, *p*-carboxyphenylboronic acid, sodium perhydrodecaborate, or sodium pentaborate were used, but these compounds had no tumor-seeking properties [6]. They could accumulate in some parts of tumor because of damaged or absent blood-brain barrier but were not able to cross the intact blood-brain barrier in the normal brain. Tumors recurred locally after treatment and the high boron concentration in the blood resulted in serious

radiation damage to skin and brain [7]. The clinical trials in the United States were therefore discontinued after 1962. BNCT clinical studies for GBM were restarted in Japan in the late 1960s utilizing sulfhydryl borane (BSH, $Na_2B_{12}H_{11}SH$) developed as a boron compound by Soloway at MGH [8]. These trials indicated that BSH accumulated selectively in tumors. Still, poor penetration of the available thermal neutron beams remained a problem. The Japanese approaches used thermal neutrons in an open surgical cavity either at the time of initial craniotomy or a re-opened craniotomy [9]. In the USA, BNCT studies were restarted in the 1990s following the improvement of neutron beams and the development of new boron compounds, especially borono-phenylalanine-fructose (BPA-F) [10]. Beams of higher-energy epithermal neutrons (0.5 eV < E_{epi} < 10 keV) were designed and constructed with the ability to deliver a significant thermal neutron fluence to deep seated (> 8cm) brain tumors minimizing damage to skin and intervening normal tissues [11, 12]. Several trials using BPA-F were completed for GBM at BNL [13-15], and for GBM and melanoma at Harvard-MIT [16]. These studies produced median survival times (~12-13 months) comparable to standard conventional therapy for GBM patients [2]. In Sweden, trials with long-term, 6 hour, infusions of BPA-F reported better median survival (18 months) of GBM patients [2]. However, histopathological examination of GBM patients after BPA-F mediated BNCT at the BNL showed tumor recurrence in high radiation dose regions as well as radiation-induced tumor necrosis [15]. Although there were some successful outcomes using these compounds, one of the main conclusions from these clinical trials was that 10B was not uniformly delivered to all tumor cells. Recent clinical trials at MIT were discontinued in 2003. Currently, BNCT clinical trials for brain tumors as well as melanoma continue in Argentina [17, 18], Europe including Finland [19], the Netherlands [20] and are to commence in the UK, Italy, and China. In Japan, clinical trials of brain cancer continue [21-23] and head and neck tumors are now being investigated [24, 25].

1-2. Dose components and biological effectiveness of BNCT radiation

The total BNCT radiation dose in tissue is comprised of several different components: the neutron-capture products of the $^{10}B(n,\alpha)^7Li$ reaction and the nonspecific

background dose from the interaction of the neutron beam with elements in tissue. In both tumor and normal tissue, radiation dose results from the 590 keV protons released from the $^{14}N(n,p)^{14}C$ (cross-section: 1.88 barns) reaction with nitrogen in tissue and the gamma rays released by the abundant amount of hydrogen in tissue from the $^{1}H(n,\gamma)^{2}H$ (cross-section: 0.33 barns) reactions. Additional dose may be contributed by the recoil protons from the contaminating fast neutrons that elastically scatter with hydrogen ($^{1}H(n,n')^{1}H$) and by gamma rays in the neutron beam [4]. These last two contributions are beam-specific and are very minor in most recent beam lines designed specifically for BNCT such as the thermal neutron beam at the MIT Research Reactor (MITR-II).

The BNCT dose components in tissue have different biological effectiveness because they have different linear energy transfer (LET) characteristics. In order to compare the total effects of BNCT or neutron irradiations with conventional photon irradiation, relative biological effectiveness (RBE) factors need to be determined experimentally. The term of compound biological effectiveness (CBE) factor is introduced in BNCT, because the biological effectiveness of the ^{10}B dose is also influenced by the microdistribution of boron in tissue which is characteristic of each boron compound.

1-3. Boron delivery agents

BNCT requires that physical and biological optimizations be performed. During the 1990s, physical optimization was completed with development of nearly optimum epithermal neutron beams [11]. As realized in the clinical trials, the success of BNCT depends upon the ability of a boron compound to preferentially and homogeneously deliver ^{10}B to malignant tissue. However, no new boron compound has been approved for clinical BNCT in over 20 years. Several groups in the USA have developed new boron compounds and the BNCT User Center at the MIT provides the pre-clinical evaluation of boron compounds [26]. This thesis includes the development and optimization for evaluation methods of boron compounds.

There are critical requirements for a promising boron delivery agent: 1) low systemic toxicity, 2) rapid clearance from blood and normal tissue and retention in tumor during irradiation, 3) highly specific uptake in tumor with high ratios of tumor-to-blood and

tumor-to-normal-tissue ^{10}B concentrations, and 4) at least 20-30 μg ^{10}B per gram of tumor to produce a significant ^{10}B capture-dose to the tumor that is approximately twice the nonspecific beam background doses that affect both tumor and normal tissue [27]. During BNCT, a maximum fluence of ~10^{12} thermal neutrons/cm^2 can be tolerated by normal brain tissue, and 10^9 atoms of ^{10}B per tumor cell are needed to create approximately 3-4 boron neutron capture events in that cell. With the assumption of 10^9 cells per one gram of tissue, 10^9 ^{10}B atoms per cell represent a bulk concentration of ~30 μg ^{10}B/g tumor [2].

Currently, only two boron compounds have been used in clinical BNCT trials: 1) the amino acid analogue *p*-boronophenylalanine (BPA, $C_9H_{12}NO_4B$) and 2) the sulfhydryl borane (BSH, $Na_2B_{12}H_{11}SH$). The chemical structures of BPA and BSH are presented in Figure 1.2. Although BPA was first synthesized in the late 1950s for BNCT, the fact that BPA penetrates the blood-brain barrier was considered as a disadvantage at the time for the treatment of brain tumors due to high doses to normal brain. Since being initially evaluated as a boron delivery agent for melanoma because of its similar structure to tyrosine, the precursor of melanin, in 1970s' Japanese studies, BPA has been actively investigated [4]. With a tumor-to-blood ^{10}B concentration ratio of ~4:1, this selective uptake of BPA in brain tumor may rely on the active amino acid transport mechanism [28]. BPA has been used in the treatment of malignant melanomas and was also utilized in the treatment of brain tumors [29]. At BNL, studies in a rat brain tumor model showed that long-term infusions (6-24 hours) of BPA-F produced better accumulation of boron in tumor cells infiltrating the normal brain compared to the 2-hour infusions [30].

BSH has been utilized for the treatment of brain tumors [31]. A small cage-structure compound, BSH is unable to cross the intact blood-brain barrier. BSH can be passively accumulated in parts of the tumor without an intact blood-brain barrier and achieve tumor-to-blood ^{10}B concentration ratios ranging from 0.9:1 to 2:1 [4]. Even though BSH has a low tumor-to-blood ^{10}B concentration ratio, BSH has been used for the treatment of brain tumors because of its exclusion from normal brain due to the blood-brain barrier [32]. However, some Japanese clinical trials reported acute and late radiation damage in normal brain because of the boron existing in the blood vessels of the normal brain during BNCT. Thus, in order to prevent the late radiation damage, a limit on the calculated ^{10}B dose of 12 Gy was suggested for the endothelial cells of the vasculature in the normal brain. This

vascular dose was calculated by applying a geometry factor that boron dose absorbed in the capillary wall was a third of the boron dose absorbed in the blood [33].

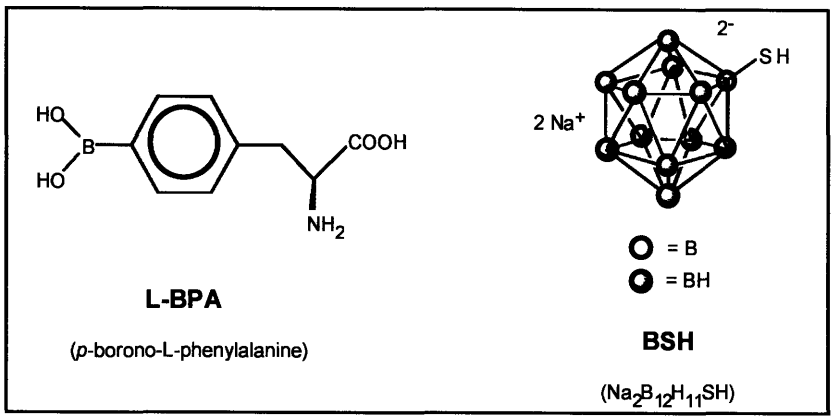

Figure 1.2. The chemical structures of p-boronophenylalanine (BPA) and the sulfhydryl borane (BSH), the two compounds used worldwide in current clinical BNCT trials [2].

Although the boron compounds BPA and BSH may be expected to provide more ^{10}B capture-dose to bulk tumors than to normal tissue, the ratio of the tumor-to-normal-tissue dose is far from what should be achieved for effective BNCT. Moreover, there are indications that BPA and BSH do not reach every tumor cell with an adequate ^{10}B concentration and that not all malignant cells are eradicated during BNCT. Thus, other classes of boron delivery agents have been designed and synthesized in attempting to attain the requirements for successful BNCT mentioned above. These types of compounds include other boron-containing amino acids, biochemical precursors of nucleic acids, DNA-targeting molecules, receptor-binding molecules, monoclonal antibodies, liposomes, and porphyrin derivatives [27]. Several review articles have comprehensively described the wide variety of boron compounds that have been synthesized [34-36].

Many compounds have been developed; however, only a few have been tested *in vitro*, with fewer tested *in vivo*, and none have yet begun a Phase I clinical study [37]. Boronated monoclonal antibodies against epidermal growth factor receptor for example have produced promising results using a glioma-bearing rat model [38, 39]. Extensive studies have demonstrated that a variety of boronated porphyrins can target various tumor types, such as glioma, mammary carcinoma, and carcinoma of head and neck [40-43].

These porphyrins have attractive properties of high boron affinity to tumor, an exceedingly high tumor-to-blood concentration ratio, and long retention time in tumors [44]. Porphyrin-mediated BNCT in the murine EMT-6 mammary carcinoma produced effective tumor response using multiple injections of the carboranylporphyrin (CuTCPH) [45]. Moreover, a radiation response study of oral mucosa showed that boron was not delivered to the sensitive epithelial stem cells of oral mucosa, suggesting that porphyrins may be of use for BNCT of head and neck tumors [46].

In conclusion, the development of better boron compounds is critical to the successful routine exploitation of neutron capture therapy as a useful modality. Moreover, the possibility of applying BNCT to a wide variety of tumor sites and tumor types makes an efficient and accurate methodology for evaluating boron compounds a very important part of boron compound development.

1-4. Research objectives and thesis organization

The overall objective of this research is to improve the effectiveness of BNCT through the identification of better boron compounds. An efficient and accurate methodology is desired to evaluate the radiobiological effectiveness of newly synthesized boron compounds. Boron compounds have to be tested with different evaluation methods depending upon their stages of compound development. An *in vitro* compound screening system is suitable in order to demonstrate promising agents with low chemical toxicity and selective intracellular uptake of compound in the early stage of compound development prior to further *in vivo* study. *In vivo* evaluation of a new boron compound is the culminating procedure for establishing the effectiveness of a compound in a small animal tumor model for BNCT since favorable animal trial results are required before clinical study in humans.

***In vitro* compound screening:** Chapter 2 describes the development of an *in vitro* compound screening method using the SCCVII mouse squamous cell carcinoma cell line; a murine model of head and neck cancer. This cell line was chosen as a representative class of tumor that could be treated in the future with BNCT. Clonogenic and colorimetric assays were utilized to assess the cell response with newly developed compounds, which are

appropriate for low molecular weight compounds that can readily permeate soft tissue. Because cell irradiations had not previously been performed for characterizing boron compounds at the MITR-II, the cell irradiation facility had to be built and optimized. Chemical synthesis is often time-consuming and expensive, so minimizing the amount of compound needed is an important factor that was considered in the design and optimization of cell irradiation facilities. In order to determine the relative intracellular accumulation of a compound, boric acid and BPA were used as reference compounds since the characteristics of cellular uptake for these compounds are well known. The comparison of the cell survival curves with boric acid, BPA, and test compounds gives an indirect estimation of relative intracellular accumulation of test compounds. The specific goals also include measuring dose, irradiating cells, and determining curves fitted to the linear-quadratic model of cell survival. To quantitatively analyze the biological efficacy of any new boron compound, CBE factors are calculated. Methodology is described for a rigorous uncertainty analysis of the neutron beam RBE and the boron compound CBE factor.

***In vivo* evaluation of boronated liposomes:** Chapter 3 provides original results from animal studies using boronated liposomes, a new class of boron delivery agent, evaluated for BNCT in the EMT-6 murine mammary carcinoma model for consistency of previous uptake studies. Liposomes are small unilamellar vesicles which consist of a phospholipids bilayer and an interior aqueous core with diameters of 60-100 nm. *In vivo* evaluations for two formulations of boronated liposomes (MAC and MAC+TAC) were completed including biodistribution, microdistribution, and therapeutic response studies. As a benchmark, the liposome results were compared with those from BPA, one of the boron compounds approved for clinical trials of BNCT. In Chapter 4, two approaches were taken to further explore the potential usefulness of liposomes for BNCT: 1) An alternative tumor model; the SCCVII mouse squamous cell carcinoma, was used to see whether there was any improvement of boron uptake and uniformity in the tumor and 2) a modified injection protocol was used in an attempt to increase the ^{10}B concentration and uniformity of uptake in the EMT-6 tumor model.

The final chapter summarizes the significance of this thesis and the general concepts of evaluating boron compounds and recommends considerations for future work.

CHAPTER TWO

METHODOLOGY FOR *IN VITRO* COMPOUND SCREENING

2-1. Introduction

With the understanding of the significance of new boron compounds and the development in drug technology such as drug delivery and targeting, there have been many studies for synthesizing new boron compounds [47-51]. These new compounds are tested in cell culture for toxicity and uptake [52-55], or may instead be directly evaluated in small animals [44, 56-60]. A simple and efficient *in vitro* study could play an important role in identifying the most promising constructs especially when several variations of a particular compound are synthesized and must be evaluated for BNCT. Besides, *in vitro* studies can minimize the quantity of compound needed as well as time and cost compared with *in vivo* systems [61]. For example, a few milligrams of compound would be required for *in vitro* studies, whereas *in vivo* studies typically need several grams of compound. *In vitro* screening to test the efficacy can derive information that is useful in designing further studies. This chapter describes the development of a methodology for *in vitro* compound screening.

A new arrangement for cell irradiations had to be designed and optimized in the vertical beam line of the thermal neutron beam at the MITR-II since cell irradiations to investigate the effects of different boron compounds had not previously been performed at the MITR-II. At Brookhaven National Laboratory, *in vitro* experiments for BNCT were carried out at the Brookhaven Medical Research Reactor (BMRR) [52]. In these experiments, single cell suspensions were placed in small vials and rotated during irradiation to uniformly administer neutron fluence [62]. However, because the BMRR had a horizontal beam channel, this layout was not suited to the vertical geometry of the MITR-II. The thermal neutron beam has been used for BNCT studies where small animals are irradiated in a removable shielding box that is part of the beam line shutter [26, 63].

Irradiation jigs for both cell culture flasks and well plates were designed and constructed to fit the configured shielding box so that cells could be reproducibly irradiated with the desired neutron fluence.

In this method development, the SCCVII mouse squamous cell carcinoma cell line was used as a head and neck cancer model but the method described can be adapted for any cell line. Most head and neck cancers are squamous cell carcinomas, originating from the mucosal lining of those regions. Tobacco use and alcohol consumption are the major risk factors for head and neck cancer [64]. The five-year survival rate is about 40 % [65]. Patients with early stage disease are often successfully treated with surgery combined with radiation therapy and chemotherapy. However, cure rates with conventional treatment have remained poor for patients with advanced stage disease [66]. Moreover, since these tumors are located around sensitive organs, such as the central nervous system, oral mucosa, and skin, a novel and targeted therapy is important to treat head and neck cancer. Therefore, the selective targeting ability as well as the high-LET dose from BNCT could be beneficial for the treatment of head and neck tumors.

Assays

Clonogenic and colorimetric assays were devised to detect and measure cell damage from the radiation exposure in the presence of newly developed boron compounds, especially for low molecular weight compounds, using only the limited quantities (a few milligrams of ^{10}B) which chemists can practically make available for testing in the early stage of compound development. The clonogenic assay or colony forming assay, is a widely-used, accepted standard method to measure the radiosensitivity of cells. Tumor cells survive when they can proliferate indefinitely and form a large colony from a single cell. After the irradiation, cells may still be viable and able to produce proteins, synthesize DNA, and even divide once or twice. However, if it cannot reproduce indefinitely, it is considered dead [67]. Therefore, for the clonogenic assay, individual tumor cells are separated and plated to grow into a colony consisting of at least 50 cells, which is defined as having reproductive integrity and represents cell survival [68]. This clonogenic assay will be used as a standard method to determine the radiobiological effectiveness of compounds in the definitive *in vitro* compound evaluation.

A colorimetric assay is generally used to determine the cytotoxic effect of a drug or radiation on the viability and proliferation of the cell. This endpoint is an alternative that is distinctly different from the reproductive integrity measured by the clonogenic assay. The tetrazolium salt, such as 3-(4,5-dimethylthiazol-2-yl)-2,5-diphenyltetrazolium bromide (MTT), is reduced by enzymatic activity in viable cells into colored formazan crystals. The amount of color produced is proportional to the number of viable cells and can be quantified using a microplate reader that measures the intensity of transmitted light at a particular wavelength [69, 70]. This colorimetric assay was used as an initial testing to facilitate a simpler and more efficient method for determining chemical toxicity and relative intracellular uptake of boron compounds using only a small quantity (less than a milligram of ^{10}B).

In order to determine relative intracellular accumulation of a test compound, boric acid and BPA were used as reference compounds because the intracellular accumulation of these compounds is well known. Boric acid is a very useful reference compound for radiobiological experiments because it is transported into cells only by diffusion and distributes uniformly inside cells *in vitro* at the same concentration as present in the growth medium (i.e. approximately 1:1 intracellular/extracellular accumulation ratio) [71]. More preferential intraceullular accumulation was shown with BPA for tumor cells because BPA is transported into cells through the cell membrane by the amino acid transport system [28]. For example, the intracellular/extracellular accumulation ratio of BPA for a rat brain tumor cell line, the 9L gliosarcoma, was 3.2 [71, 72]. Even though the boron uptake into the cells depends on the cell lines, a study to evaluate intracellular/extracellular accumulation ratio with various tumor cell lines showed BPA preferentially accumulated in the tumor cells [72]. Thus, BPA was also expected to have a higher intracellular accumulation in the SCCVII cells used in the studies described here. Cell survival experiments with these reference compounds (boric acid and BPA) and test compounds give an indirect estimation of relative intracellular accumulation for a test compound. To demonstrate the *in vitro* method, the boronated porphyrin, BOPP, is studied as a test compound.

Cell survival curves

The response of cells to radiation is measured as a function of radiation dose using clonogenic and colorimetric assays and these results are given as cell survival curves. A cell survival curve describes the relationship between the radiation dose and the proportion of surviving cells after the radiation exposure, which is generally represented by plotting the surviving fraction on a logarithmic scale on the y-coordinate against the radiation dose on a linear scale on the x-coordinate. The shape of the cell survival curve is different for radiation with different LET. High-LET radiations produce a cell survival curve that is almost a straight line on a log–linear plot. Low-LET radiation yields curves with an initial slope followed by a shoulder region that becomes nearly straight at higher doses [67]. The shoulder region is generally accepted to represent the ability of cells to repair sub-lethal damage. Numerous mathematical models have been proposed to describe the shape of cell survival curves, which are based on the random nature of energy deposition by radiation. The linear- quadratic model is now most often used to describe the cell survival curve, assuming that there are two ways to cause cell killing that is presumed to arise from a double stranded break in the DNA caused by the radiation. The linear component (α) describes cell killing by a single track of radiation; the quadratic component (β) represents cell killing by two separate events in the same target.

$$SF(D) = exp(-\alpha D - \beta D^2) \tag{1}$$

where SF(D) is the surviving fraction at a certain dose D, and α and β are constants.

Biological weighting factors

Different types of radiation produce different levels of biological response for the same absorbed dose. When radiation is absorbed in a cell or tissue, the energy is deposited through ionization and excitation along the tracks with a pattern that is characteristic of the type of radiation involved. Also, when neutrons interact with tissue, neutrons set in motion a charged particle spectrum that consists of proton, alpha particle, and heavier ions. X- or γ-rays produce only electrons with a low ionization density; whereas heavier charged particles (such as protons, alpha particles, and heavier ions such as Li) generate a much more dense pattern of ionizations. The term linear energy transfer (LET) represents the ionization density of the radiation. This difference in LET of the radiation governs the

biological effects observed from a given dose of neutrons, protons, and alpha particles compared with that of low-LET radiations such as X- or γ-rays, and electrons [67].

The relative biological effectiveness (RBE) is a practical method to compare the biological effects of different radiations. The RBE for a test radiation is determined by comparing the dose of a reference radiation (generally 250 kVp X-rays) that produces the same biological effect as a dose of test radiation. Thus, for the same biological endpoint,

$$RBE = \frac{Dose\ from\ reference\ radiation}{Dose\ from\ test\ radiation} \tag{2}$$

The RBE changes with the type of radiation and its energy, the type of cell or tissue, the biological endpoint, the radiation dose, the dose rate, and fractionation [67]. In BNCT, the biological effectiveness of the boron dose from $^{10}B(n,\alpha)^{7}Li$ reaction is dependent not only on these properties but also on the microscopic distribution of boron in tissue that is characteristic of a given boron compound. An additional term called the compound biological effectiveness (CBE) factor was introduced to describe the overall biological effectiveness of the boron neutron capture dose component. The CBE factor is calculated for a certain endpoint by comparing neutron beam irradiation in the presence of boron compound with X-ray irradiation [4].

$$X\text{-}ray\ Dose = [Beam\ Dose][Beam\ RBE] + [Boron\ Dose][CBE\ factor] \tag{3}$$

Present study

This chapter describes the development of the methodology for *in vitro* compound screening using the clonogenic and colorimetric assays. The specific goals include designing and optimizing the cell irradiation facility at the thermal neutron beam in the MITR-II, measuring dose, irradiating cells, and the determining cell survival curves fitted with the linear-quadratic model. Cell survival experiments with reference compounds (boric acid and BPA) and a test compound (BOPP) give an indirect estimation of relative intracellular accumulation for BOPP. To demonstrate the *in vitro* method, the boronated porphyrin, BOPP, is studied as a test compound. To quantitatively analyze the biological efficacy of a test compound, CBE factors are calculated after determining the beam RBE. A rigorous analysis of the uncertainty of all measured and derived quantities is included. Also, the advantages and limitations of the developed method are discussed.

2-2. Materials and methods

2-2-1. Thermal neutron irradiation facility

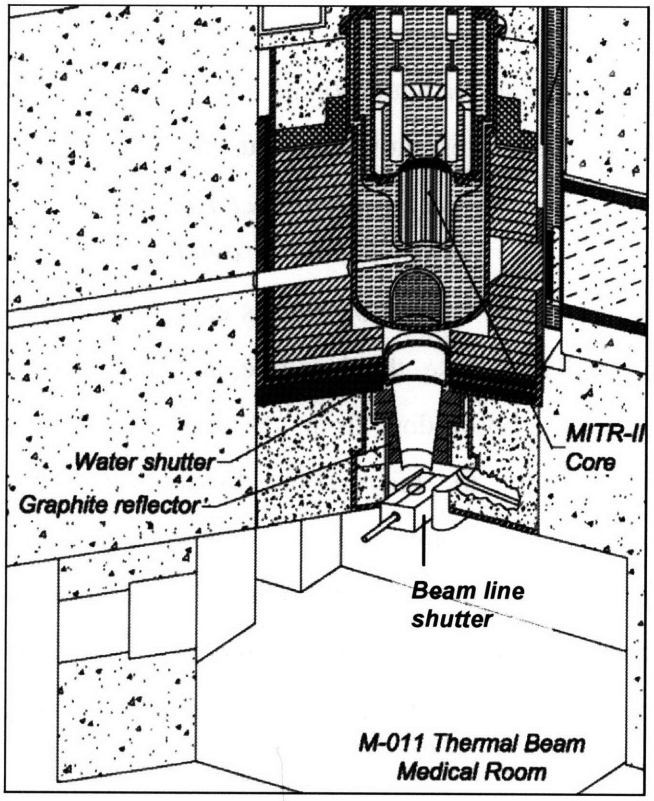

Figure 2.1. The cross-section view of the MITR-II with the M-011 thermal neutron irradiation facility directly beneath of the core. (This image is kindly provided by Dr. Kent Riley.)

The MITR-II has a 5 MW maximum operating power and contains a number of experimental facilities. The core is comprised of highly enriched uranium fuel elements, which are cooled and moderated by light water. Neutrons from the core are reflected and moderated by a heavy water tank below the core, producing a peak thermal neutron flux of $\sim 1 \times 10^{14}$ n/cm^2-s at 5 MW power. Thermal neutrons are collimated by the surrounding graphite walls of the beam line. The high intensity of thermal neutrons at the position of the field delimiter, $\sim 5 \times 10^{9}$ n/cm^2-s, and very low photon and fast neutron contamination of the thermal neutron beam facility, is well suited for preclinical cell culture experiments or small animal studies and for clinical studies of superficial tumors [26]. The beam is turned on by first emptying a water tank beneath the D_2O reflector. Beam shutters of lead and neutron-absorbing boral (boronated aluminum) are then opened and a bismuth photon

shield and collimator are move into the beam line together with the shielding box containing animals or cells. Figure 2.1 illustrates the cross-section view of the MITR-II with the M-011 thermal neutron irradiation facility directly beneath of the core.

2-2-2. Experimental arrangement at MITR-II

An experimental setup to reproducibly position cell cultures was designed for the shielding box that is part of the beam line shutter in the M-011 thermal neutron beam of the MITR-II. This box efficiently absorbs low energy neutrons in the beam producing very little secondary radiation and helps minimize activation inside the medical room. During the irradiation, cells are attached to the bottom of the tissue culture flask (clonogenic assay) or a 96-well plate (colorimetric assay). Platforms to position flasks or 96-well plates in the shielding box were designed and built. Acrylic plates and nylon bars were used to make the platform considering practical use, durability, low residual radioactivity after the irradiation, and light weight due to the vertical position of thermal neutron beam. Also, in order to minimize the amount of boron compound used for screening, two flasks with smallest growth area of 12.5 cm^2 or one 96-well microplate (0.37 cm^2 per well, 35.5. cm^2 total) were employed for each irradiation. Scatterers made of acrylic plate were put around the flasks or 96-well plates to provide a more uniform dose distribution where cells were placed during irradiation. Elastic neutron scattering with the hydrogenous plastic will return some neutrons that would otherwise be lost from the beam.

2-2-3. Dose measurements at MITR-II

Gold foil activation analysis was used to measure thermal neutron flux. Bare gold foils (12-18 mg, 0.005 cm thick) were positioned on the bottom of flasks containing 1 ml of growth medium to reproduce the cell irradiation condition, and then irradiated for approximately 30 minutes. Smaller gold foils (3-4 mg, 0.005 cm thick) were placed at the bottom of several wells in a 96-well plate and covered with 100 μl of growth medium, and then irradiated for a similar duration. ^{197}Au reacts with neutrons to form ^{198}Au that emits a 411 keV photon during decay. The 2200 m/s neutron flux was determined from measurement of ^{198}Au activity on foils using a calibrated high purity germanium detector.

Nitrogen dose from $^{14}N(n,p)^{14}C$ reactions and ^{10}B dose from $^{10}B(n,\alpha)^{7}Li$ reactions were determined by multiplying the measured 2200 m/s flux by kerma coefficients of 7.88×10^{-12} Gy/cm^2 and 8.66×10^{-8} Gy/cm^2, respectively.

The dual chamber technique [73] was applied to measure photon and fast neutron (E_n > 0.5 eV) absorbed doses. An A-150 tissue-equivalent ionization chamber filled with tissue-equivalent gas (64.4 % CH_4, 32.4 % CO_2, and 3.2 % N_2 by partial pressure) measured the total dose from photons and neutrons. A carbon (graphite) walled ionization chamber filled with CO_2 gas, which has little response to neutrons, was used to repeatedly measure the photon dose. The gas flow rate of both chambers was 20 ml/min, and the voltage was +250 V. During measurements, chambers were positioned in the center of a flask near the bottom and next to a second flask containing 1 ml of growth medium or in the middle of a 96-well plate through a hole made for dosimetry. All details of these dosimetry methods including the dual chamber technique and gold foil analysis are described elsewhere [73]. Beam monitor counts were recorded and calibrated by these absorbed dose measurements. Ultimately, these beam monitor counts control beam delivery during cell irradiations to 1 % precision. Overall uncertainties associated with the dosimetry are 5 % for thermal neutron, 5 % for photon, and 7 % for boron component [26, 74].

2-2-4. Cell culture conditions

The SCCVII mouse squamous cell carcinoma cell line was generously provided by Brookhaven National Laboratory. The cells were grown in Dulbecco's Modified Eagle's Medium (DMEM, Mediatech) supplemented with 10 % fetal bovine serum (SeraCare Life Science), 1 % 200mM L-glutamine (Mediatech), and 1 % 5,000 I.U./ml penicillin – 5,000 μg/ml streptomycin (Mediatech) at 37 °C in an atmosphere of 5 % CO_2. The cell doubling time is about 15 hours. The cells were sub-cultured every 5-7 days. To maintain consistency of cell characteristics, new cells were started from cryogenically preserved stocks after ~24 passages (about 5 months).

2-2-5. Cell counting

Cell numbers were counted using a Z2 Coulter Counter from Beckman Coulter. When cells suspended in an electrolyte are passed through a small aperture, the counter detects changes in electrical conductance. The counter displays cell concentration and size distribution of the counted cells. Five measurements were carried out on 1 ml suspensions from each flask and averaged to get the final result. Cell numbers measured with the Coulter Counter were periodically cross-checked with results from manual counting using a hemocytometer and agreed to within 5 %.

2-2-6. Boron compounds

Boric acid (H_3BO_3, 94.56 % ^{10}B enriched) was used as the reference boron compound that uniformly distributes inside and outside cells [71]. BPA-fructose solution (p-boronophenylalanine, > 99 % ^{10}B enriched, L-isomer) was prepared as a positive control that preferentially accumulates inside tumor cells [72].

As a test compound, the boronated porphyrin BOPP (tetrakis-carborane carboxylate ester of 2,4-bis-(alpha,beta-dihydroxyethyl)-deutero-porphyrin IX, ^{10}B enriched) was dissolved in phosphate-buffered saline (PBS 1x) and stored at 4 °C in darkness, because porphyrins are sensitive to visible light. Experiments with BOPP solution were carried out under low intensity light [75]. The BOPP was synthesized by Professor Steve B. Kahl from the University of California, San Francisco and the solutions for testing were kindly prepared by M.Alejandra Dagrosa from Constituyentes Atomic Center, Argentina.

2-2-7. Boron analysis

The ^{10}B concentration of each boron solution was measured using Prompt Gamma Neutron Activation Analysis (PGNAA) in the MITR-II. PGNAA detects the 478 keV photons produced from boron neutron capture reactions in ^{10}B [76]. Boron solutions were diluted into growth medium to make the desired ^{10}B concentration for each experiment. ^{10}B concentrations of diluted solutions were confirmed with PGNAA. The uncertainty of measurement is less than 5 %.

2-2-8. Cell irradiation

Two flasks or a 96-well plate were positioned on the platform in the shielding box (see Figure 2.2) which was placed in the beam line. Cells were irradiated with graded doses of the thermal neutron beam with and without boron compound in the medium. Boron dose is calculated with ^{10}B concentration in the growth medium. Based on the beam monitor counts calibrated by dosimetry measurements, the desired neutron fluence was given with 1 % precision. Also, cells were irradiated with graded doses of X-rays. A Phillips RT250 unit in the MIT Nuclear Science and Engineering Department was used, operating at 250 kVp and 15 mA with 0.4 mm Sn plus 0.25 mm Cu added filtration and a focus-to-target distance of 23cm. The average X-ray dose rate to the cells at the bottom of the flask was 1.0 Gy/min and this was measured with an air-filled graphite ionization chamber periodically to check for consistency. The administered doses have an estimated uncertainty of approximately 3 % based upon calibration precision of the ionization chamber, positioning errors, and output constancy of the machine.

2-2-9. Fitting survival data to the linear-quadratic model

The linear-quadratic model has been used to fit survival data from the clonogenic and colorimetric assay cell survival experiments, by means of the TableCurve 2D software, version 5.01 (SYSTAT Software Inc., 2002). This program uses an automated curve fitting process to find the ideal model using weighted, least square curve-fitting. Data points were weighted with the inverse square of the standard deviation. The coefficients of α and β with the standard errors from the linear-quadratic equation, $SF(D) = exp(-\alpha D - \beta D^2)$ were obtained, using the coefficient of determination, R^2, as a measure of the goodness-of-fit. Also, chi-square statistics were calculated to verify the goodness-of-fit [77, 78].

2-2-10. Calculations of RBE and CBE

The fitted linear-quadratic equations were used to interpolate the doses of X-ray and neutron beam corresponding to a specified surviving fraction. Surviving fractions of 0.02 for the clonogenic assay and 0.2 for the MTT assay were chosen because those were suitable ranges for each assay based on results of X-ray irradiations. The RBE of the

thermal neutron beam was then obtained using equation (2) in 2-1. CBE values for the boron compounds were obtained using equation (3) in 2-1 after determining the beam RBE and the neutron beam and boron dose components for a given surviving fraction.

2-2-11. Uncertainty analysis

In order to analyze uncertainties of RBE and CBE, total uncertainties of interpolated doses were estimated by propagating the uncertainties from curve fitting and dose measurement. The fitting uncertainty of dose was determined using the standard errors of the fitting-coefficients, α and β, and these fitting uncertainties were averaged for each assay (2.8 % for clonogenic assay and 3.5 % for MTT assay). The estimated uncertainty in the dose measurement for both clonogenic and MTT assay was 3 % for X-rays, 5 % for the neutron beam, and 7 % for boron, which includes 5 % uncertainty in the boron concentration measurement.

The estimated uncertainty in the neutron beam RBE was calculated using error propagation [77, 78] associated with the X-ray and neutron beam endpoint doses.

$$\sigma_{RBE} = RBE \times \sqrt{\left(\frac{\sigma_{X\text{-}rays\ Dose}}{X\text{-}ray\ Dose}\right)^2 + \left(\frac{\sigma_{Neutron\ beam\ Dose}}{Neutron\ beam\ Dose}\right)^2} \tag{4}$$

Next, the uncertainty of CBE for each boron compound was obtained using error propagation through all components of the CBE equation as follows:

$$\sigma_{CBE} = CBE \times \sqrt{\left(\frac{\sigma_{X\text{-}ray\ Dose\text{-}(Neutron\ beam\ Dose \times RBE)}}{X\text{-}ray\ Dose - (Neutron\ beam\ Dose \times RBE)}\right)^2 + \left(\frac{\sigma_{Boron\ Dose}}{Boron\ Dose}\right)^2}$$

$$\sigma_{X\text{-}ray\ Dose\text{-}(Neutron\ beam\ Dose \times RBE)} = \sqrt{\sigma^2_{X\text{-}ray\ Dose} + \sigma^2_{(Neutron\ beam\ Dose \times RBE)}} \tag{5}$$

$$\sigma_{(Neutron\ beam\ Dose \times RBE)} = (Neutron\ beam\ Dose \times RBE) \times \sqrt{\left(\frac{\sigma_{Neutron\ beam\ Dose}}{Neutron\ beam\ Dose}\right)^2 + \left(\frac{\sigma_{RBE}}{RBE}\right)^2}$$

2-3. Clonogenic assay

2-3-1. Experimental arrangement and dosimetry

The initial arrangement shown in Figure 2.2 used two T12.5 flasks completely filled with growth medium turned upside down. This arrangement positioned cells that were attached to the bottom of the flasks closer to the thermal neutron beam and provided a simple geometry for dosimetry. However, to fill a flask completely, almost 43 ml of medium was needed and so this would require a large amount of compound. For example, a boron solution with a concentration of 10 μg ^{10}B/ml would require 430 μg ^{10}B in one flask. Cells must be irradiated with several graded doses of neutrons and at least a few milligrams of ^{10}B compound would be required for this test, which may exceed the quantity available. Such a large amount of new compound may not be practical for preliminary cell culture studies.

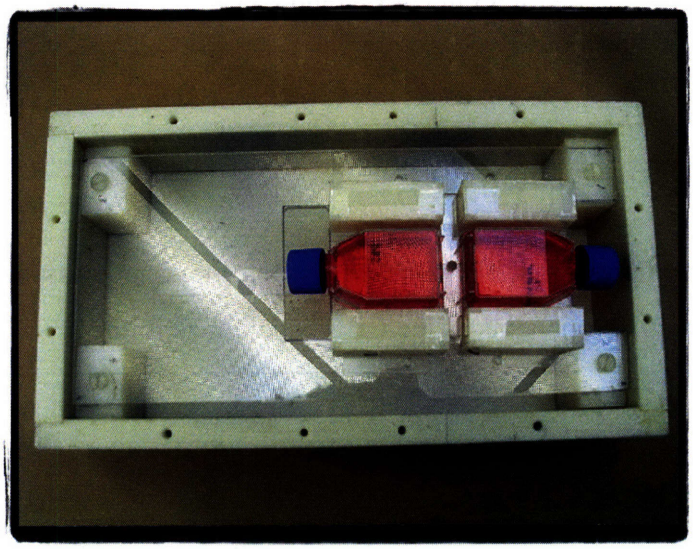

Figure 2.2. Initial arrangement with inverted T12.5 flasks which are completely filled with growth medium for cell irradiations with the thermal neutron beam at MITR-II.

An optimized new arrangement for the clonogenic assay was with two T12.5 flasks in the normal position, each containing 1 ml of growth medium. Scatterers made of acrylic plate surround the flasks, and this also served to guide flasks into the same position for every experiment. Beneath the platform, a thick scatterer was used to help backscatter useful thermal neutrons and create a more uniform dose profile over all the cells. This setup requires less than a milligram of ^{10}B. Figure 2.3 shows the schematic view of the experiment setup for the clonogenic assay.

The thermal neutron flux normalized to the reactor operating at 5 MW of 8.5 (± 0.4) $x10^9$ n/cm^2-s, was determined from the average of several gold foil measurements at different positions through the bottom of two flasks. The nitrogen and boron capture dose rates were determined as 14.2 ± 0.7 cGy/min and 4.4 ± 0.3 cGy/min per μg ^{10}B/ml, respectively, assuming a nitrogen concentration of 3.5 %. Dual ionization chamber measurements determined a photon absorbed dose rate of 26.9 ± 1.3 cGy/min with negligible fast neutron contamination in the thermal neutron beam. With 10 μg^{10}B/ml concentration, the boron capture dose is 52 % of the total absorbed dose (Table 2.1). Estimated uncertainties for dose measurement were 5 % for the nitrogen capture dose, 5 % for photon dose, and 7 % for boron dose which includes uncertainties of thermal neutron flux measurement and boron concentration measurement.

Table 2.1. The absorbed dose rates for cells in flasks containing 1 ml of medium normalized to 5 MW, the full power of the reactor.

Thermal neutron flux (n/cm^2-s)	Absorbed dose rate (cGy/min)			
	Nitrogen	Fast neutron	Photon	Boron (per μg ^{10}B /ml)
8.5 (± 0.4) x 10^9	14.2 ± 0.7	< 0.1	26.9 ± 1.3	4.4 ± 0.3

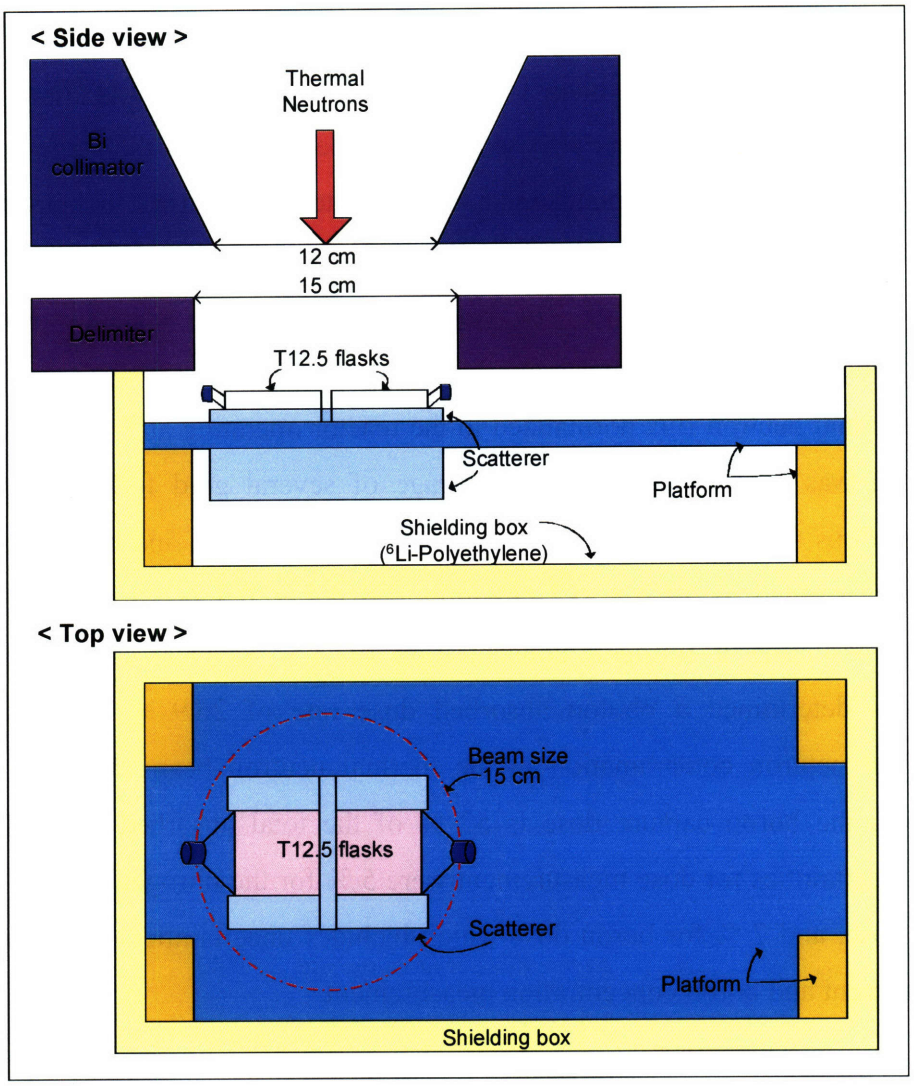

Figure 2.3. Schematic view of the setup to carry out the thermal neutron irradiation for clonogenic assay in the MITR-II. Two T12.5 flasks were irradiated simultaneously in the 15 cm diameter circular field. Plastic scatterers were positioned to produce more uniform irradiation of the flasks.

2-3-2. Cell survival experiment

SCCVII cells (~3×10^5) were plated into each T12.5 flask (growth area of 12.5 cm^2) with 5 ml of growth medium one day before the irradiation. To remove the trypsin from the cell suspension and increase the plating efficiency, cell suspensions were centrifuged and

the supernatant removed. Then, cells were resuspended with new growth medium and plated in the flask. Flasks were incubated overnight (approximately 20 hours) to allow cells to attach to the bottom. Two hours before the irradiation, growth medium was replaced with medium containing the desired amount of boron. Two flasks were irradiated together with graded doses of thermal neutron beam. For X-ray irradiations, cells were plated in T25 flasks (growth area of 25 cm^2) with 5 ml of growth medium and incubated overnight to allow attachment. Then, cells in T25 flasks were irradiated with graded doses of X-rays. Control flasks which received no irradiation were kept in the thermal neutron beam control room at the MITR-II or in the X-ray machine room during the experiment.

After the irradiation, cells were trypsinized with 0.25 % trypsin containing 0.1 % EDTA for 3 minutes in the incubator (37 °C, 5 % CO_2), and then resuspended with growth medium. After cells for each flask were counted 5 times with the Coulter Counter, a known number of cells was plated into 100x20 mm Petri dishes. Five replicate dishes were used for each flask. The medium was changed at 5 days after cells were plated. After 7-10 days, medium was removed, and the colonies were fixed and stained with 1 % methylene blue in 95 % ethanol for 5-10 minutes. Dishes were washed with flowing water and dried at room temperature. Colonies containing more than 50 cells were counted. This procedure is briefly illustrated in Figure 2.4.

The surviving fraction (SF) was calculated as:

$$SF(\%) = \frac{number\ of\ colonies}{number\ of\ seeded\ cell \times (plating\ efficiency/100)}$$

The plating efficiency (PE) from non-irradiated control plate is determined from the following formula:

$$PE(\%) = \frac{number\ of\ colonies}{number\ of\ seeded\ cell} \times 100$$

The plating efficiency varies due to experimental or cell variability. Thus, every experiment included a control group to determine plating efficiency.

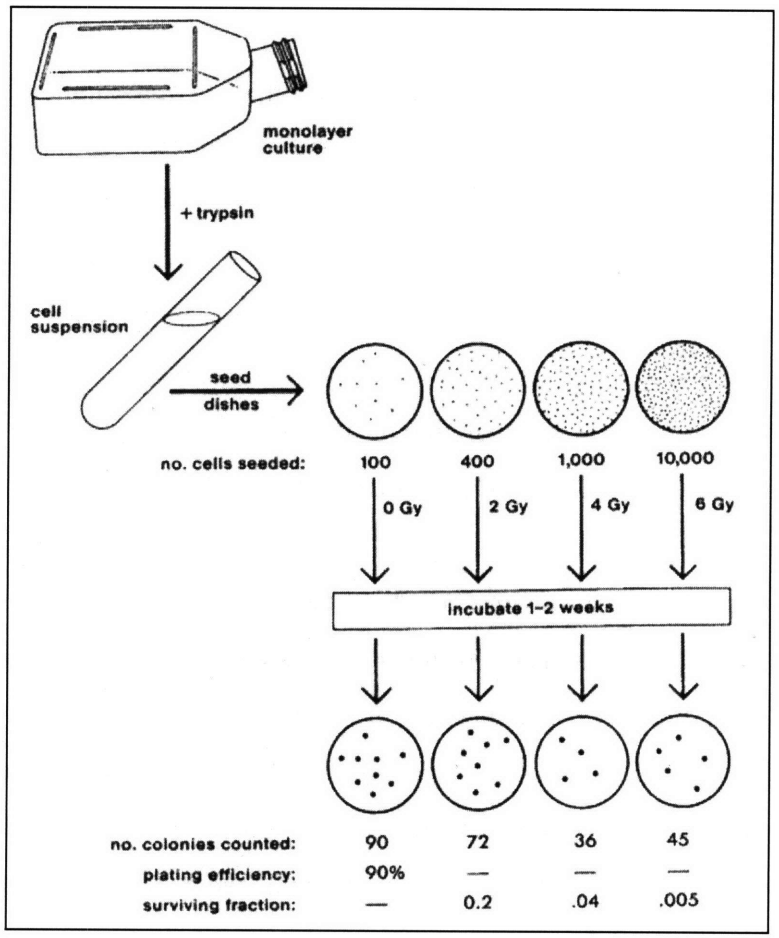

Figure 2.4. Outline of experimental procedure for the colony forming assay [67]. Cells are irradiated with graded dose of radiation (thermal neutrons or X-rays) and resuspended in the growth medium by trypsinization. Known number of cells are plated into Petri dishes and incubated for 7-10 days. The numbers of colonies are counted and used for calculation of surviving fractions with the plating efficiency determined from non-irradiated control plate.

2-3-3. Survival curve

Figure 2.5 presents the fitted survival curves using the clonogenic assay for SCCVII cells irradiated with 250 kVp X-rays, the thermal neutron beam, and the thermal neutron beam in the presence of 5 and 10 μg ^{10}B/ml boric acid. The survival data points of neutron beam irradiation with 2.3 μg ^{10}B/ml BPA are also shown in Figure 2.5. The x-axis shows total absorbed dose which is the sum of the beam and boron doses. Boron doses were calculated from the measured boron concentration in the medium. The data represent four

independent X-ray and neutron beam irradiation experiments and a single experiment with each boron compound. Error bars indicate the relative errors with error propagation through the whole procedure (from cell counting to colony counting) of five replicate dishes. Average plating efficiencies were 44 % for X-ray experiments and 20 % for neutron experiments. This lower plating efficiency in the neutron experiments was attributed to the cells being left at room temperature for longer period during the irradiation in the MITR-II.

With X-rays, the surviving fraction slowly decreased as dose increased. Thermal neutron beam irradiation produced a greater decrease in survival fraction than X-rays, but the survival curves of X-ray and neutron beam were relatively similar due to the high percentage of photon dose component (65 %) in the neutron beam. Neutron beam irradiation in the presence of boron compound clearly produced additional cell killing effect. Greater cell killing was observed with an increased boron concentration from boric acid. Only the survival data points with BPA are shown in Figure 2.5 without a fitted curve due to the limited number of data points. Still, the points show that the cell killing effect of BPA is comparable to twice the concentration of boric acid (5 μg ^{10}B/ml) in the low dose range.

Table 2.2 lists the fitting coefficients (α and β) and the goodness-of-fit (R^2 and χ^2) of the survival curves fitted using the linear-quadratic model. Curves of X-rays, neutron beam, and 5 μg ^{10}B/ml boric acid had an initial shoulder region; while curves of 10 μg ^{10}B/ml boric acid showed straight lines with $\beta = 0$. The goodness-of-fit values of R^2 and P (probability) from χ^2 test approach 1.0 which indicates that survival curves fit the linear-quadratic model well.

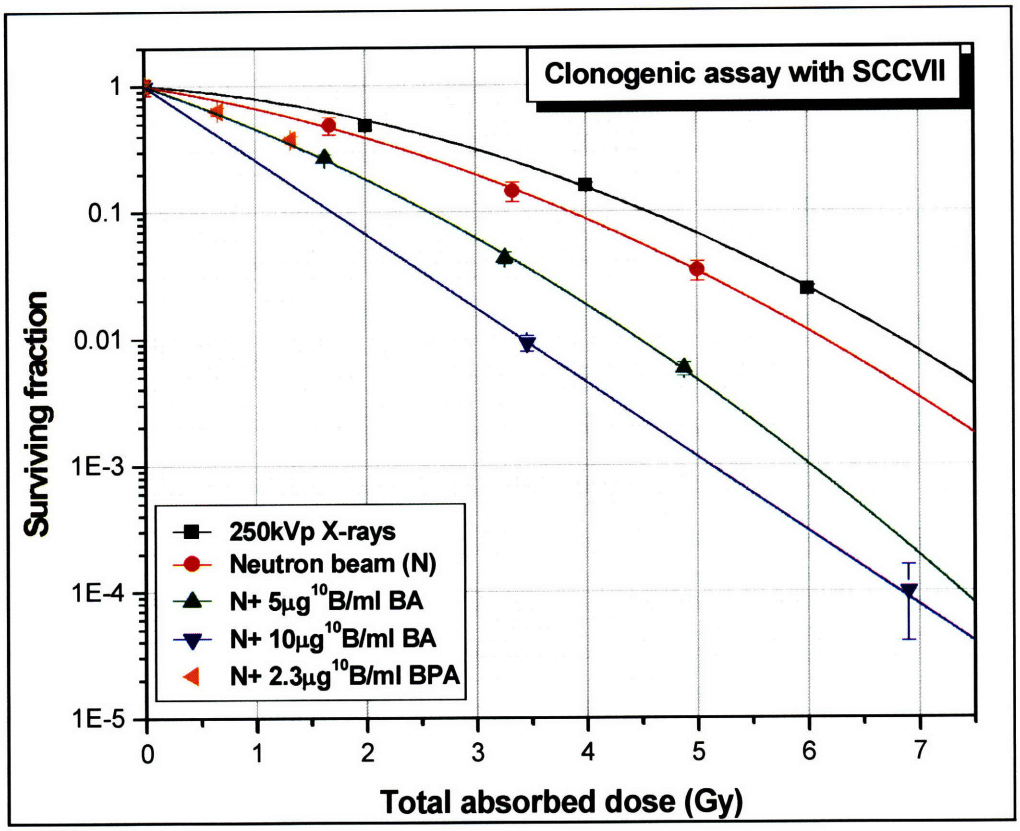

Figure 2.5. Survival curves fitted using the linear-quadratic model for SCCVII cells irradiated with 250 kVp X-rays, the thermal neutron beam, and the thermal neutron beam in the presence of 5 and 10 μg ^{10}B/ml boric acid (BA) and survival data points for 2.3 μg ^{10}B/ml BPA using the clonogenic assay. Results are expressed as the average ± uncertainty for surviving fractions and error bars are shown when these are larger than the symbols.

Table 2.2. Fitting coefficients (α and β) for the linear-quadratic model and goodness-of-fit (R^2 and χ^2) for X-rays, the neutron beam, the neutron beam with 5 and 10 μg ^{10}B/ml boric acid (BA) when using the clonogenic assay.

Radiation	SF = exp (- αD - βD^2)		Goodness-of-fit	
	α	β	R^2	χ^2
X-rays	0.163 ± 0.036	0.076 ± 0.007	0.9971	0.0027 (p=1.0)
Neutron beam (N)	0.338 ± 0.031	0.068 ± 0.007	0.9984	0.0011 (p=1.0)
N + 5 μg 10B/ml BA	0.703 ± 0.030	0.074 ± 0.008	0.9990	0.0003 (p=1.0)
N + 10 μg 10B/ml BA	1.351 ± 0.005	0	0.9998	0.9546 (p=0.8122)

2-3-4. Toxicity

To ensure that the results observed in Figure 2.5 are due primarily to radiation effects, a toxicity study was performed under similar experimental conditions. An experiment was performed using boric acid to determine whether chemical toxicity during the 24 hour incubation period before irradiation contributed to the cell kill observed during clonogenic assay cell survival experiments. Cells were exposed to 40 μg ^{10}B/ml boric acid solution for 24 hours. Before irradiation with thermal neutrons, the cells were washed and new growth medium was added to completely remove boric acid during irradiation. Control cells that had no boric acid showed 22 % plating efficiency and cells exposed to 40 μg ^{10}B/ml boric acid for 24 hours had a plating efficiency of 16 %. This lower plating efficiency may be due to the chemical toxicity of boric acid. Surviving fractions for this test were not considered significantly different for the two groups relative to the anticipated radiation damage that will be induced by the additional boron present in the cell during thermal neutron beam irradiations (Figure 2.6). This implies that chemical toxicity itself does not affect the cell response to the radiation for the clonogenic assay and the effect of chemical toxicity was incorporated into the plating efficiency.

2-3-5. Calculation of RBE and CBE with uncertainty analysis

Table 2.3 shows the doses with uncertainties at surviving fraction of 0.02 for X-rays, the neutron beam, and the neutron beam in the presence of boric acid. A surviving fraction of 0.02 was chosen since the clonogenic assay has a large dynamic range for measuring survival that can span three to four logs (10^{-3}-10^{-4}). The values for the beam RBE and the CBE factor of boric acid with estimated uncertainties are also presented in Table 2.3. Total uncertainties on the interpolated dose at the endpoint were estimated to be 4 % for X-rays, 5.7 % for the neutron beam, 7.5 % for boron using the clonogenic assay.

The beam RBE of the MITR-II was 1.1 ± 0.1 for SCCVII cells at 0.02 surviving fraction. This beam RBE value is close to 1 due to the high proportion of photon dose component (~ 65 %) in the thermal neutron beam. The CBE values for boric acid were 2.4 ± 0.3 for 5 μg ^{10}B/ml and 3.1 ± 0.3 for 10 μg ^{10}B/ml. The CBE value appears to increase with increasing concentration of boric acid, but this difference is not statistically significant.

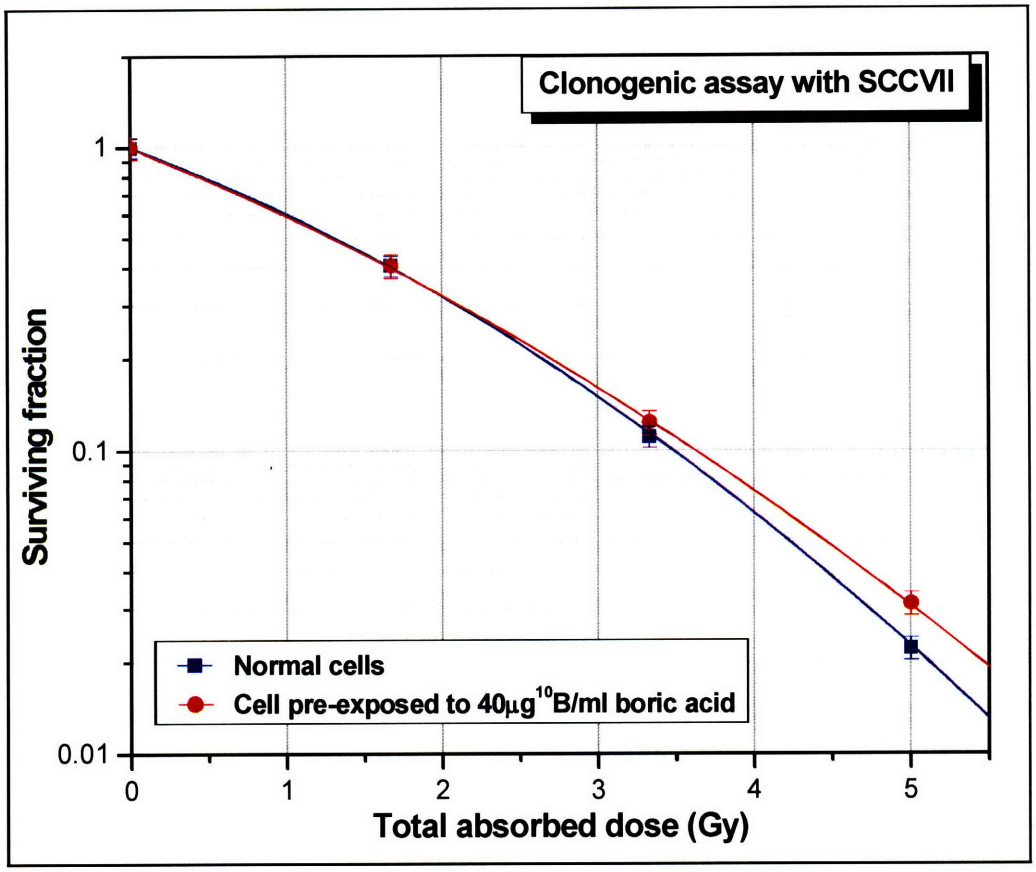

Figure 2.6. Survival curves fitted using the linear-quadratic model for SCCVII cells irradiated with the thermal neutron beam using the clonogenic assay. One group of cells received no pre-treatment with boric acid; the other group of cells were exposed to 40 μg ^{10}B/ml boric acid for 24 hours, then washed free of the boric acid. No boron was present during irradiations.

Table 2.3. Interpolated doses and RBE/CBE at surviving fraction of 0.02 for X-rays, the neutron beam, the neutron beam in the presence of 5 and 10 μg ^{10}B/ml boric acid (BA) using the clonogenic assay and SCCVII cells.

Radiation	Dose (Gy)	RBE/CBE
X-rays	6.2 ± 0.3	
Neutron beam (N)	5.5 ± 0.3	1.1 ± 0.1
N + 5 μg ^{10}B/ml BA	3.9 ± 0.3	2.4 ± 0.3
N + 10 μg ^{10}B/ml BA	2.9 ± 0.2	3.1 ± 0.3

2-4. Colorimetric assay

2-4-1. Experimental arrangement and dosimetry

A 96-well plate was prepared for neutron irradiations without using all outermost wells because gold foil measurements showed that corner wells have approximately 25 % lower thermal neutron flux than those in the middle. As with the flasks, a scatterer made of acrylic plate was put around the 96-well plate, which also helped to keep the plates in the same position for every experiment. In addition, a thick scatterer was placed underneath the plate with a hole in the center to improve uniformity of the thermal neutron flux in the outer wells. Figure 2.7 illustrates the arrangement of 96-well plate for cell irradiations.

The average thermal neutron flux (excluding the edge wells) was 7.7 (± 0.4) $\times 10^9$ n/cm^2-s, and fast neutron contamination was again trivial (< 0.1 cGy/min). With 10 μg ^{10}B/ml concentration, the boron capture dose produces 46 % of the total absorbed dose (Table 2.4). Estimated uncertainties were 5 % for the nitrogen capture dose, 5 % for photon dose, and 7 % for boron dose.

Table 2.4. The absorbed dose rates for cells in a 96-well plate containing 100 μl of medium in each well normalized to 5 MW reactor power.

Thermal neutron flux (n/cm^2-s)	Absorbed dose rate (cGy/min)			
	Nitrogen	Fast neutron	Photon	Boron (per μg ^{10}B /ml)
7.7 (± 0.4) x 10^9	12.8 ± 0.6	< 0.1	34.4 ± 1.7	4.0 ± 0.3

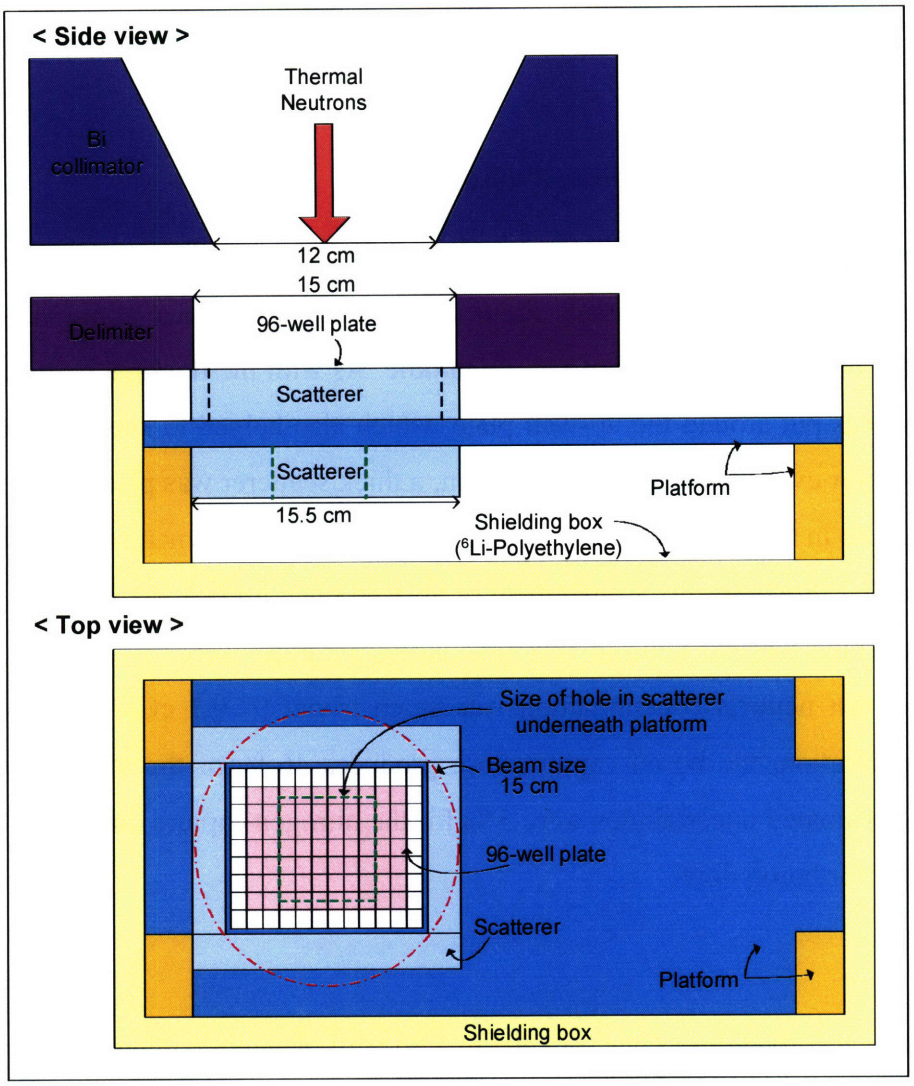

Figure 2.7. Schematic view of the setup to carry out thermal neutron irradiations for the colorimetric assay in the MITR-II. A 96-well plate was irradiated in the 15 cm diameter circular field. Plastic scatterers were positioned to produce more uniform irradiation of the plate. Only the shaded wells in the 96-well plate were used for experiments.

2-4-2. Preliminary study

The colorimetric assays are based on the conversion of tetrazolium salt to a colored product by enzymatic activity of viable cells. The amount of color produced, which is directly proportional to the number of viable cells, can be measured using a microplate reader that measures the optical density in each well, using the appropriate light wavelength. The first colorimetric assay evaluated was based on a reagent known as WST-1. The WST-1, tetrazolium salt (4-[3-(4-Iodophenyl)-2-(4-nitrophenyl)-2H-5-tetrazolio]-1,3-benzene

disulfonate), is cleaved to form a formazan dye by a mitochondrial enzyme in direct proportion to the number of viable cells present. An assay kit is available including a WST-1 reagent (Roche Applied Science). Due to simpler processing step and higher sensitivity, the WST-1 assay has advantages over other cell proliferation agents for some applications: e.g. those that only measure chemical toxicity [79]. However, numerous preliminary experiments showed that this assay is too sensitive for use in our radiation response assay. To compare OD of non-irradiated control cells with that of irradiated cells showing measurable radiation damage, a practical number of cells have to be plated in each well allowing 4-5 days of growth time after irradiation. For example, with WST-1, OD numbers of the control cells after 5 days of growth time were mostly out of reading range (OD > 3) even though only 100 cells were initially plated in each well. Due to this limitation, an alternative colorimetric assay was evaluated: the more generally used MTT colorimetric assay.

The MTT tetrazolium salt, 3-(4,5-dimethylthiazol-2-yl)-2,5-diphenyltetrazolium bromide, is reduced into purple formazan crystals. The MTT assay kit (Roche Applied Science) available includes a MTT labeling reagent and a solubilization solution. Figure 2.8 shows the average OD numbers using WST-1 and MTT assays as a function of SCCVII cells initially plated in each well. These numbers were measured right after cells were plated and no irradiation was involved. Higher OD numbers from the WST-1 assay were measured for increasing numbers of cells in each well than those from the MTT assay. This means that with the MTT assay each well can contain more cells and still have an OD reading in the measurable range.

In order to determine the growth time, preliminary experiments were performed with varying growth times from 3 to 6 days, and the optimum was found to be 5 days. Over a 5 day period, however, depletion of nutrients in the medium could lead to sub-optimal growth. An additional preliminary study (Figure 2.9) was carried out to evaluate the OD after 5 days growth as a function of cells plated in each well and to determine the effect of changing the medium during the incubation period. Since the colorimetric assays are based on cell growth differences between non-irradiated control cells and irradiated cells, the loss of cells during the procedure of pipetting for medium changing could be a potential problem. OD numbers were measured at 5 days with and without a medium change 3 days

after cell plating. Cells with medium change produced slightly higher average OD number than cells without medium change, especially for higher cell numbers initially plated. This indicates that OD numbers decrease more due to lack of nutritious medium than due to possible cell loss during medium change. In Figure 2.9, a cell density of 500-1000 cells/well maximizes cell growth after the 5 day period selected to use for the MTT assay. This may result from further medium depletion or confluence of cells at the higher cell densities. Thus, our protocol specifies a cell density of 500 cells/well and the addition of medium 3 days after cell plating to feed the cells and to avoid potential differences in their subsequent growth. Also, all 96-well plates should have blank wells containing only medium or medium with boron compound present to obtain an accurate blank OD number, although medium only measured as a function of incubation time appears to be relatively constant.

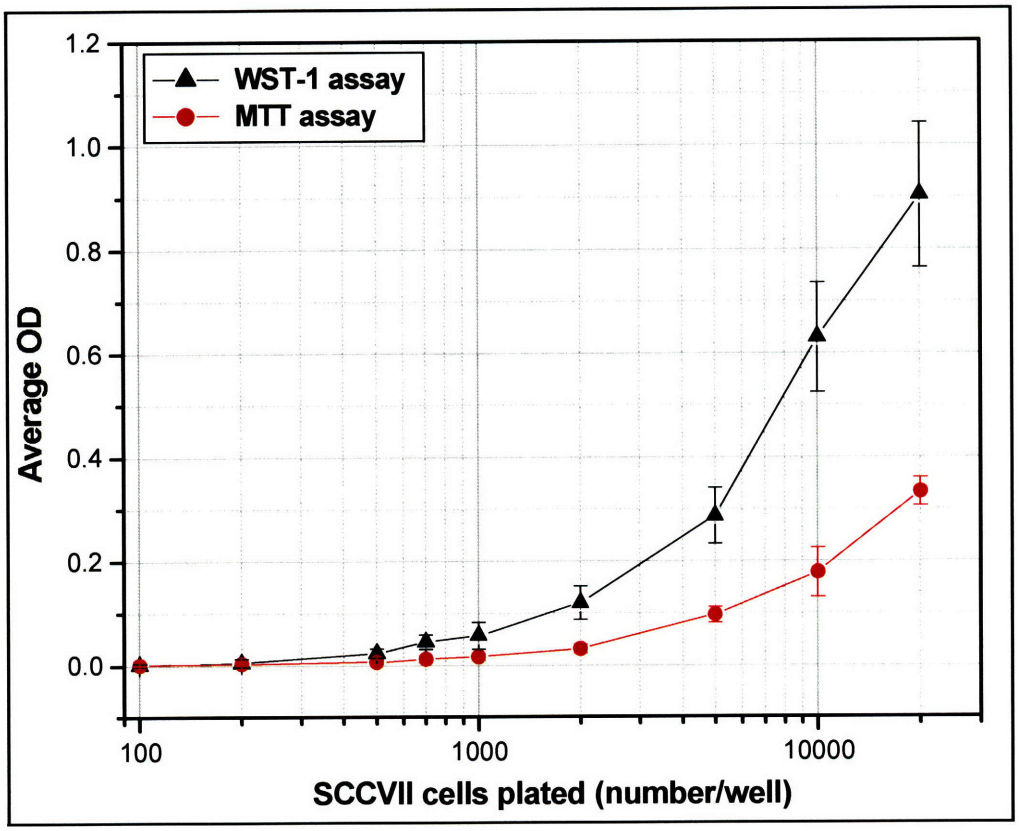

Figure 2.8. Average optical density (OD) numbers as a function of SCCVII cell number plated in one well using WST-1 and MTT assays. These OD numbers were measured right after cells were plated.

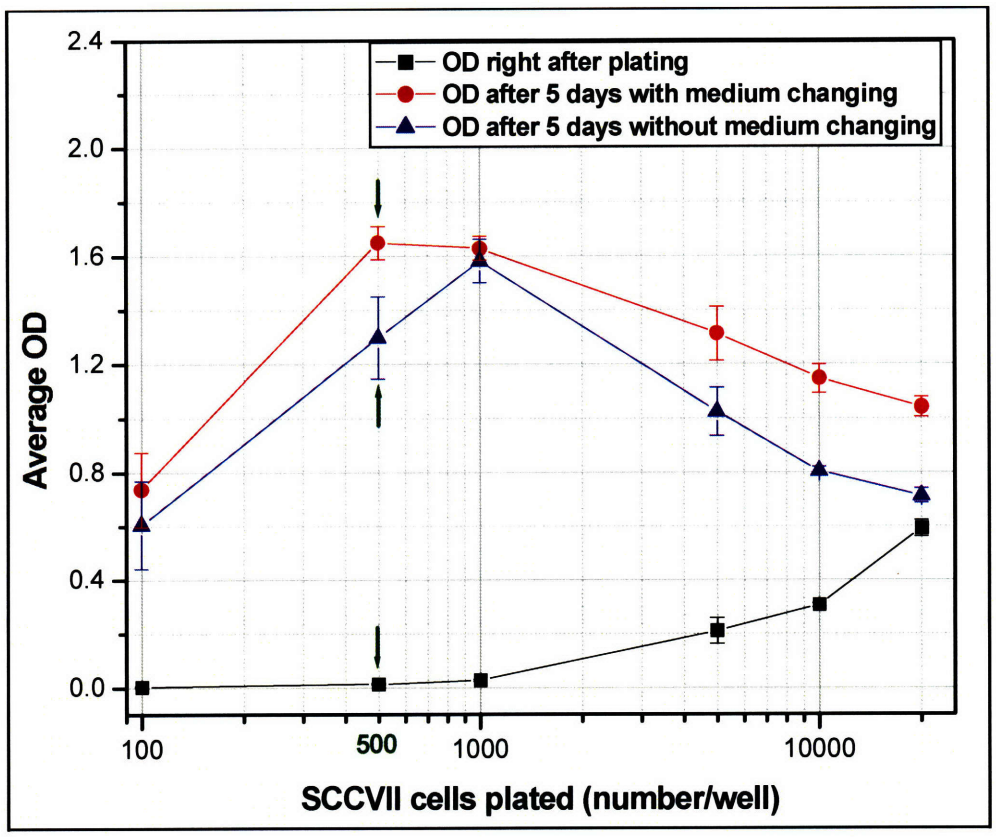

Figure 2.9. Average OD using the MTT assay as a function of SCCVII cells plated initially in each well. OD numbers were measured right after cell plating or 5 days after cell plating. Also, OD numbers were compared with medium changing at 3 days after plating or without medium changing. Arrows indicate the cell numbers in well (500 cells/well) for our protocol. Lines are drawn connecting the data to help guide the eye.

2-4-3. Cell survival experiment

A single cell suspension of SCCVII cells was prepared and the cell density was counted with the Coulter Counter. A total of 500 cells were plated in each well of the 96-well plate with 100 μl growth medium. This plating density of cells, 500 cells/well, was determined by preliminary experiments to give a useful range of OD. For neutron beam irradiation with boron compound, cells were plated in growth medium containing boron compound at the desired boron concentration. Then, plates were incubated overnight (~20 hours) to allow the cells to attach to the bottom of well. The 96-well plate was then irradiated with graded doses of thermal neutron beam or X-rays. Control plates which

received no irradiation were kept in the thermal neutron beam control room at the MITR-II or in the X-ray machine room during the experiment.

To demonstrate the study for determining efficacy of a test compound, cells were plated with boric acid for a reference, BPA for a positive control, and BOPP for a test compound. Each plate used the same boron concentration for these three boron compounds (see Figure 2.10 as an example). Boron concentrations of approximately 5, 10, 20, or 40 μg ^{10}B/ml were used in the presence or absence (blanks wells) of cells, with one plate for each concentration in each plate. Separate plates were irradiated with different neutron exposure times to produce total absorbed doses of approximately 1.7 and 3.3 Gy.

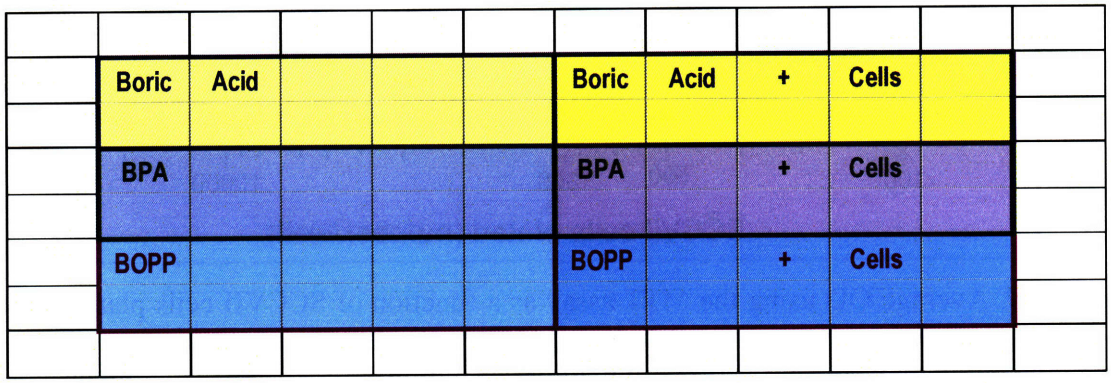

Figure 2.10. Example of experiment design in a 96-well plate for testing a new compound. Here, BOPP is the compound being tested. 10 wells contain each compound-only solution as blank (without cells) and another 10 wells contain cells together with the compound at the same concentration.

After the irradiation, plates were returned to the 37 °C incubator. After two days, 100 μl of medium was added to each well to supply enough nutrients to the growing cells. After two more days, 100 μl of medium was removed from each well being careful not to touch the bottom of the well to avoid removing any cells. Then, 10 μl of MTT reagent was added to each well. After 4 hours of incubation, 100 μl of solubilization solution was added to each well, and the plates were incubated again for ~23 hours. Finally, OD numbers were measured against a background control as blank using a microplate reader (Figure 2.11, Bio-TeK Instrument, Inc.) at 570 nm wavelength. The reference wavelength is 660 nm.

The survival was expressed as the fractional OD, which is equivalent to surviving fraction from the clonogenic assay, by the relative percentage of OD compared to non-irradiated control cells [80].

$$Fractional\ OD = \frac{OD_{irradiated} - OD_{blank(irradiated)}}{OD_{control} - OD_{blank(control)}}$$

Blank means that there are no cells, but there is medium alone or medium containing boron compound in the well.

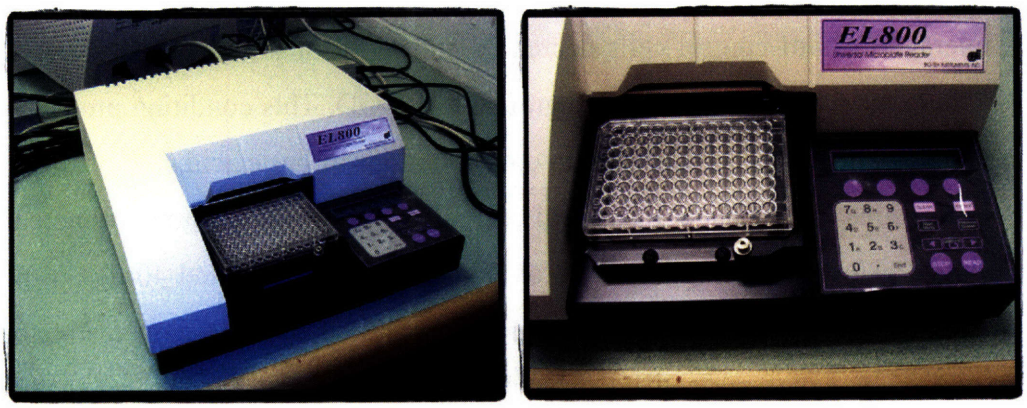

Figure 2.11. Microplate reader (EL800, Bio-Tek Instrument, Inc.) and a 96-well plate.

2-4-4. Survival curves

Figure 2.12 shows fitted survival curves for SCCVII cells irradiated with X-rays, with the neutron beam, and with the thermal neutron beam in the presence of different boron concentrations of boric acid, BPA, and BOPP with the measured boron concentrations shown in the graphs. The x-axis shows total absorbed dose which is the sum of the beam and boron doses. Boron doses were calculated from the measured boron concentration in the medium. The data represent three independent X-ray and neutron beam only experiments and a single experiment for the boron compound. Error bars indicate the relative errors with error propagation from standard deviations of OD numbers of 10-20 wells.

Like the clonogenic assay, survival curves of X-rays and the neutron beam were close due to the high fraction of photon dose component (73 %) in the neutron beam.

Neutron beam irradiations in the presence of boric acid and BPA clearly produced an additional cell killing effect. Cell survival was expected to decrease as a function of increasing boron concentration due to the increasing percentage of high-LET radiation component. Boric acid showed that cell survival decreased as boron concentration increased up to 20 μg ^{10}B/ml. Boric acid with 40 μg ^{10}B/ml produced large uncertainty because of too much cell killing from chemical toxicity. Figure 2.13 presents primary data, average OD numbers, as a function of total absorbed dose (Gy) for different boron concentrations of boric acid. These primary data were used to obtain the fractional OD by normalizing to the average OD of non-irradiated control (0 Gy) cells. Due to the chemical toxicity, average ODs of control cells decreased and those of irradiated cells were in the very low OD range which is close to background blank OD. This condition produced large estimated uncertainties for the higher boron concentrations of boric acid.

In irradiations with BPA, cell survival decreased as boron concentration increased up to 10 μg ^{10}B/ml. However, with higher boron concentrations of 20 and 40 μg ^{10}B/ml, cell survivals were similar to those of lower boron concentrations due to the overestimations of survivals caused by excessive cell kill from high boron concentrations. Due to the large uncertainty in BOPP experiments because of chemical toxicity, it is difficult to see how much effect different boron concentrations of BOPP produced to cells. The primary data for BOPP are not shown here, but a trend of decreased average OD with increasing boron concentration similar to that shown in boric acid (Figure 2.13) was observed.

The fitting coefficients of linear-quadratic equations and the goodness-of-fit for each curve are given in Tables 2.5 to 2.8. Curves of X-rays and the neutron beam showed an initial shoulder region; on the other hand, curves of neutron beam irradiations with all boron compounds showed straight lines with $\beta = 0$. The values of R^2 and P (probability) from χ^2 test were close to 1.0, demonstrating that survival curves fit the linear quadratic model well. None of the boron compounds with approximately 20 μg ^{10}B/ml fit perfectly because of overestimated survivals for higher dose points due to either chemical toxicity or the excessive cell killing.

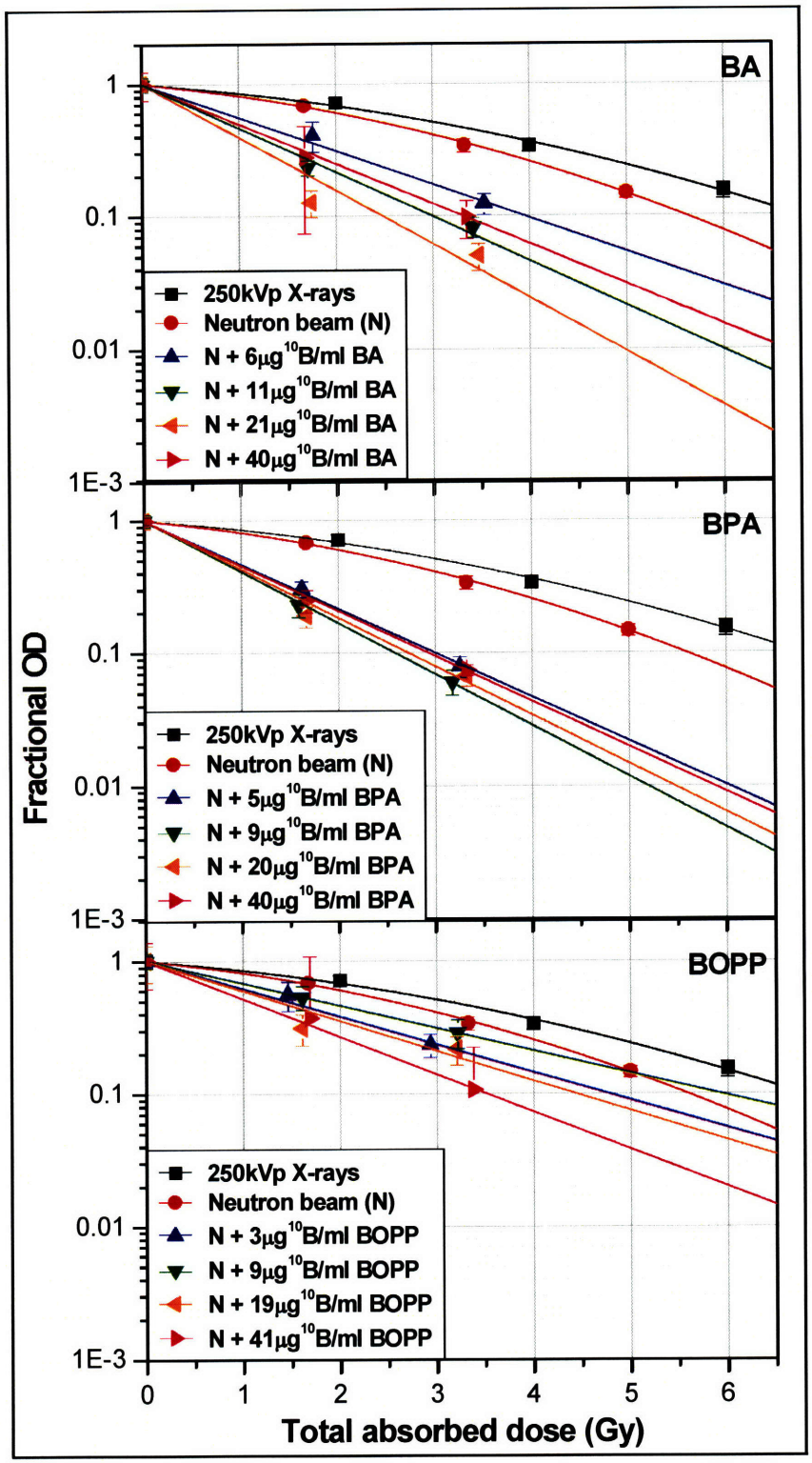

Figure 2.12. Survival curves fitted with the linear-quadratic model using the MTT ssay for SCCVII cells irradiated with 250 kVp X-rays, the thermal neutron beam, and the thermal neutron beam in the presence of boric acid (BA), BPA, and BOPP with increasing boron concentrations. The fractional OD of cells is plotted on a log scale against total absorbed dose on a linear scale. Curves for compounds were fitted up to ~3.5 Gy and extrapolated beyond that dose.

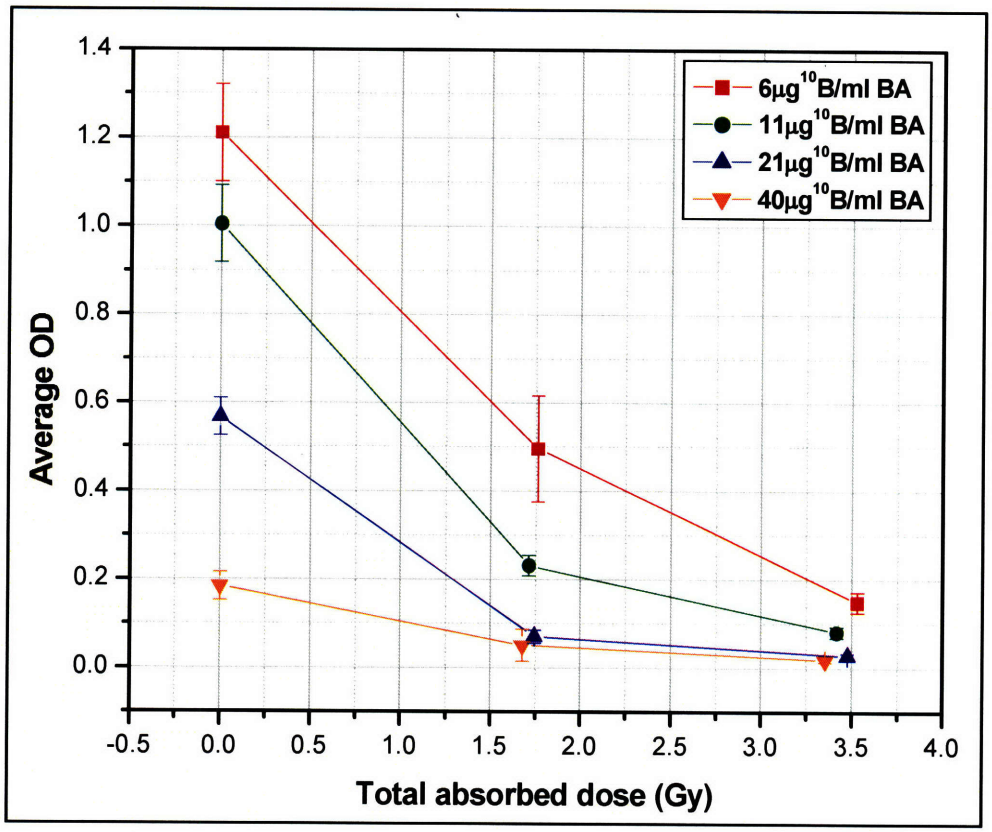

Figure 2.13. Average OD measured after 5 days of growth time using the MTT assay as a function of total absorbed dose (Gy) for the SCCVII cells irradiated with the neutron beam in the presence of boric acid (BA) at different boron concentrations. Lines are drawn connecting the data to help guide the eye.

Table 2.5. Fitting coefficients (α and β) for the linear-quadratic model and goodness-of-fit (R^2 and χ^2) for X-rays and neutron beam irradiations using the MTT assay.

Radiation	SF = exp (- αD - βD^2)		Goodness-of-fit	
	α	β	R^2	χ^2
X-rays	0.128 ± 0.032	0.031 ± 0.006	0.9952	0.0028 (p=1.0)
Neutron beam (N)	0.162 ± 0.017	0.045 ± 0.004	0.9994	0.0009 (p=1.0)

Table 2.6. Fitting coefficients (α and β) for the linear-quadratic model and goodness-of-fit (R^2 and χ^2) for neutron beam irradiations with 6, 11, 21, and 40 μg ^{10}B/ml boric acid (BA) using the MTT assay.

Radiation	SF = exp (- αD - βD^2)		Goodness-of-fit	
	α	β	R^2	χ^2
N + 6 μg ^{10}B/ml BA	0.585 ± 0.178	0	0.9946	0.0078 (p=0.9998)
N + 11 μg ^{10}B/ml BA	0.770 ± 0.041	0	0.9736	0.0062 (p=0.9999)
N + 21 μg ^{10}B/ml BA	0.930 ± 0.111	0	0.9171	0.6581 (p=0.8830)
N + 40 μg ^{10}B/ml BA	0.697 ± 0.012	0	0.9979	0.0039 (p=0.9999)

Table 2.7. Fitting coefficients (α and β) for the linear-quadratic model and goodness-of-fit (R^2 and χ^2) for neutron beam irradiations with 5, 9, 20, and 40 μg ^{10}B/ml BPA using the MTT assay.

Radiation	SF = exp (- αD - βD^2)		Goodness-of-fit	
	α	β	R^2	χ^2
N + 5 μg ^{10}B/ml BPA	0.764 ± 0.014	0	0.9991	0.0010 (p=0.9999)
N + 9 μg ^{10}B/ml BPA	0.888 ± 0.013	0	0.9990	0.0007 (p=1.0)
N + 20 μg ^{10}B/ml BPA	0.843 ± 0.054	0	0.9556	0.5744 (p=0.9023)
N + 40 μg ^{10}B/ml BPA	0.784 ± 0.009	0	0.9988	0.0016 (p=1.0)

Table 2.8. Fitting coefficients (α and β) for the linear-quadratic model and goodness-of-fit (R^2 and χ^2) for neutron beam irradiations with 3, 9, 19, and 41 μg ^{10}B/ml BOPP using the MTT assay.

Radiation	SF = exp (- αD - βD^2)		Goodness-of-fit	
	α	β	R^2	χ^2
N + 3 μg ^{10}B/ml BOPP	0.483 ± 0.021	0	0.9958	0.0077 (p=0.9998)
N + 9 μg ^{10}B/ml BOPP	0.389 ± 0.001	0	0.9999	0.00001 (p=1.0)
N + 19 μg ^{10}B/ml BOPP	0.517 ± 0.076	0	0.6359	0.3484 (p=0.9507)
N + 41 μg ^{10}B/ml BOPP	0.652 ± 0.013	0	0.9993	0.0052 (p=0.9999)

2-4-5. Toxicity

To investigate further the large uncertainty in the survival curves for boric acid and BOPP using the MTT assay, the chemical toxicity of these two boron compounds was determined by OD numbers for SCCVII cells incubating with increased boron concentrations for 5 days without any irradiation involved. Figure 2.14 illustrates that the toxicity of boric acid and BOPP increases as the boron concentration increases. This explains why the observed OD numbers for the non-irradiated control cells with boric acid and BOPP were very low after 5 days of growth time (see Figure 2.13). Five days incubation time was necessary to allow measurable growth (OD) in the irradiated cells. OD numbers of a blank reference of BOPP solution (without cells) show a slight increase as the boron concentration increased (Figure 2.14). OD numbers of cells in higher boron concentrations of boric acid or BOPP (40 μg ^{10}B/ml) are very low and similar to the OD number of the blank, compound-only solution. This is the reason the survival fractions for higher concentrations of boric acid and BOPP had very large uncertainty and were overestimated: even without irradiation there was very little cell growth due to the chemical toxicity, and thus, very little OD signal remained to measure the radiation effects. This chemical toxicity information was taken account into surviving curves when normalizing average OD numbers of irradiated cells with those of non-irradiated cells.

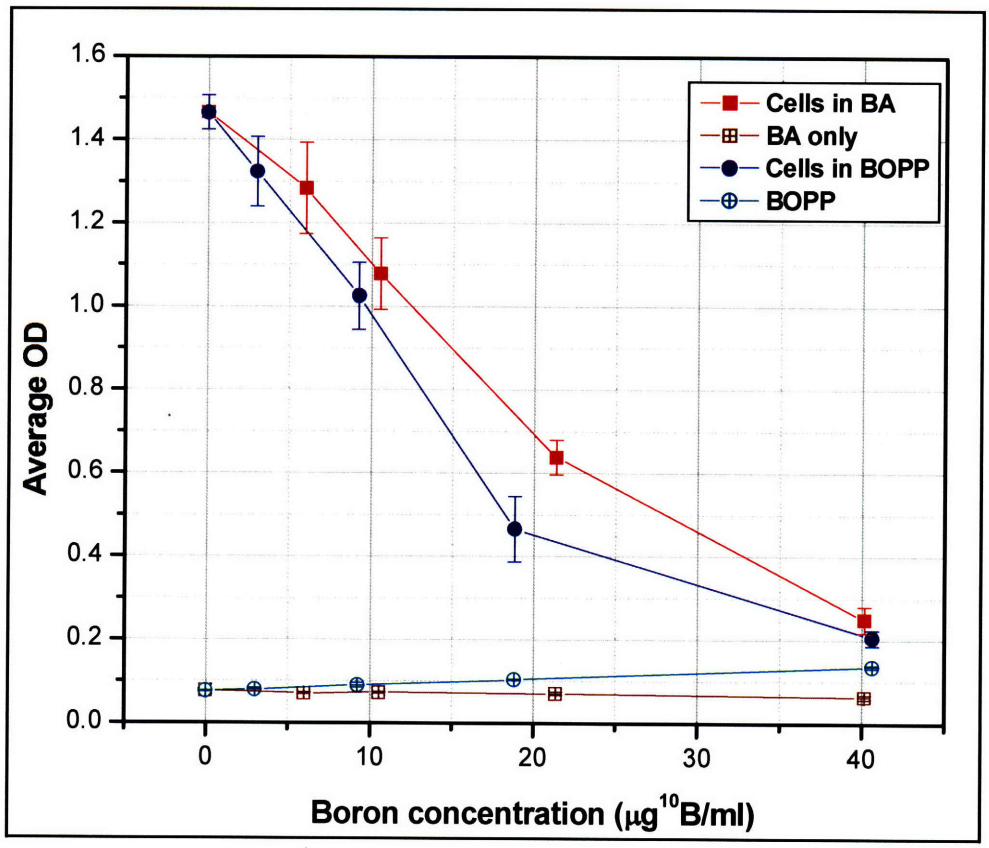

Figure 2.14. Average OD numbers for SCCVII cells using the MTT assay as a function of boron concentration with boric acid (BA), and BOPP measured 5 days after cell plating. OD numbers were measured for wells containing cells in boron solution or for wells containing only boron solution. Lines are drawn connecting the data to help guide the eye.

2-4-6. Calculation of RBE and CBE with uncertainty analysis

Tables 2.9 to 2.12 show the doses with estimated uncertainties at surviving fraction of 0.2 for X-rays, neutron beam, and neutron beam in the presence of boron compound. A surviving fraction of 0.2 was chosen since the MTT assay could measure only fractional survivals in the range of the first two logs (SF > 0.01). The values for the RBE of the neutron beam and the CBE factor of each boron compound with estimated uncertainty are also presented in these tables. Total uncertainties of 4.6 % for X-rays dose, 6.1 % for neutron beam dose, and 7.8 % for boron dose were estimated with the MTT assay. The beam RBE was 1.2 ± 0.1 for SCCVII cells at surviving fraction of 0.2. This RBE value is similar to that derived from the clonogenic assay and is close to 1 due to the high fraction of photon dose (73 %) in the neutron beam.

The uncertainties determined by combining the averaged fitting uncertainty together with dose measurement uncertainty do not accurately represent the uncertainties for the points where cell killing is too high due to either chemical toxicity or high boron capture reaction. The low CBE value at 40 μg ^{10}B/ml from boric acid is due to overestimated survival resulting from the high chemical toxicity. For 20 and 40 μg ^{10}B/ml of BPA, the CBE factors were lower because of excessive cell killing. The test compound, BOPP, showed low CBE values at high boron concentration from 10 to 40 μg ^{10}B/ml since the chemical toxicity is dominant to cell killing. These conditions identify a useful boron concentration, 5-10 μg ^{10}B/ml, for *in vitro* evaluation. The derived results with underestimated uncertainty are not statistically meaningful, so they are shaded in Tables 2.10 to 2.12.

Table 2.9. Interpolated doses and RBE at surviving fraction of 0.2 for X-rays, the neutron beam using the MTT assay.

Radiation	Dose (Gy)	RBE
X-rays	5.4 ± 0.3	
Neutron beam (N)	4.5 ± 0.3	1.2 ± 0.1

Table 2.10. Interpolated doses and CBE at surviving fraction of 0.2 for the neutron beam with different concentrations of BA using the MTT assay. Shaded results have uncertainties that are underestimated due to excessive cell killing and they are not considered statistically meaningful.

Radiation	Dose (Gy)	CBE
N + 6 μg ^{10}B/ml BA	2.8 ± 0.2	3.5 ± 0.5
N + 11 μg ^{10}B/ml BA	2.1 ± 0.1	4.1 ± 0.4
N + 21 μg ^{10}B/ml BA	1.7 ± 0.1	4.2 ± 0.4
N + 40 μg ^{10}B/ml BA	2.3 ± 0.2	2.7 ± 0.3

Table 2.11. Interpolated doses and CBE at surviving fraction of 0.2 for the neutron beam with different concentrations of BPA using the MTT assay. Shaded results have uncertainties that are underestimated due to excessive cell killing and they are not considered statistically meaningful.

Radiation	Dose (Gy)	CBE
N + 5 μg ^{10}B/ml BPA	2.1 ± 0.1	6.1 ± 0.7
N + 9 μg ^{10}B/ml BPA	1.8 ± 0.1	5.3 ± 0.6
N + 20 μg ^{10}B/ml BPA	1.9 ± 0.1	3.8 ± 0.4
N + 40 μg ^{10}B/ml BPA	2.1 ± 0.2	3.1 ± 0.3

Table 2.12. Interpolated doses and CBE at surviving fraction of 0.2 for the neutron beam with different concentrations of BOPP using the MTT assay. Shaded results have uncertainties that are underestimated due to excessive cell killing and they are not considered statistically meaningful.

Radiation	Dose (Gy)	CBE
N + 3 μg ^{10}B/ml BOPP	3.3 ± 0.2	3.3 ± 0.7
N + 9 μg ^{10}B/ml BOPP	4.1 ± 0.3	1.4 ± 0.2
N + 19 μg ^{10}B/ml BOPP	3.1 ± 0.2	2.1 ± 0.2
N + 41 μg ^{10}B/ml BOPP	2.5 ± 0.2	2.5 ± 0.2

The CBE values with the same compound at different boron concentrations (approximately 5, 10, and 20 μg ^{10}B/ml) using the MTT assay are shown in Figure 2.15. The CBE factors for a given compound were not statistically significantly different with different boron concentrations for boric acid and BPA. CBE factor should be independent of boron concentration for each boron compound since CBE is normalized to the boron dose component.

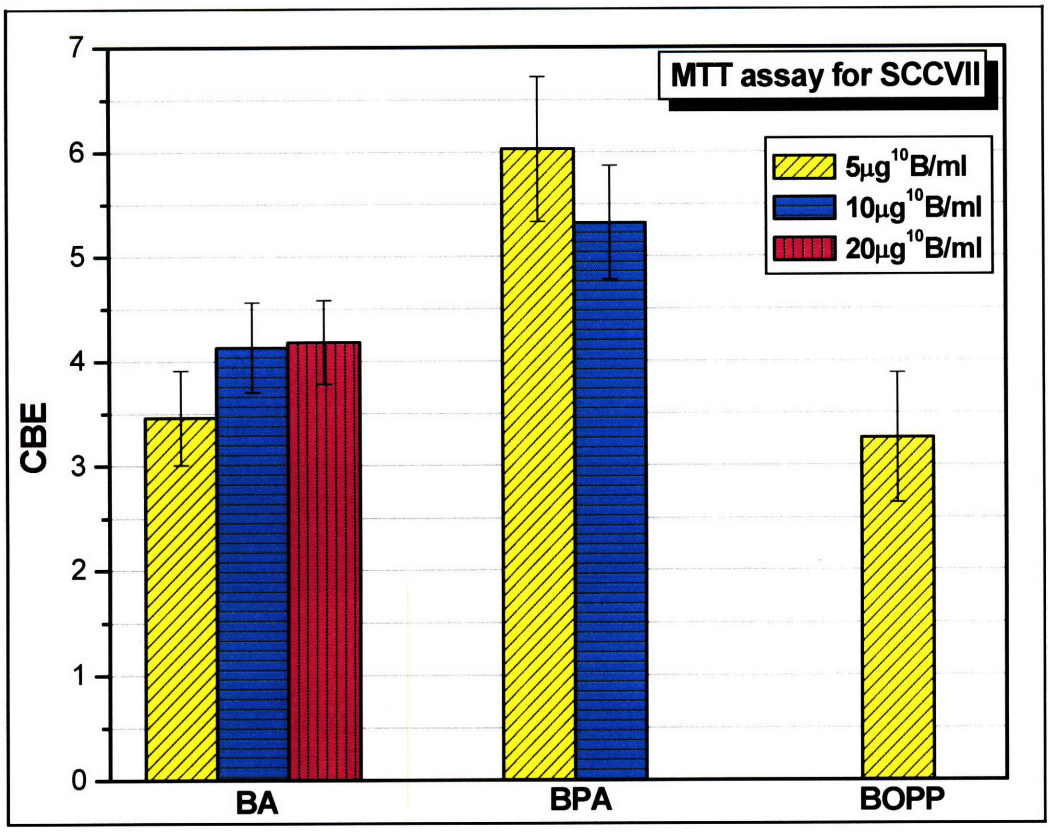

Figure 2.15. The CBE values for boric acid (BA), BPA, and BOPP at 5, 10, and 20 μg ^{10}B/ml using the MTT assay. This graph compares the CBE values of different boron concentrations for each boron compound.

2-4-7. Evaluation of a test compound

A direct comparison of survival at the same total absorbed dose is another approach to compare the efficacy of a boron compound at the same boron concentration. Figure 2.16 plots survival curves for SCCVII cells irradiated with the thermal neutron beam in the presence of boric acid, BPA, and BOPP with approximately equivalent boron concentrations so as to directly compare the radiation induced effects of the different boron compounds. Gray arrows point to the survivals (fractional OD) for each boron compound with the same boron concentration at the same total absorbed dose of 3 Gy which is chosen as a suitable dose point. At a total absorbed dose, 3 Gy, higher survival was observed from the test compound, BOPP, than the reference compound, boric acid, which indicates that the test compound is less effective than boric acid and it does not accumulate preferentially inside the SCCVII cells. The BPA, serving as a positive control due to the known ability to accumulate inside cells showed a lower survival than boric acid.

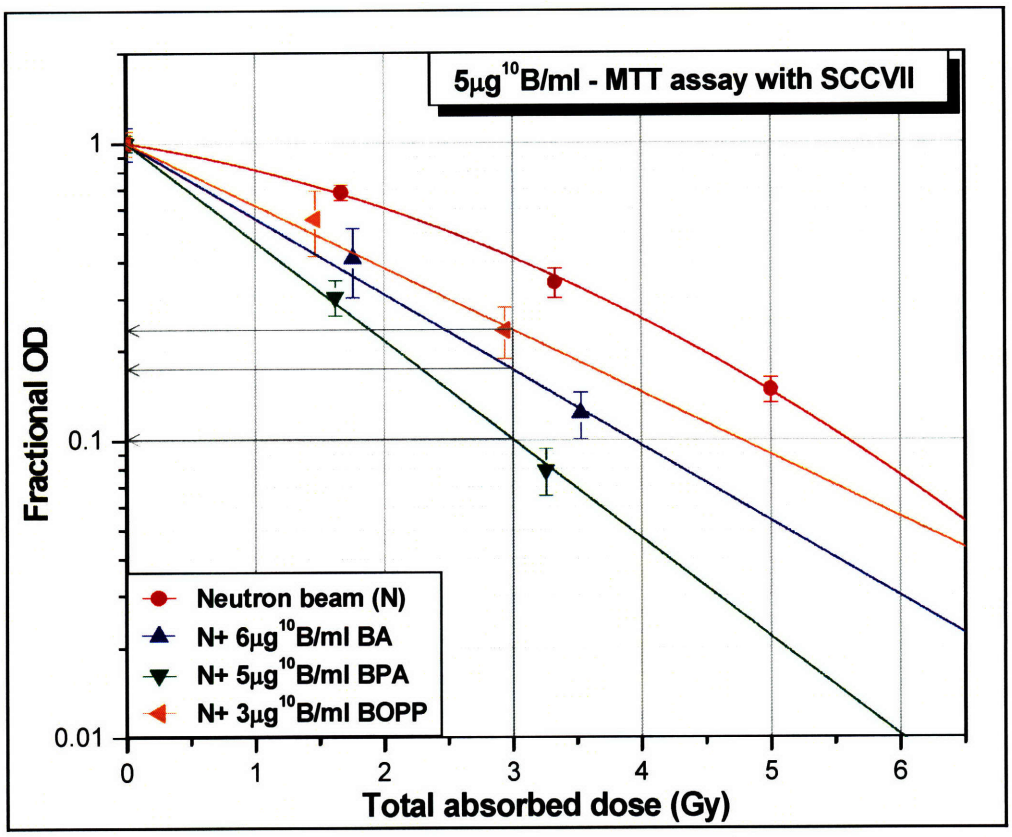

Figure 2.16. Survival curves using the MTT assay for SCCVII cells irradiated with the neutron beam and with the neutron beam in the presence of boric acid (BA), BPA, and BOPP. Graphs are represented with approximately the same boron concentration (5 μg ^{10}B/ml) from three different compounds. Gray arrows indicate survivals (fractional OD) for each compound at total absorbed dose of 3 Gy.

The efficacy of the test compound, BOPP, was also evaluated by comparing CBE factors with those of boric acid and BPA at the same boron concentration. As described in the previous section, CBE factors for higher boron concentration of these boron compounds were underestimated due to the chemical toxicity or the excessive cell killing. Thus, CBE values of these compounds with 5 μg ^{10}B/ml were analyzed. Figure 2.17 shows a significantly larger CBE value (6.1 ± 0.7) from BPA than those of boric acid and BOPP. The comparable CBE values of boric acid and BOPP (3.5 ± 0.5 and 3.3 ± 0.7, respectively) indicate that BOPP has similar biological effectiveness with boric acid and does not preferentially accumulate in the SCCVII cells.

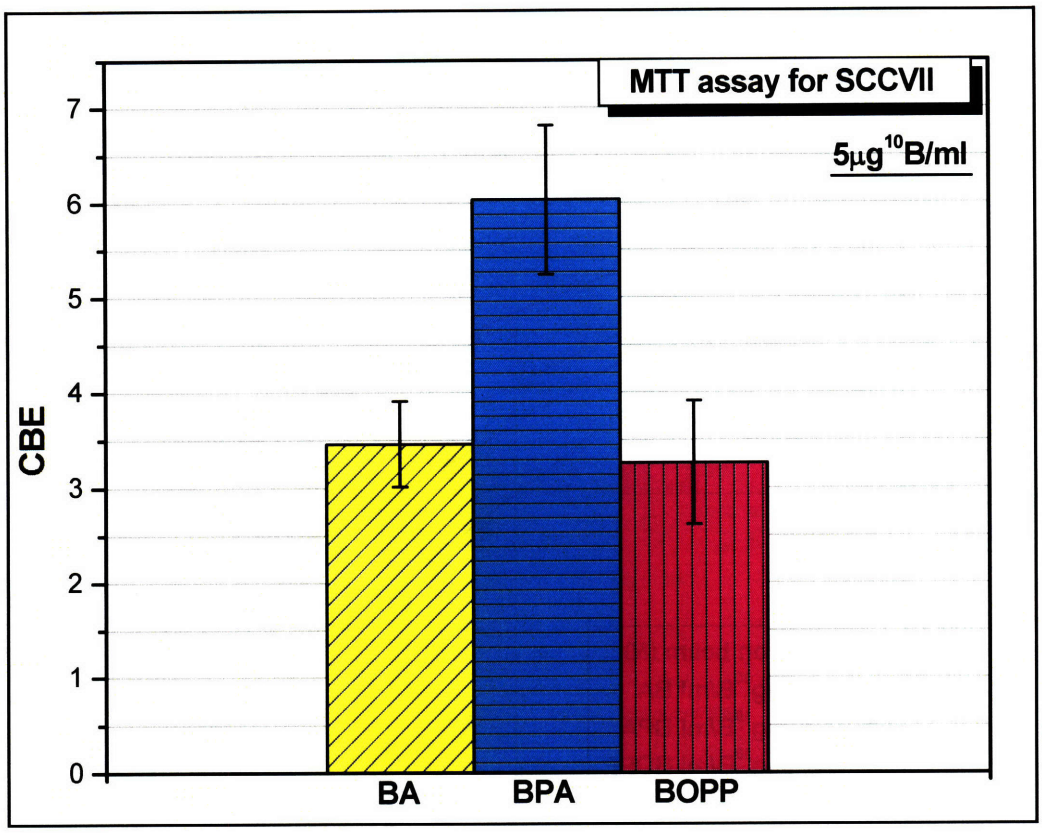

Figure 2.17. The CBE values for boric acid (BA), BPA, and BOPP at 5 μg ^{10}B/ml using the MTT assay.

2-5. Comparison between clonogenic and colorimetric assays

Figures 2.18 and 2.19 compare survival curves (fractional OD) from the colorimetric (WST-1 and MTT) assay to the survival curves for clonogenic assay for SCCVII cells irradiated with 250 kVp X-rays and with the thermal neutron beam only, respectively. Initial optimization experiments were focused on producing good agreement between WST-1 and clonogenic assays, and so experimental conditions of 100 cells/well (for 2 and 4 Gy of X-rays and 1.7 and 3.3 Gy of neutron beam) or 200 cells/well (for 6 Gy of X-rays and 5 Gy of neutron beam) with 5 days growth time were used for the WST-1 assay. The WST-1 and clonogenic assays showed good correlation up to 6 Gy from X-ray irradiation (Figure 2.18). When the same protocol used for the WST-1 assay was applied to thermal neutron beam irradiations, however, surviving fraction from the WST-1 assay was much

higher than from the clonogenic assay (Figure 2.19). Since the thermal neutron beam consists partly of high-LET radiations, overestimated survivals may result from insufficient cells in each well or a longer cell growth delay caused by high-LET radiation. Experimental conditions such as cell density and the growth time for each dose point could be optimized for agreement between the two different assays. In these figures, the protocol for the MTT assay used a cell density of 500 cells/well with 5 days of growth time, which was not optimized for making it agree with the clonogenic assay but rather for examining the effects of boron compounds.

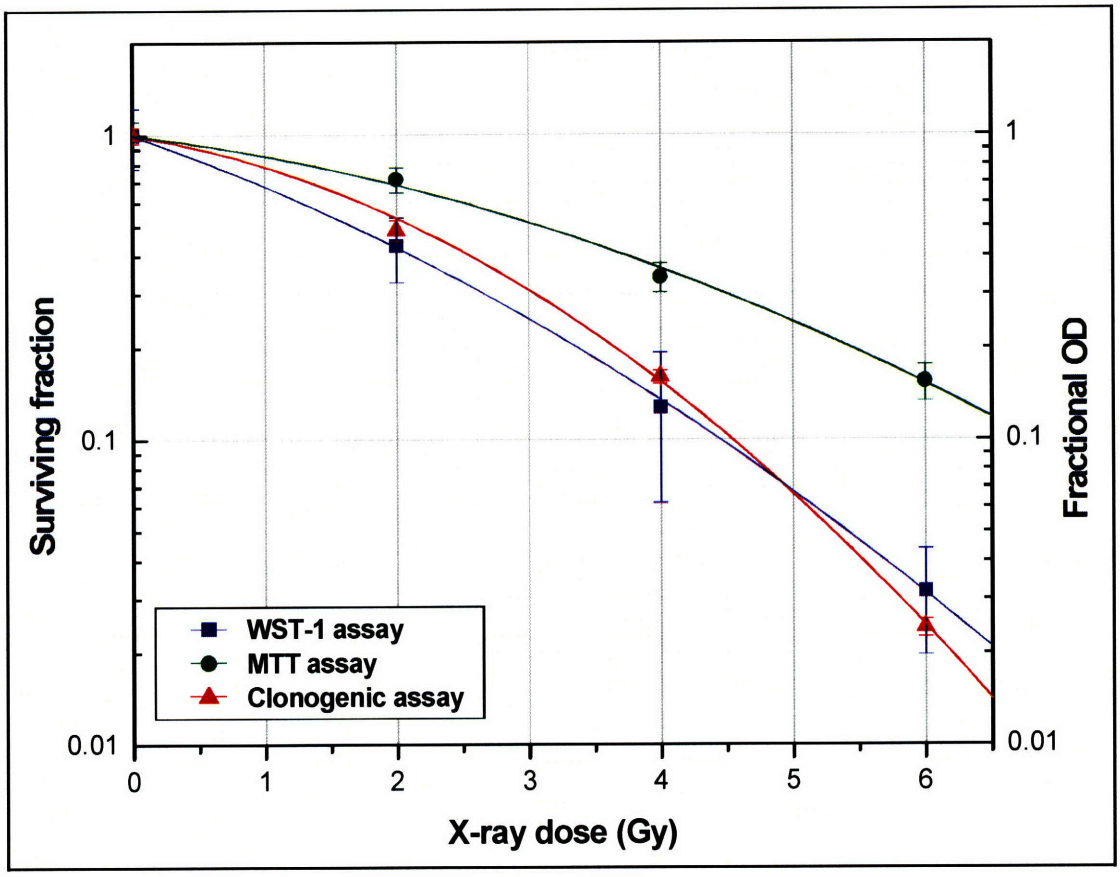

Figure 2.18. Survival curves fitted with the linear-quadratic model using the colorimetric (WST-1 and MTT) and clonogenic assays for SCCVII cells irradiated with 250 kVp X-rays.

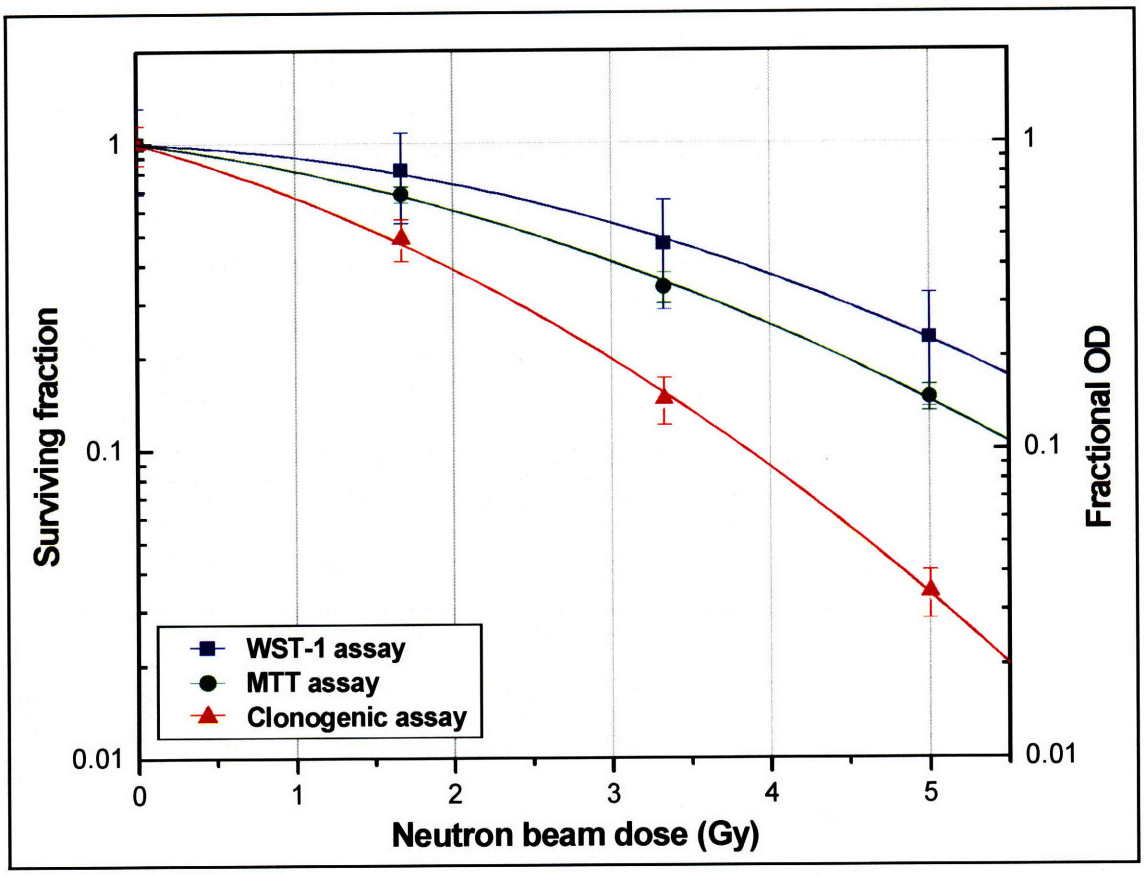

Figure 2.19. Survival curves fitted with the linear-quadratic model using the colorimetric (WST-1 and MTT) and clonogenic assays for SCCVII cells irradiated with the thermal neutron beam.

2-6. Discussion

The clonogenic assay is generally considered to be the well-accepted standard to test radiosensitivity of the proliferating tumor cells by directly measuring the reproductive integrity of individual cells. Despite its worldwide use in basic research, the clonogenic assay has some disadvantages. It takes a long time, around 2 weeks to allow colonies to grow to the size needed for counting. There is also no standard in colony counting procedures, and manual counting of colonies can therefore be subjective and time consuming. Moreover, this method is difficult to apply to cell lines with very low plating efficiency. The number of cells initially plated in a Petri dish is critical for obtaining accurate results when counting the number of colonies. For example, if too many live cells

are plated, the numbers of colonies are impossible to count due to overlapping colonies. Or, at very low cell densities, cells cannot form colonies well and counting statistics are poor. When testing a new compound with an unknown boron effect, the number of cells to initially plate cannot be practically predicted and experiments must often be repeated to get the best results. This limiting factor requires more quantity of boron compound to be tested.

When evaluating new compounds which may only be available in small amounts at the early stages of their development, the quantity of testing boron compound is a critical factor for developing the evaluation method. In the initial geometry for the clonogenic assay, when flasks were filled with medium because they were up-side down in the beam, 43 ml of medium was necessary to completely fill a T12.5 flask. If 10 μg ^{10}B/ml of boron concentration is used for testing, 430 μg ^{10}B is needed in each flask. Eight flasks irradiated with 4 graded doses will require 3.5 mg ^{10}B, and it is frequently not feasible to produce this much compound for preliminary *in vitro* tests. With the optimized setup using upright flasks and 1 ml of medium, only 80 μg ^{10}B is needed for 8 flasks. However, 8 flasks might not be enough for 4 graded doses. For example, if the survival of cells exposed with a large radiation dose mainly from boron dose is reduced by three logs (SF = 10^{-3}), at least four T12.5 flasks are required to plate enough cells in the Petri dishes for counting. Therefore, a few hundred micrograms of boron would be needed for the clonogenic assay. If the data from this experiment proves insufficient for any reason (such as low cell plating, contamination), then further experiment would be required to complete the survival curve which in turn would require more compounds.

The colorimetric assay uses 96-well plates which need 100 μl of medium per well. Again using 10 μg ^{10}B/ml, the colorimetric assay needs only 40 μg ^{10}B when 10 wells are used for one boron compound in 4 different plates to give 4 graded doses as with the clonogenic assay. For initial testing a new compound which has an unknown characteristics, this assay is capable of identifying at least some measurable boron effect from cell irradiations as well as determining chemical toxicity with this small quantity. Besides using a very small quantity of boron, the MTT assay has several advantages over the clonogenic assay. It is a semi-automated method which rapidly and objectively assesses the number of viable cells using a microplate reader. Since several boron compounds can be tested in one

96-well plate, it saves a lot of time in the entire experiment and especially in the use of neutron beams. Also, it can be applied to cell lines which have very low plating efficiency.

However, the colorimetric assay has serious limitations. A measurable OD from the MTT assay is between ~0.02 and 3.0, which means that the right amount of cell growth must be obtained to produce a reasonable OD. Approximately 5 days of growth time is required for SCCVII cells after an irradiation, but this may be different for other cell lines with different cell cycle delay and proliferation inhibition [81]. Non-irradiated control cells have to be still in the measurable OD range at the time of assay and this limits the number of cells initially plated, which is 500 cells/well for SCCVII cells. This limited number of cells means that the total absorbed dose (beam + boron dose) is also limited to low levels (< ~3 Gy) as well as the boron concentration to avoid killing too many cells and making the OD too low. Also, during growth time, cells are exposed to the boron compound and so chemical toxicity can mask the effects of radiation damage. A long exposure to compounds with high toxicity like boric acid and a test compound, BOPP, results in very low OD numbers that are difficult to discern accurately from background OD level, producing very large uncertainties on the resulting fractional OD.

Since growth delay from radiation damage varies with cell line, the colorimetric assay requires considerable effort to optimize a standard protocol for each cell line, especially the number of cells initially plated in each well, growth time, and practical range of doses including useful boron concentration. Possible improvements to the colorimetric assay, that would separate curves further (statistically significantly) include changing the medium after irradiation to avoid toxic effects from the compound and increasing the growth time to be able to accurately measure OD after higher radiation doses.

Some reports have shown good correlation in direct comparison between MTT colorimetric and clonogenic assays for determining chemosensitivity [81-83] or radiosensitivity [69, 80, 84, 85]. After lengthy optimization of the protocol of X-ray irradiation, WST-1 and clonogenic assay showed comparable survival curves (see Figure 2.18). However, when the same protocol was applied to neutron beam irradiations, the survival curves showed significant differences between two techniques. Since the purpose of applying this colorimetric assay is to establish a simple and efficient method for compound screening, it was decided not to develop this protocol to get good agreement but

instead to observe if the presence of boron was having an effect. The colorimetric assay is perfectly capable of useful boron compound screening, without such optimization to agree with clonogenic assay data.

This colorimetric assay was chosen as an initial testing since it could facilitate a simpler and more efficient method of compound evaluation for determining chemical toxicity and relative intracellular uptake of compounds using very small quantity which would be only a few hundred micrograms of ^{10}B. Thus, boronated porphyrin, BOPP was tested as an example for the usefulness and practicality of the colorimetric assay. In this chapter, the clonogenic assay could not be used to evaluate BOPP because of insufficient quantity.

Survival data were fitted to the widely-accepted linear-quadratic model in order to describe radiation sensitivity of cells with a simple equation [86]. Only two parameters are used to simulate the basic mechanism of cell killing; a lethal double-stranded break in the DNA. Most damage from high-LET radiation is lethal and the quadratic component becomes zero. Thus, a survival curve of high LET-radiation presents simply as an exponential function. Since a linear-quadratic model is practical to represent survival data in the first two decades of cell killing, this model described cell survival well, especially the MTT assay which had most surviving fractions in the first two decades [67]. Also, this model with only two parameters helped to accurately interpolate dose and reduced the extent of uncertainty on the calculations of RBE and CBE. As there were only 3-4 survival points for each irradiation, survival curves fit the linear-quadratic model well.

Cell irradiations in the presence of a reference compound, boric acid, exhibited decreased cell survival with increasing boron concentration using the clonogenic assay and this trend also apparent with MTT assay up to 20 μg ^{10}B/ml. Boric acid accumulates in the cells by diffusion and the boron concentration inside cells therefore increases with increased boron concentration in the medium. This 1:1 ratio of intracellular/extracellular boron concentration was proven for GS-9L rat gliosarcoma [71] and was assumed to also hold for SCCVII cells. At 40 μg ^{10}B/ml, the chemical toxic effects of boric acid became too large to obtain statistically meaningful results with the MTT assay.

BPA, a positive control compound, showed more cell-killing than boric acid at the same boron concentration and this indicates that BPA is preferentially accumulated in the

cells. This was shown also in the boron accumulation study for BPA with several tumor cell lines [71]. With the MTT assay, survival curves using BPA at 5 and 10 μg ^{10}B/ml showed a slight increased effect with increasing boron concentration; however, with 20 and 40 μg ^{10}B/ml BPA, this tendency was not observed. The extremely high boron dose seems to kill most of plated cells (which for the MTT assay is fixed at 500 cells/well) and this resulted in very low OD numbers causing an overestimation of cell survival for high boron concentration. Therefore, the choice of a useful boron concentration in the medium is approximately 5-10 μg ^{10}B/ml for any boron compound to be tested using the MTT assay.

Comparing the survival curve of a test compound with those for boric acid is an indirect estimation of the intracellular boron accumulation and a test compound, BOPP, showed non-selective accumulation inside SCCVII cells. *In vitro* study by others with BOPP reported that it entered human glioma cells through the low density lipoprotein pathway [87]. The survival curves using the MTT assay with BOPP were not distinguishable from each other especially considering the error bars and this agrees with literature report that similar amounts of BOPP may be present in the cells during irradiations regardless of the BOPP concentration in the medium [87]. Also, the survival with BOPP was similar to that of boric acid at the same concentration especially considering the estimated uncertainties as was reported in studies using V79 Chinese hamster ovary cells [61]. Cytotoxicity experiments for rat C6 glioma cells proved that BOPP was toxic [88], which agrees with our toxicity observation for SCCVII cells.

The mixture of different-LET radiations during BNCT has different effectiveness in biological systems. In order to quantitatively compare the efficacy of different types of radiation, the neutron beam RBE relative to 250 kVp X-rays was determined. Thus, the RBE of 250 kVp X-rays is defined as 1. The RBE of the neutron beam including the high-LET components for SCCVII cells was 1.1 ± 0.1 at surviving fraction of 0.02 using the clonogenic assay and 1.2 ± 0.1 at surviving fraction of 0.2 using the MTT assay. A higher surviving fraction of 0.2 was chosen for the colorimetric assay since the dynamic range of this assay was limited. This value agreed with the beam RBE (1.2 ± 0.1) from previous small animal experiments with rat lung irradiation at the thermal neutron beam of the MITR-II [89]. The RBE varies mostly from quality of radiation, types of biological system, and the chosen biological endpoint. Thus, the RBE values are different for neutron beams

that have different beam characteristics. The RBE of the BMRR beam for example was 2.6 for 9L gliosarcoma cells, and this high RBE mainly resulted from a high percentage (43 %) of fast neutron dose component in the neutron beam [62].

The CBE factor was introduced to quantitatively compare the biological efficacy of different boron compounds. The CBE, also, depends on characteristics of the boron compound, types of biological system, and a given biological endpoint. Especially, microscopic distribution of boron in the cell primarily affects CBE factor due to the short ranges of particles produced by the boron neutron capture reaction. As there is no straightforward and reliable method to measure intracellular boron concentration at the time of irradiation *in vitro*, the boron dose component is calculated using the boron concentration measured in the growth medium. A CBE value of a test compound larger than that of boric acid can be interpreted as preferential intracellular accumulation relative to the boron concentration in the medium.

The CBE values of a particular boron compound did not vary statistically significantly for different boron concentrations using both clonogenic and colorimetric assays. Thus, the average CBE value of boric acid from different boron concentrations is 2.8 ± 0.2 at a surviving fraction of 0.02 for the clonogenic assay (5-10 μg ^{10}B/ml) and 3.9 ± 0.3 at a surviving fraction of 0.2 for SCCVII cells using the MTT assay (5-20 μg ^{10}B/ml). BPA showed a significantly higher average CBE, 5.7 ± 0.4, at a surviving fraction of 0.2 using the MTT assay (5-10 μg ^{10}B/ml), which verifies that BPA can more accumulate inside SCCVII cells. This larger CBE value of BPA than that of boric acid was also reported in the study of 9L gliosarcoma cell irradiation with the neutron beam of the BMRR (RBE = 2.6) [62]. The CBE values was 3.4 for boric acid (at a surviving fraction of 0.1 and 0.01) and 9.8 (at surviving fractions of 0.1) for BPA using the clonogenic assay [62].

The uncertainty analysis for CBE value has not been comprehensively investigated during *in vitro* and *in vivo* studies for BNCT. In this chapter, the uncertainty analysis was started with calculating the fitting uncertainty of interpolated dose using the standard errors of the fitting coefficients (α and β). These fitting uncertainties were averaged for each assay (2.8 % for the clonogenic assay and 3.5 % for the MTT assay) and combined with the dosimetry measurement uncertainty (3 % for X-rays, 5 % for neutron beam, and 7 % for

boron). Total uncertainties on the interpolated dose at the endpoint were estimated to be 4 % and 4.6 % for X-rays, 5.7 % and 6.1 % for the neutron beam, 7.5 % and 7.8 % for boron using the clonogenic and MTT assays, respectively. The uncertainty of beam RBE was approximately 7 % for the clonogenic and MTT assays. The estimated uncertainties of CBE for the 5 and 10 μg ^{10}B/ml were ~12 % for boric acid, ~11 % for BPA, and ~18 % for BOPP. Relatively large uncertainties of CBE cause difficulty in precisely comparing the efficacy of a test compound to those of boric acid and BPA. This large uncertainty also indicates that investigators should be very careful when a general CBE factor is applied to another study for the same endpoint using a different biological system (e.g. humans). This large uncertainty must be recognized as a major source of experimental error especially for a study in which the dose-response relationship is steep and a slightly different dose would cause a large change in outcome.

An alternative approach to compare the efficacy of each boron compound can be considered due to the large uncertainty of CBE obtained by comparing with X-ray irradiation. Since boric acid is used as a reference boron compound, the efficacy of a test compound can be directly compared with that of boric acid at the same boron concentration. For this, a new parameter (C) which is defined as 1 for boric acid can be introduced in the following equation.

$$\begin{aligned}&(Dose_{Beam})_{BA}\times(RBE)+(Dose_{Boron})_{BA}\times(1)\\&=(Dose_{Beam})_{testing\ compound}\times(RBE)+(Dose_{Boron})_{testing\ compound}\times(C)\end{aligned}$$

Using this relation, if a test compound produces this new parameter (C) larger than 1 like BPA (2.2 ± 0.2), this test compound is more effective than boric acid. The new parameter of the test compound, BOPP is less than one, indicating that BOPP is not as effective as boric acid. This "effectiveness" can be also interpreted as relative intracellular accumulation compared with the boron concentration in the medium.

In conclusion, the optimized *in vitro* compound screening includes:

1) identifying the chemical toxicity of a new compound using the MTT assay,

2) determining boron effects from cell irradiation in the presence of a test compound compared with boric acid and BPA at the same boron concentration of 5-10 μg^{10}B/ml using the MTT assay,

3) optimizing experimental conditions (especially, the number of cells initially plated in the Petri dish) for the clonogenic assay,
4) verifying promising boron compound for further *in vivo* study using the clonogenic assay.

2-7. Summary

In vitro compound screening was established in the laboratory for determining initial suitability of boron compounds by assessing preferential intracellular uptake. Boric acid is used as the reference for identifying intracellular uptake since it uniformly distributes in the intra- and extra-cellular compartments. If cell irradiation in the presence of a test compound produces more cell killing than in the presence of boric acid at the same concentration in the growth medium, then the test compound is considered to be preferentially accumulating in tumor cells. In this work, cell irradiation with BPA produced significantly more cell killing than with boric acid, consistent with earlier *in vitro* studies using 9L gliosarcoma cells [62]. The test compound, BOPP, produced similar cell killing with the reference boric acid, as was reported in studies using V79 Chinese hamster ovary cells [61]. The BOPP chemical toxicity data from the colorimetric assay is also consistent with published report [88].

Using the colorimetric assay requires only limited quantities of compound (approximately a hundred micrograms of ^{10}B) and can determine data relevant to chemical toxicity and intracellular uptake which otherwise would not be obtainable from the clonogenic assay. This preliminary information is useful for optimizing subsequent studies using the clonogenic assay. The survival data obtained from the colorimetric assay is used to estimate the number of cells required for plating in the clonogenic assay and minimizes the amount of compound necessary to obtain a full survival curve from which the relevant radiobiological data can be determined.

CHAPTER THREE

IN VIVO EVALUATION OF BORONATED LIPOSOMES

3-1. Introduction

In vivo evaluation in a small animal model of a new boron compound is the critical procedure to establish the potential radiobiological effectiveness of a new compound for BNCT. Low molecular weight compounds which have shown promising results during *in vitro* screening process can be candidates for such further study. In addition, *in vivo* evaluation may be the first testing performed on some high molecular weight compounds for which *in vitro* testing is not particularly suitable. Moreover, some compounds may be designed for specific metabolic modification as part of their targeting mechanism and would require testing in specific tumor models. For example, a nucleoside that needs phosphorylation by thymidine kinase (TK) [49] to remain inside cells could be tested in TK+ and TK- tumors to demonstrate that the metabolic targeting is actually working.

In vivo testing requires neutron irradiation when the ^{10}B distribution is optimal (i.e. high concentration and good selectivity in tumor) for tumor therapy. Thus, the first step of *in vivo* testing is a biodistribution study to ensure enough boron is delivered to tumor by the test compound and to measure uptake in other tissues, such as blood, skin, and other important organs, as a function of time after injection. This data is essential for later studies testing efficacy as the best time post administration for an irradiation has to be determined. A boron compound that delivers sufficient ^{10}B to tumor warrants a tumor therapeutic response study to evaluate the therapeutic effectiveness of this compound at the time chosen for BNCT based on the biodistribution study. The microscopic distribution of ^{10}B within the tumor greatly affects the uniformity of radiation dose absorbed within the tumor, and thus the effectiveness of the therapy. A microscopic analysis of the ^{10}B biodistribution within the tumor should be performed if possible as this can provide information to help explain the observed radiation effects.

Liposomes are small unilamellar vesicles with a membrane of phospholipid bilayer that are widely studied for drug delivery. They have very low toxicity due to the similarity to biomembranes and liposomes are therefore generally safe for use in the humans without serious side effects [90]. They can deliver drugs either through diffusion or through endocytic action. The attractive property of liposomes as a boron delivery vehicle for BNCT is their ability to accumulate in tumors. This feature results from the increased permeability through leaky tumor vessels and slower clearance from tumors than normal tissues [91]. Thus, an active tumor-targeting property is thought not to be required for the incorporated boron species within the liposomes. In addition, this specificity of liposomes allows the delivery of greater quantities of boron at lower administered doses [92].

Professor M. Frederick Hawthorne's research group at the University of Missouri, Columbia, has spent many years developing liposomes that incorporate ^{10}B-containing molecules as boron delivery agents. Some of these boronated liposomes showed promising *in vivo* uptake in EMT-6 murine mammary tumors [92-95]. Metastatic brain tumors or recurrent disease from primary breast cancer have been suggested as possible candidates for BNCT. Liposomes may be especially attractive for metastatic brain tumors because the blood-brain barrier keeps liposomes out of normal brain but is often comprised in tumors. Also, recurrent tumors which usually spread all over the chest wall are difficult to treat with surgery or conventional radiation therapy because of radiation damage to normal tissues from the initial treatment. Thus, the selective targeting ability of BNCT can be an advantage in the treatment of this tumor.

In this chapter, an *in vivo* evaluation study of boronated liposomes supplied by Professor Hawthorne's research group is performed for BNCT in a murine mammary carcinoma, EMT-6 tumor model. A current best compound in BNCT, BPA, was used as a positive control to compare the effectiveness of BNCT.

3-2. Materials and methods

3-2-1. Tumor model

The EMT-6 murine mammary carcinoma was used as a tumor model of breast cancer. The EMT-6 tumor was chosen for evaluating the effectiveness of liposomes to build upon

promising preliminary biodistribution studies of boronated liposomes in this model have already reported to show selective tumor uptake and long-retention of boron in tumor relative to normal tissues [92-95].

The EMT-6 cell line (kindly provided by Brookhaven National Laboratory) was grown in Dulbecco's Modification of Eagle's Medium (DMEM, Mediatech) supplemented with 10% fetal bovine serum (SeraCare Life Science), 1 % 200 mM L-glutamine (Mediatech), and 1 % 5,000 I.U./ml penicillin – 5,000 μg/ml streptomycin (Mediatech) at 37 °C in an atmosphere of 5 % CO_2. Cells were used for transplantation when the monolayer reached ~90 % confluence. Each female BALB/c mouse was anesthetized with isoflurane, and then 10^6 EMT-6 cells in a volume of 0.1 ml were injected subcutaneously on the lower back.

3-2-2. Liposomes

Liposomes are small unilamellar vesicles which consist of a phospholipid bilayer composed of distearoylphosphatidyl choline (DSPC) and cholesterol and an interior aqueous core [92]. The liposomes produced by the Hawthorne group for this project generally had diameters of 60-100 nm and contained 24 mg total lipid/ml (Figure 3.1). There are two ways for incorporating boron species (Figure 3.2): (1) MAC-16, lipophilic boron compounds, [nido-7-$CH_3(CH_2)_{15}$-7,8-$C_2B_9H_{11}$]$^-$, are embedded within the phospholipid bilayer, or (2) TAC, hydrophilic, a water-soluble boron compound, $[B_{20}H_{17}NH_3]^{3-}$, is trapped within the aqueous core of the liposome. In addition, both types of boron compounds can be combined within the same liposomal formulation, which is called MAC+TAC.

In our experiments, we used MAC-16 and MAC+TAC, which were prepared in hypertonic solution. Liposome solutions were provided in batches of ~7-10 ml. Each batch had a different liposome size and boron concentration. Liposome mean diameter varied from 59-70 nm. Solution concentrations varied from 475 to 580 in μg ^{10}B/ml for MAC-16 solutions and from 1215 to 2195 in μg ^{10}B/ml for MAC+TAC solutions. From these solutions, injected doses for therapy studies were maximized with concentrations of 580 and 2195 μg ^{10}B/ml for MAC-16 and MAC+TAC solutions, respectively. The injected

doses are indicated in each table and graph. Thus, different batches of liposome solutions were used for biodistribution studies. When data were compared from different biodistribution studies, these were normalized to the same injection dose.

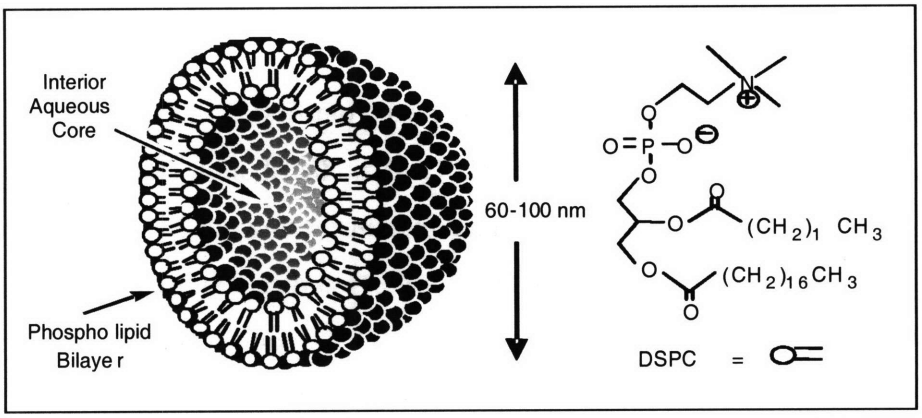

Figure 3.1. A cross-sectional view of a small unilamellar vesicle and the structure of distearoylphosphatidyl choline (DSPC) which makes up the phospholipid bilayer.

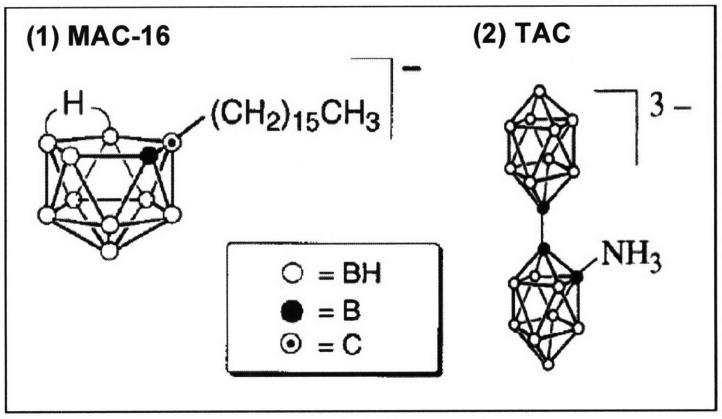

Figure 3.2. Structures of (1) MAC-16, the lipophilic boron species, [nido-7-$CH_3(CH_2)_{15}$-7,8-$C_2B_9H_{11}$]$^-$, which is embedded in the bilayer and (2) TAC, the hydrophilic ion, $[B_{20}H_{17}NH_3]^{3-}$, which is encapsulated in the aqueous core.

3-2-3. Biodistribution study

Murine biodistribution studies used female BALB/c mice (17-22 g), with EMT-6 tumors implanted subcutaneously on the lower back at 8 days before the experiments. Each mouse received an i.v. injection of 0.2 ml liposome solution into the retro-orbital sinus

while under brief isoflurane anesthesia. Retro-orbital injections do not damage the eye or affect the vision. Also, retro-orbital injections showed comparable uptake results to tail vein injections. Five to seven tumor-bearing mice were used at each time point of sacrifice and were euthanized by isoflurane overdose. Blood was removed directly from the heart, and tumor and liver were collected for boron analysis. Tumor volume at the time of sacrifice ranged from 50 to 200 mm^3.

A biodistribution study of MAC-16 was carried out first at sacrifice times of 6, 24, 30, and 48 hours after injection. An initial MAC+TAC biodistribution study was performed at 30 hours after injection, which was determined by considering our MAC-16 biodistribution study and the published liposome biodistribution studies. Subsequently, a complete MAC+TAC biodistribution study was carried out for the sacrifice times of 6, 18, 24, 30, and 48 hours which were chosen based on previous studies [92-94].

A BPA biodistribution study was included for comparison. BPA (0.2 ml, 4.3 mg^{10}B/ml) was injected intraperitoneally (i.p.) as the BPA-fructose complex (BPA-F) to improve the solubility. Tumor and blood were collected at 2, 4, and 6 hours after administration.

Macroscopic ^{10}B quantification of blood and tissues was carried out using PGNAA in the MITR-II. PGNAA is a non-destructive analytical technique and does not restrict the shape, size, or chemical form of samples. PGNAA detects the 478 keV photons produced from boron neutron capture reactions in ^{10}B: the detection limit is 1 μg ^{10}B [76].

3-2-4. Tumor therapeutic response study

Tumor therapeutic responses were evaluated using female BALB/c mice (17-22g) bearing EMT-6 tumors implanted subcutaneously on the back 8 days prior to the experiments. Experiments involved irradiation of tumors with graded doses of thermal neutrons in the presence of liposomes (MAC-16 and MAC+TAC), thermal neutrons in the presence of BPA, thermal neutrons alone, or 250 kVp X-rays. Additional controls included mice whose tumors received no irradiation. Five to eleven mice were used for each irradiation group.

Animal irradiations were performed using the vertical M011 thermal neutron beam in the MITR-II and using a shielding box made of lithiated-polyethylene (Li-Poly; 93 % ^{6}Li-enriched Li_2CO_3 dispersed in polyethylene; 7.5 % total Li by weight; Reactor Experiments, Sunnyvale, CA [89]). The lid of the box has a 10 cm x 2 cm irradiation aperture providing a narrow irradiation field across the backs of the mice. Four mice, which were anesthesized with ketamine-xylazine, were positioned side-by-side under the lid of the box (Figure 3.3). Then, the shielding box was mounted in the thermal neutron beam line shutter that turns the beam on and positions the shielding box aperture in the center of the neutron field. The absorbed dose rates on the tumor site with thermal neutron beam were presented in Table 3.1.

Table 3.1. The absorbed dose rates on the tumor site with the thermal neutron beam at the MITR-II.

Absorbed dose rate (cGy/min)			
Nitrogen	Fast neutron	Photons	Boron (per μg ^{10}B/g)
13.0 ± 0.6	< 0.1	19.8 ± 1.0	4.0 ± 0.2

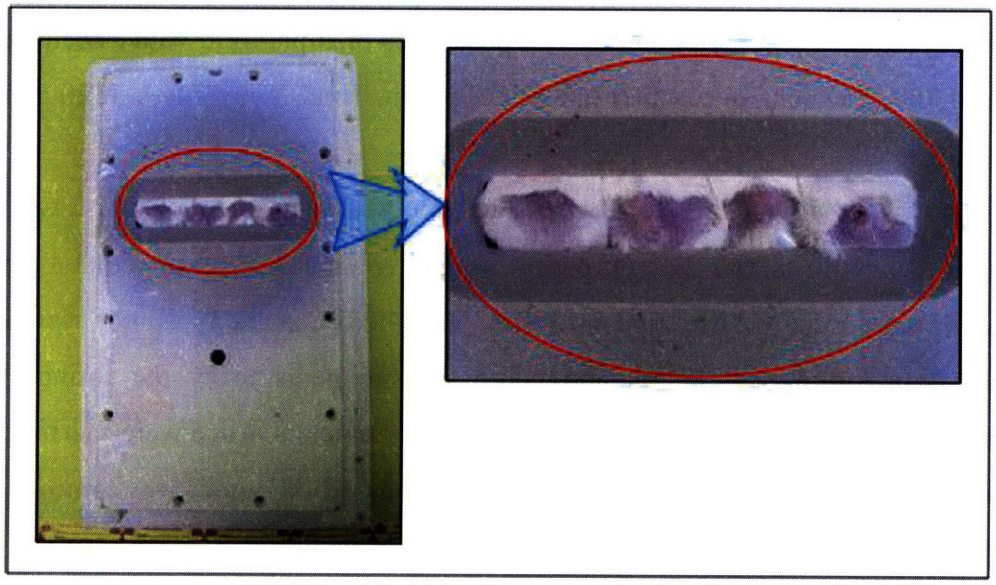

Figure 3.3. Positioning 4 anesthesized mice under the lid of the shielding box that provides narrow irradiation field across the backs of the mice during irradiation in the thermal neutron beam at the MITR-II.

Neutron irradiations with liposome-mediated BNCT were carried out at 30 hours after retro-orbital injection of 0.2 ml of the liposome solution with neutron beam doses of 4, 6, and 8 Gy. This dose range was selected knowing that 10 Gy neutron beam is not well tolerated by the animals and we want to give graded doses up to that maximum so as to be able to establish a dose response. The quantity of boron in each injected dose was maximized based on the concentration of a stock solution supply (5.8 μg ^{10}B/gbw (gram of body weight) for MAC-16, 22.0 μg ^{10}B/gbw for MAC+TAC). BPA-mediated BNCT used irradiations 4 hours after i.p. injection of 0.2 ml BPA-F and neutron beam doses of 6 and 8 Gy. Injected dose of BPA-F (43 μg ^{10}B/gbw) was maximized based on the solubility of BPA.

In addition, to see whether there was any therapeutic effectiveness when liposomes target tumor vasculature, the irradiations were tried at 30 minutes after liposome injection while the blood boron concentration was still high. At the time of irradiation, blood boron concentration was ~40 μg ^{10}B/g from MAC-16 and ~100 μg ^{10}B/g from MAC+TAC. In this case, a neutron beam dose of 8 Gy was used to see the maximum effect.

A Phillips RT250 unit in the MIT Nuclear Science and Engineering Department was used for X-ray irradiations operating at 250 kVp and 15 mA utilizing filtration of 0.4 mm Sn plus 0.25 mm Cu. The same shielding box for the thermal neutron irradiations was used with the top of the box replaced by 5 mm-thick lead having the same 10 cm x 2 cm irradiation aperture. The irradiation box was positioned on a platform with a focus-to-target distance of 10 cm which gave a dose rate of 2 Gy/min. Total X-ray doses of 20 and 30 Gy were administered.

To evaluate the tumor response, tumor volume was measured daily for 2 weeks after irradiations. After the initial 2-week period, tumor volume was measured 2-3 times per week until only mice whose tumors were controlled remained. Tumor volume was calculated from orthogonal length and width measurements using the formula for an ellipsoid $V = (ab^2)/2$, where a is the larger of the two diameters. Mice were sacrificed if the tumor became necrotic or its volume exceeded 500 mm^3. If the tumor was controlled, mice were kept and observed for 6 months to check for tumor recurrence.

3-2-5. Microdistribution study

To observe microscopic distribution of boron, MAC-16 liposome incorporated with fluorescent rhodamine phospholipids incorporated into the bilayer were first tried. At 30 hours after retro-orbital injection of fluorescent liposomes, tumor was harvested and immediately frozen in Tissue-Tek with dry ice, and then it was stored in the -80 °C freezer. Sections of tissue sample were cut at ~4 μm using a cryotome (Thermo Electron Corporation), and then mounted on a microscope slides. This would be useful for determining liposome distribution in tumor. Although the fluorescent marker was not directly attached to the boron species, it showed co-localized position of boron and liposomes.

High resolution quantitative autoradiography (HRQAR) is a powerful tool that can visualize tracks from boron-neutron capture reactions superimposed on tissue histology from thin (2-4 μm) frozen tissue sections [96]. This technique has been developed in Professor Otto K. Harling's laboratory in the MIT Nuclear Reactor Laboratory and the Department of Nuclear Science and Engineering [97, 98].

HRQAR analysis within the tumor was performed at one time point; the optimum time as indicated by the biodistribution studies (30 hours after retro-orbital injection of liposome solution and 4 hours after BPA-F i.p. injection). Thin tissue sections were mounted on microscope slides coated with 2 polymers and then irradiated with thermal neutrons. Since one of two polymers was a thin layer of nuclear track detector, α particle tracks from boron neutron capture reactions were recorded. After several procedures including tissue staining and track etching, the boron microscopic distribution was visible as black dots of etched tracks together with the stained tissue histology that are viewed under a light microscope. HRQAR images were produced by Thomas Harris and Dr. Kent Riley, and detailed methods are described in the reference [96, 97].

3-3. Results

3-3-1. Biodistribution study

3-3-1-1. MAC-16 biodistribution study

Table 3.2 and Figure 3.4 show boron concentrations in tumor, blood, and liver as a function of time after MAC-16 administration. All tumors in each time group were added together and measured together to increase the ^{10}B signal in PGNAA. Thus, the ^{10}B concentrations in tumor have a 5 % error in measurement from PGNAA. However, blood and liver were each measured separately and error bars represent standard deviation (SD) of 7 mice. While boron concentrations in blood and liver decreased slowly over the time period, boron continued to accumulate in the tumor. The maximum boron concentration in tumor of 18.4 ± 0.9 μg $^{10}B/g$, was reached at 30 hours after injection with the tumor to blood (T/B) boron concentration ratio of 0.90. The average blood and liver values at 30 hours were 20.5 ± 4.2 μg $^{10}B/g$ and 12.0 ± 2.9 μg $^{10}B/g$, respectively.

Table 3.2. ^{10}B concentrations at different times after MAC-16 retro-orbital injection with an injected dose of 4.8 μg ^{10}B/gbw (gram of body weight). Results are expressed as the mean ± SD for 7 mice except tumor. The tumor errors represent a 5 % error in measurement from the PGNAA.

Time after MAC-16 administration (hrs)	^{10}B concentration (μg $^{10}B/g$)		
	Tumor	Blood	Liver
6	11.6 ± 0.6	42.9 ± 3.7	20.1 ± 1.9
24	16.8 ± 0.8	22.9 ± 4.6	12.6 ± 2.7
30	18.4 ± 0.9	20.5 ± 4.2	12.0 ± 2.9
48	15.9 ± 0.8	10.6 ± 1.6	6.2 ± 1.5

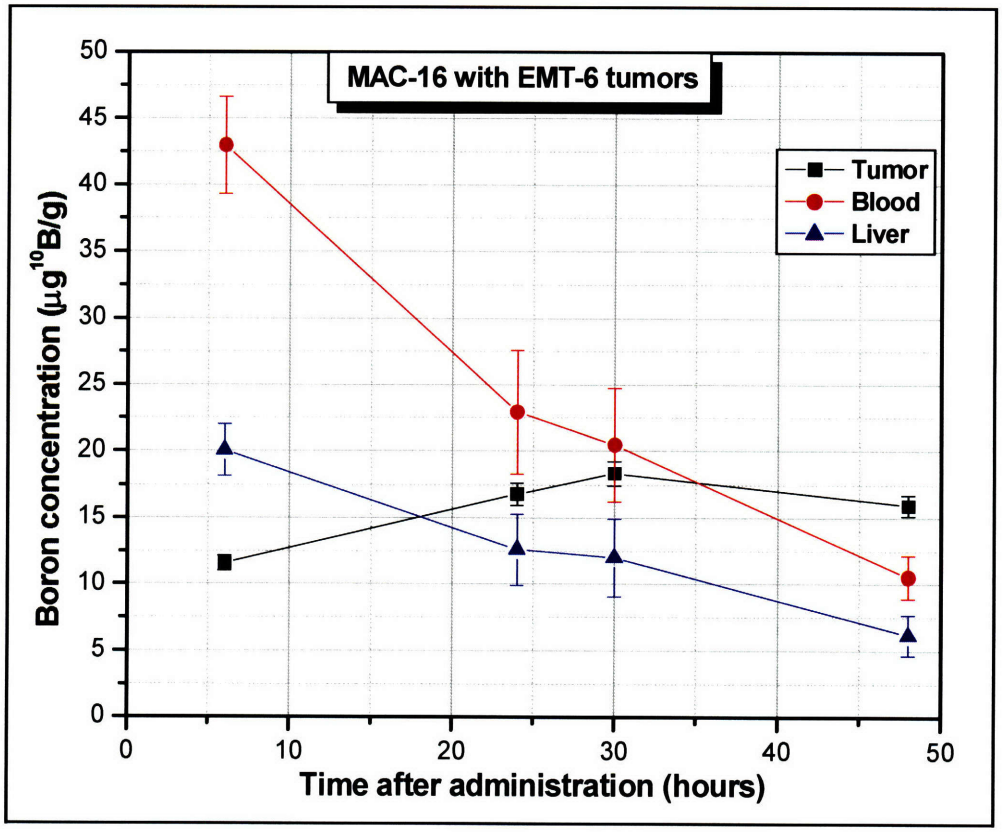

Figure 3.4. ^{10}B concentrations (μg ^{10}B/g) versus time (hours) post-injection for MAC-16 with retro-orbital injection dose of 4.8 μg ^{10}B/gbw. Points represent the mean ± SD for 7 mice except tumor which is a single measurement on several pooled tumors. The tumor error bars represent a 5 % error in measurement from the PGNAA. Lines are drawn connecting the data to help guide the eye.

These experiments were repeated to confirm the uptake data for the most promising time point (i.e. 30 hours). Table 3.3 shows boron concentrations in blood and tissues at 30 hours after MAC-16 administration. Injection dose was increased 18 % due to the use of a different batch of MAC-16 solution. However, ^{10}B concentration in the tumor was comparable to the previous study. The large SD (34 %) on the ^{10}B concentrations in tumor may mask any effects of the increased injected dose. ^{10}B concentrations in blood and liver were different from previous study, which could be due to the different liposome size in each batch of MAC-16 solution.

Table 3.3. ^{10}B concentrations at 30 hours after retro-orbital injection of MAC-16 with an injected dose of 5.8 μg ^{10}B/gbw. Results are expressed as the mean ± SD for 5 mice.

Time after MAC-16 administration (hrs)	^{10}B concentration (μg ^{10}B/g)		
	Tumor	Blood	Liver
30	18.3 ± 6.3	13.9 ± 2.1	21.0 ± 4.0

3-3-1-2. MAC+TAC biodistribution study

Table 3.4 presents boron concentrations of tissues at 30 hours after MAC+TAC administration. The biodistribution study of MAC+TAC shows an average ^{10}B concentration in tumor of 32.2 μg ^{10}B/g at 30 hours after injection with a T/B ratio of 0.63. This ^{10}B concentration in tumor meets one of the requirements for new boron compounds to deliver sufficient ^{10}B to tumor to allow therapeutic doses of radiation to the tumor during BNCT. Although MAC+TAC produced a relatively high ^{10}B concentration in liver, 75.7 μg ^{10}B/g, this can be tolerated because the liver will be located under the shielded from neutrons during the irradiation.

Table 3.4. ^{10}B concentration in tissues at 30 hours after MAC+TAC retro-orbital injection of 15 μg ^{10}B/gbw. Results are expressed as the mean ± SD with 5 mice for tumor and liver and with 3 mice for blood.

Time after MAC-16 administration (hrs)	^{10}B concentration (μg ^{10}B/g)		
	Tumor	Blood	Liver
30	32.3 ± 11.0	51.2 ± 2.5	75.7 ± 5.3

As was done for MAC-16, an additional MAC+TAC biodistribution study at the 30 hour-time-point was performed to confirm the consistency of experiments. Table 3.5 presents ^{10}B concentrations in blood and tissues at 30 hours after MAC+TAC administration for the repeated experiment. Due to the higher injected dose, the average ^{10}B concentration in tumor, 42.9 μg ^{10}B/g, seems higher than previous results, 32.3 μg ^{10}B/g;

however, the large SD (~30 %) on the ^{10}B concentrations in tumor masks the effect of the increased injected dose.

Table 3.5. ^{10}B concentrations at 30 hours after retro-orbital injection of MAC+TAC with an injected dose of 22.0 μg ^{10}B/gbw. Results are expressed as the mean ± SD for 5 mice.

Time after MAC-16 administration (hrs)	^{10}B concentration (μg ^{10}B/g)		
	Tumor	Blood	Liver
30	42.9 ± 11.9	58.1 ± 10.9	71.4 ± 11.4

A complete biodistribution with MAC+TAC solution was carried out from 6 to 48 hours after retro-orbtial injection using an injected dose of 12.2 μg ^{10}B/gbw (Table 3.6 and Figure 3.5). The maximum ^{10}B concentration in tumor reached approximately 24 μg ^{10}B/g between 18 and 30 hours after liposome injection. This result agreed with previous experiments after normalizing data to the same injected dose. Boron in blood was cleared out during the observation time and washout was also evident in liver with a slower rate. All skin samples (which were not presented in Table 3.6 and Figure 3.5) showed very low ^{10}B concentrations, most at or below the detection limit of ~1 μg ^{10}B/g and none greater than 4 μg ^{10}B/g.

Table 3.6. ^{10}B concentrations after retro-orbital injection of MAC+TAC with an injected dose of 12.2 μg ^{10}B/gbw. Results are expressed as the mean ± SD for 3-5 mice.

Time after MAC+TAC administration (hrs)	^{10}B concentration (μg ^{10}B/g)		
	Tumor	Blood	Liver
6	16.1 ± 2.5	79.2 ± 8.2	63.8 ± 7.1
18	26.0 ± 4.2	53.3 ± 0.8	44.6 ± 4.9
24	23.2 ± 2.9	37.7 ± 3.0	55.4 ± 4.6
30	25.2 ± 7.2	28.7 ± 3.7	55.6 ± 3.2
48	20.0 ± 6.6	11.6 ± 3.6	37.0 ± 8.8

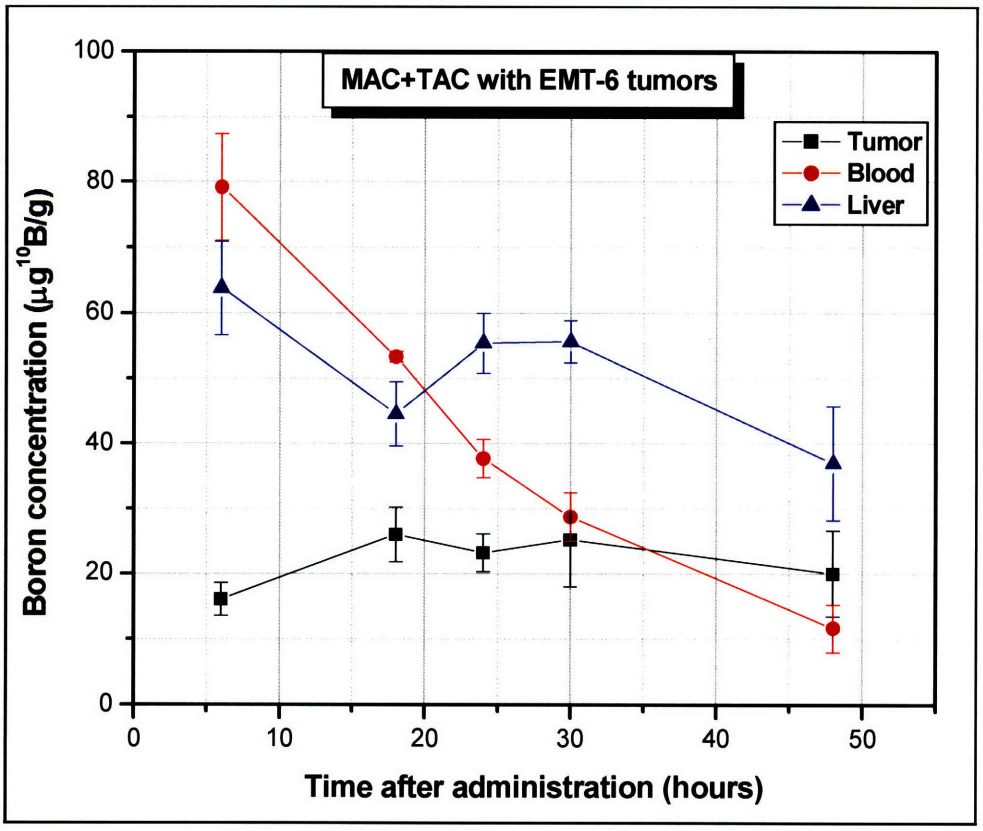

Figure 3.5. ^{10}B concentrations (μg ^{10}B/g) versus time (hours) after retro-orbital injection of MAC+TAC with an injected dose of 12.2 μg ^{10}B/gbw. Points represent the mean ± SD for 3-5 mice. Lines are drawn connecting the data to help guide the eye.

An additional experiment from 30 to 96 hours confirmed that ^{10}B uptake in the tumor decreased after the 30-hour time point. Figure 3.6 shows boron concentrations of this additional experiment combined with the previous data (Figure 3.5) normalized to the same injected doses. Boron in the blood and liver is continuously cleared out and also boron in tumor starts washout after 30 hours.

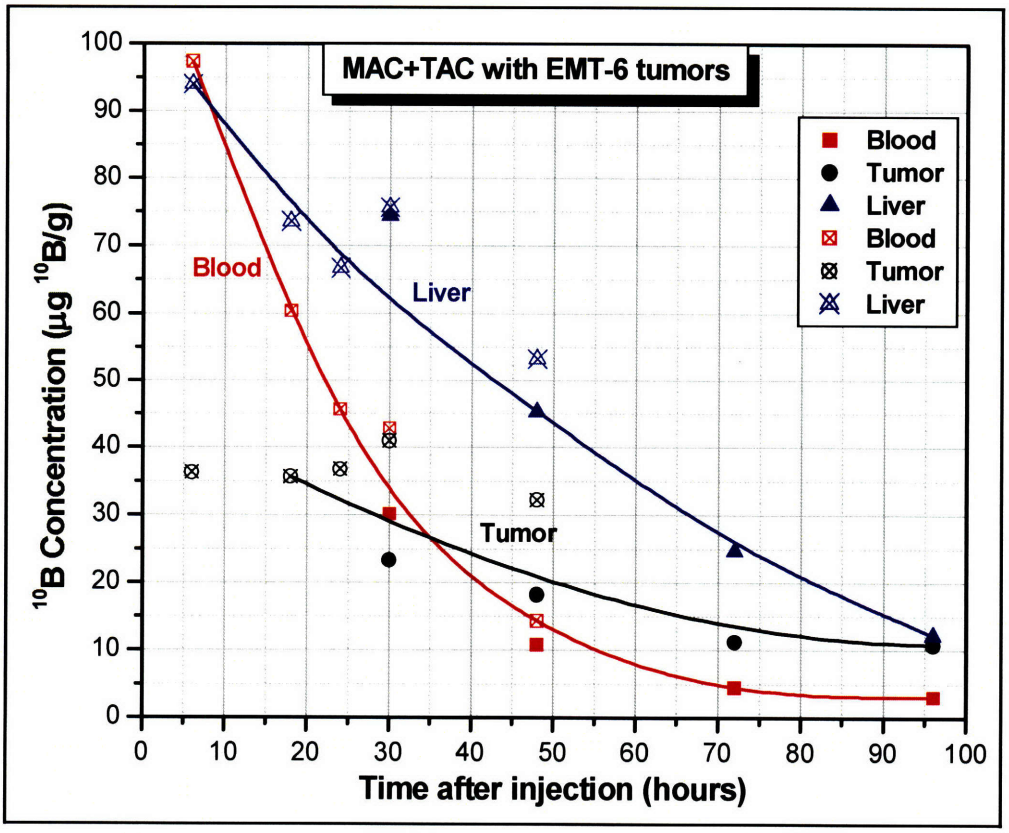

Figure 3.6. ^{10}B concentrations (μg ^{10}B/g) versus time (hours) of MAC+TAC. Solid symbols present data with i.d.= 17.8 μg ^{10}B/gbw and open & cross symbols show data from the earlier experiment (i.d.= 12.2 μg ^{10}B/gbw) normalized to the same injected dose using a factor of 1.47. Solid lines show the trend of boron concentrations.

3-3-1-3. BPA biodistribution study

Figure and Table 3.7 show the ^{10}B concentrations in tumor and blood as a function of time. Unlike liposomes, BPA is a small molecule and shows fast blood clearance and tumor uptake. The average ^{10}B concentration in tumor at 4 hours after BPA-F i.p. injection was 21.6 μg ^{10}B/g with a T/B ratio of 2.3. Average ^{10}B concentrations in tumor from MAC-16 at 30 hours after administration were comparable (20 μg ^{10}B/g) with those from BPA (at 4 hours) and a tumor therapeutic response study and a microdistribution study were therefore deemed useful to evaluate the effectiveness of boronated liposomes.

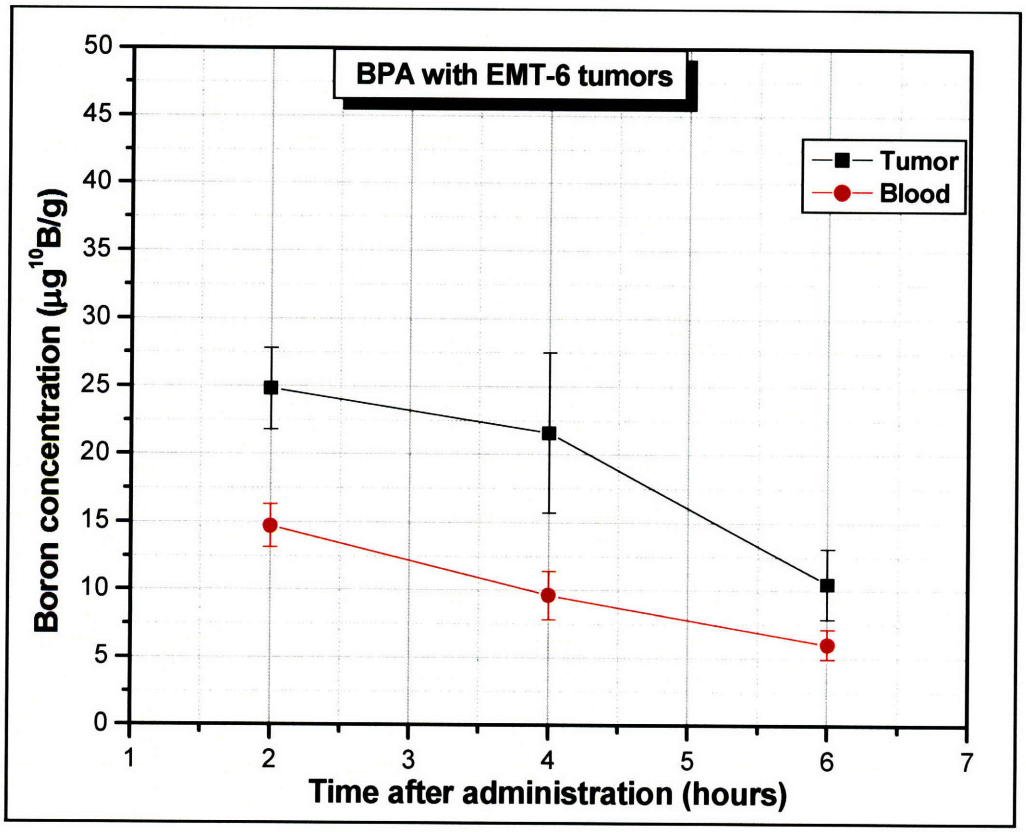

Figure 3.7. ^{10}B concentrations (μg ^{10}B/g) versus time (hours) after BPA-F injection (0.2 ml, i.p. 43.0 μg ^{10}B/gbw). Points represent the mean ± SD for 5 mice. Lines are drawn connecting the data to help guide the eye.

Table 3.7. ^{10}B concentrations at different times after BPA-F i.p. injection of 43.0 μg ^{10}B/gbw. Results are expressed as the mean ± SD for 5 mice.

Time after BPA-F administration (hrs)	^{10}B concentration (μg ^{10}B/g)	
	Tumor	Blood
2	24.8 ± 3.0	14.7 ± 1.6
4	21.6 ± 5.9	9.6 ± 1.8
6	10.5 ± 2.6	6.0 ± 1.1

3-3-2. Tumor therapeutic response study

Table 3.8 summarizes the fraction of tumors controlled for the different treatment groups. BPA-mediated treatment showed a superior result attaining 62.5 % tumor control. MAC-16, delivered 30 hours before irradiation with 6 Gy of thermal neutron beam was the best for liposomes, with 27.3 % tumor control. Although MAC+TAC showed almost twice the ^{10}B concentration in tumor relative to MAC-16, and a higher neutron beam dose (8 Gy) was used with the MAC+TAC liposomes, no improvement in tumor control was observed. An additional experiment using the same conditions was performed to confirm these results. However, this repeat experiment did not control any tumors. A single pilot study using liposomes administered 30 minutes before irradiation to produce vascular damage into tumor did not control any tumors.

Figures 3.8 to 3.12 present measured tumor volumes of each mouse after irradiation for the 6 Gy neutron beam alone and 6 Gy neutron beam in the presence of MAC-16, MAC+TAC, or BPA, respectively. All groups have evident growth delay post-irradiation with varying recovery rates. In the 6 Gy neutron beam alone group, growth suppression was initially maintained for ~6-7 days post-irradiation, but the tumors were quick to recover. The 6 Gy neutron beam in the presence of MAC-16 groups for both the first and the repeated experiments show a longer growth delay period of ~11-13 days post-irradiation. Growth suppression periods of ~14-16 days or ~16-18 days post-irradiation were observed in the 6 Gy neutron beam in the presence of MAC+TAC or BPA, respectively. Some animals were sacrificed with tumors at smaller than 500 mm^3 due to apparent necrosis of the tumor.

Table 3.8. Fractions of tumors controlled with different treatments.

Treatment	Fraction of tumors controlled
No treatment	0/7
20 Gy X-rays	1/5
30 Gy X-rays	4/5
4 Gy thermal neutron beam	0/8
6 Gy thermal neutron beam	0/8 (Figure 3.8)
8 Gy thermal neutron beam	0/8
MAC-16 (30 hr) – 4 Gy beam (+ 9.8 Gy boron)	0/11
MAC-16 (30 hr) – 6 Gy beam (+ 14.6 Gy boron)	3/11 (Figure 3.9)
MAC-16 (30 hr) – 6 Gy beam (+ 14.6 Gy boron) (Repeat)	0/8 (Figure 3.10)
MAC-16 (30 hr) – 8 Gy beam (+ 19.5 Gy boron)	1/8
MAC+TAC (30 hr) – 4 Gy beam (+ 19.5 Gy boron)	0/8
MAC+TAC (30 hr) – 6 Gy beam (+ 29.3 Gy boron)	1/8 (Figure 3.11)
MAC+TAC (30 hr) – 8 Gy beam (+ 39.0 Gy boron)	2/8
MAC-16 (30 min) – 8 Gy beam (+ 39.0 Gy boron – blood)	0/8
MAC+TAC (30 min) – 8 Gy beam (+ 97.6 Gy boron – blood)	0/6
BPA (4 hr) – 6 Gy beam (+ 14.6 Gy boron)	5/8 (Figure 3.12)

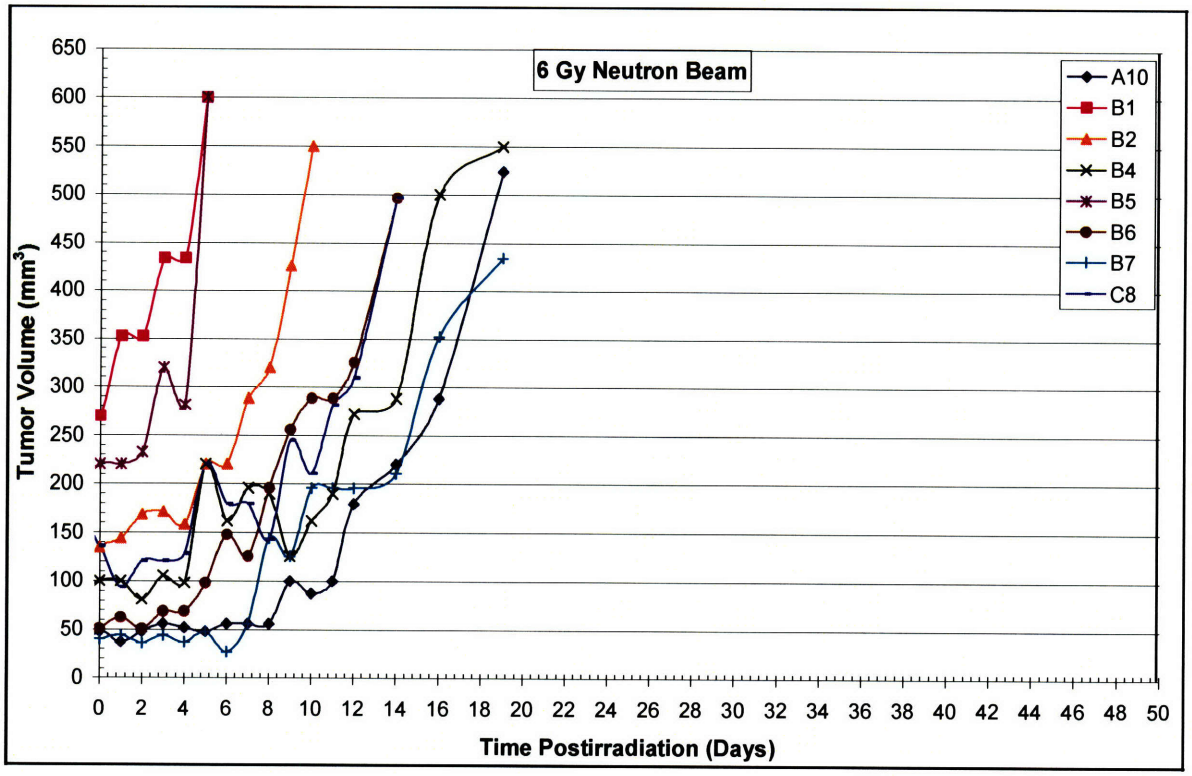

Figure 3.8. Tumor volume (mm^3) versus time (days) after 6 Gy neutron beam irradiation. Each line indicates tumor volume for each mouse.

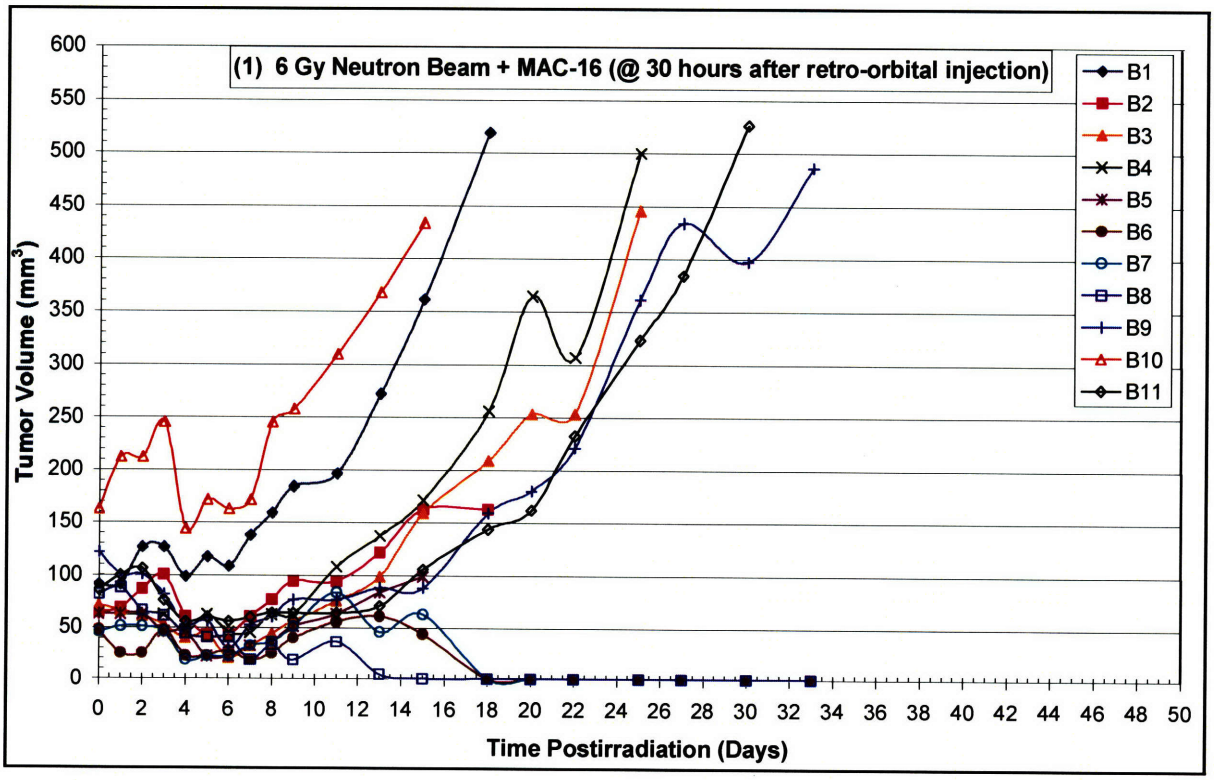

Figure 3.9. Tumor volume (mm^3) versus time (days) after 6 Gy neutron beam irradiation in the presence of MAC-16. Each line indicates tumor volume for each mouse.

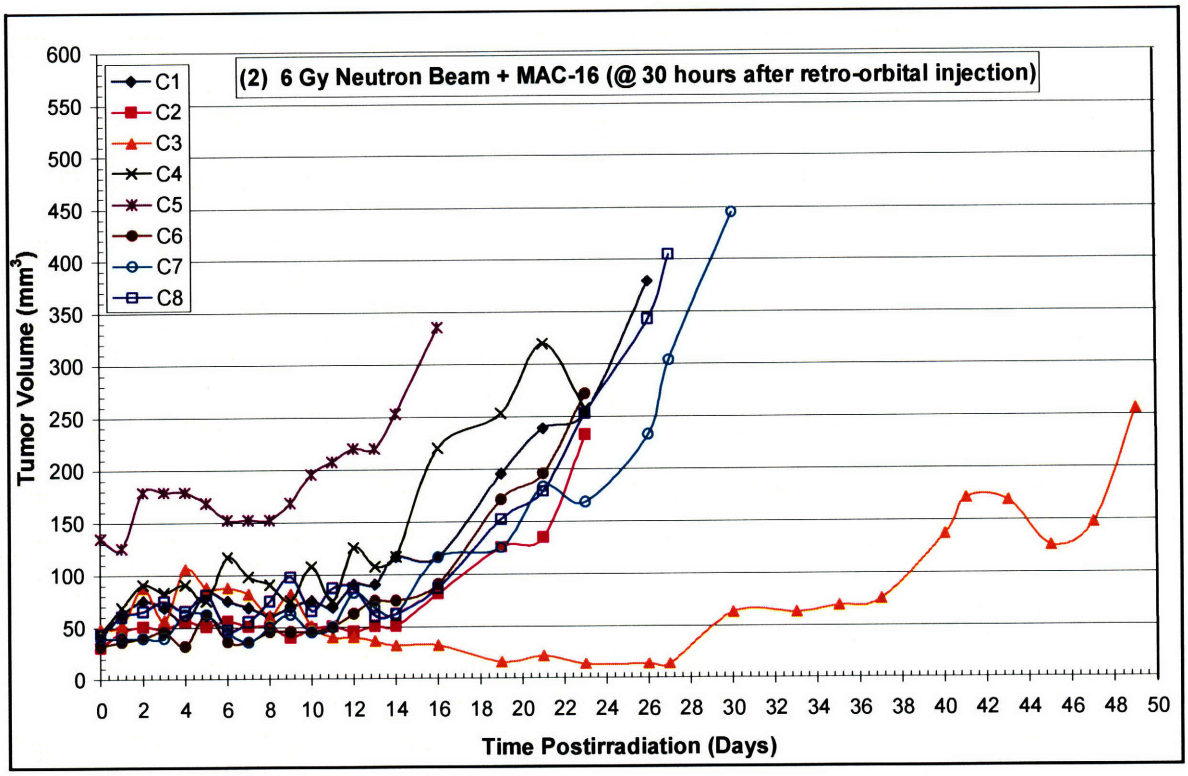

Figure 3.10. Tumor volume (mm^3) versus time (days) after 6 Gy neutron beam irradiation in the presence of MAC-16 (repeated). Each line indicates tumor volume for each mouse.

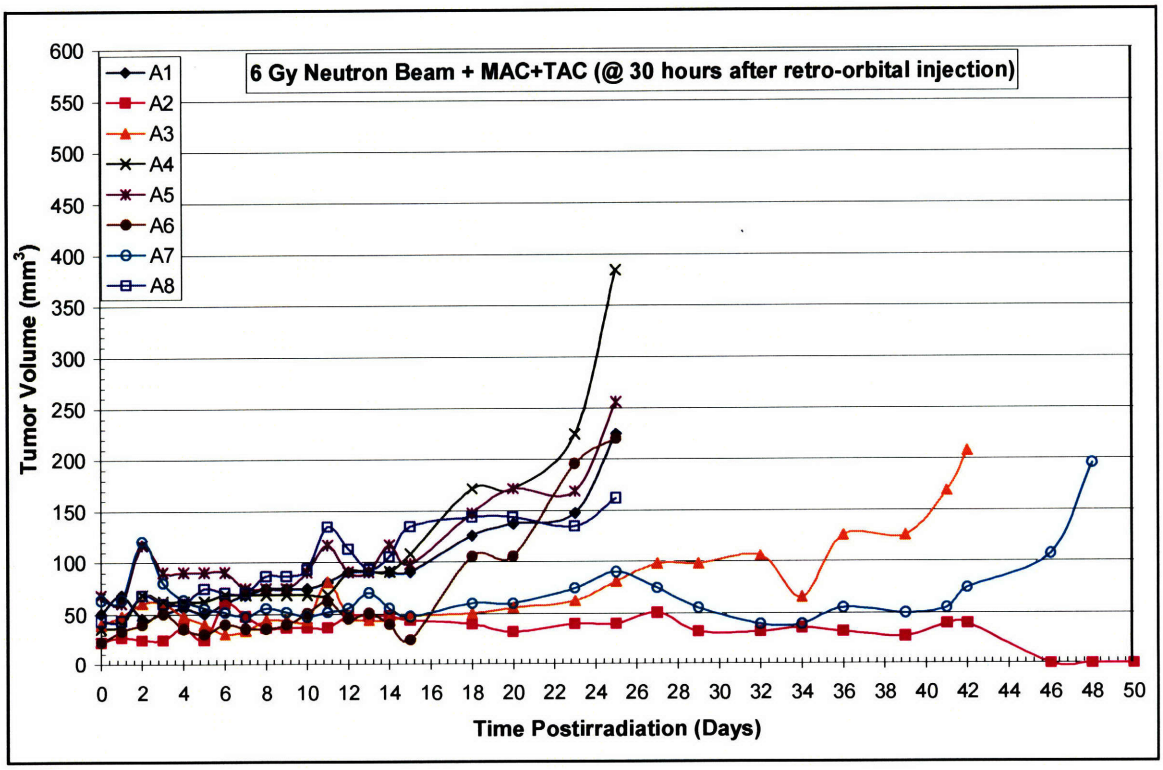

Figure 3.11. Tumor volume (mm^3) versus time (days) after 6 Gy neutron beam irradiation in the presence of MAC+TAC. Each line indicates tumor volume for each mouse.

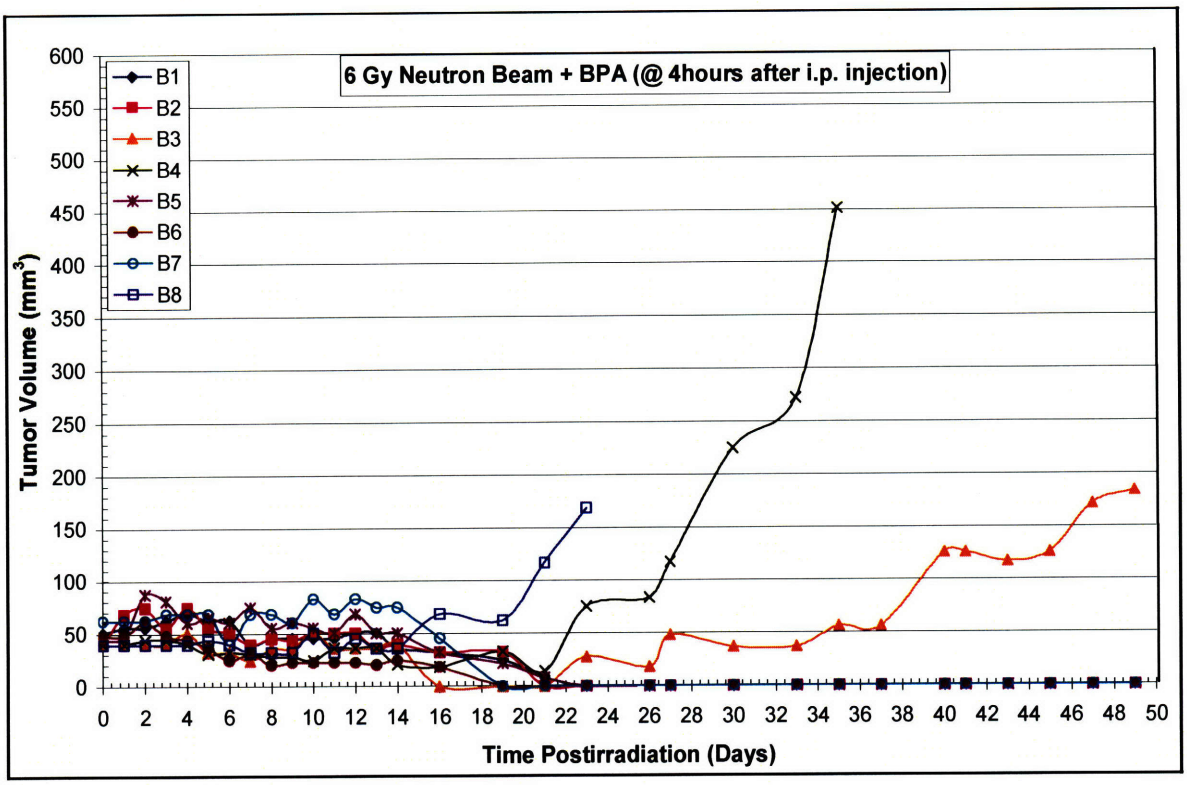

Figure 3.12. Tumor volume (mm^3) versus time (days) after 6 Gy neutron beam irradiation in the presence of BPA. Each line indicates tumor volume for each mouse.

3-3-3. Microdistribution study

Figure 3.13 (A) is an unstained frozen section of EMT-6 tumor from a BALB/c mouse which received a retro-orbital injection of fluorescent liposomes 30 hours before sacrifice. Fluorescence microscopy showed that the liposomes (brown) were located almost exclusively at the edges of the tumor. This non-uniformity was independently confirmed using HRQAR images with liposomes. Figure 3.13 (C) and (D) are HRQAR images of the EMT-6 tumor after MAC-16 injection via the retro-orbital sinus, which was the same condition with the therapy. Boron neutron capture reactions appear as small black dots on the image, called tracks. Tracks are evident only near the periphery of the tumor. However, in Figure 3.13 (B), when delivered by BPA using the same condition with the therapy, tracks are uniformly distributed throughout the tumor interior. Although BPA and MAC-16 have similar bulk ^{10}B concentrations in the tumor, they showed very different uptake patterns on a microscopic scale.

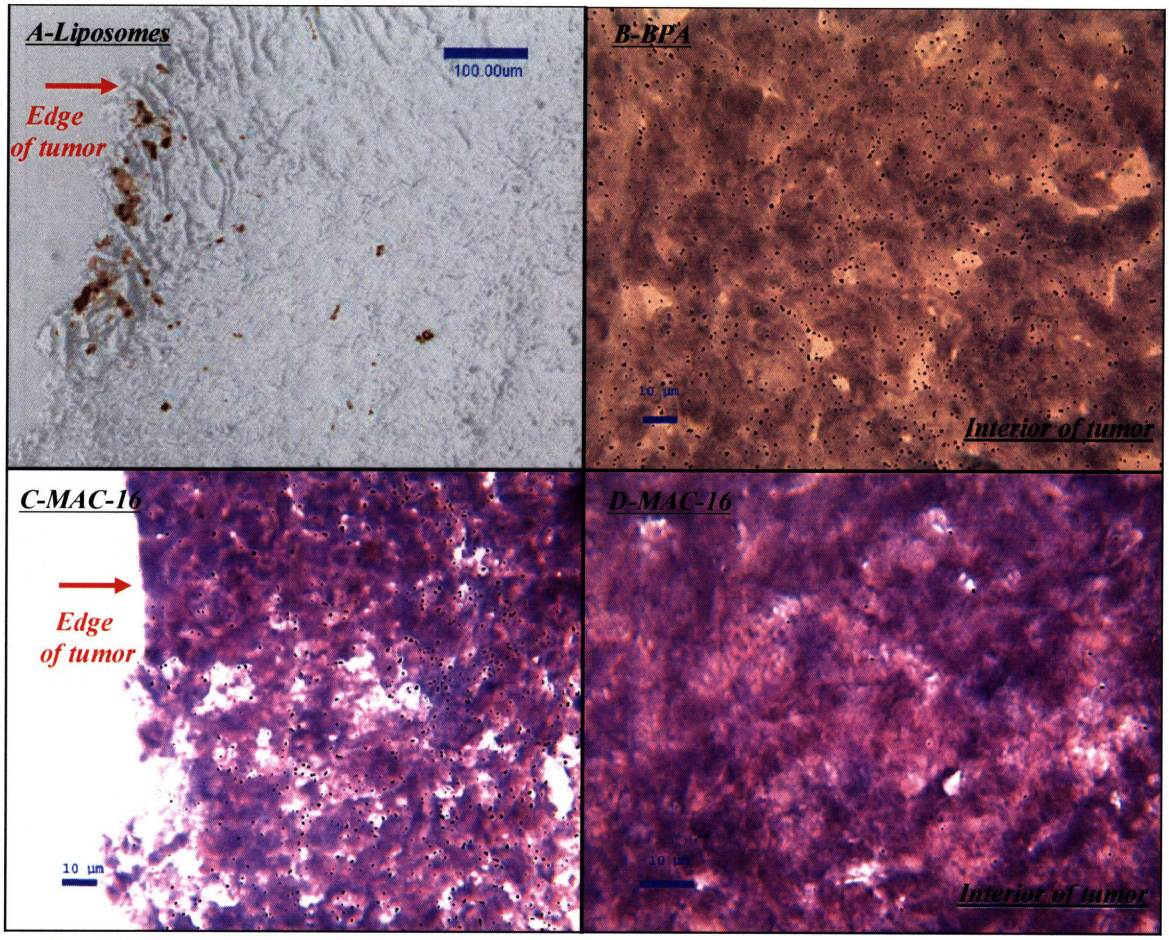

Figure 3.13. Microdistribution images of the EMT-6 tumor. A) Liposomes labeled with a fluorescent marker (brown) that are concentrated at the edge of the tumor. Scale bar: 100 µm. B) HRQAR image of the tumor that received a BPA injection to visualize boron-neutron capture particle tracks (black dots) superimposed on the histology, that are uniformly distributed throughout the tumor interior. Scale bar: 10 µm C-D) HRQAR images of the tumor received MAC-16 injection superimposed on the histology, where tracks are evident only near the periphery of the tumor. Scale bar: 10 µm. (HRQAR images produced by Thomas Harris.)

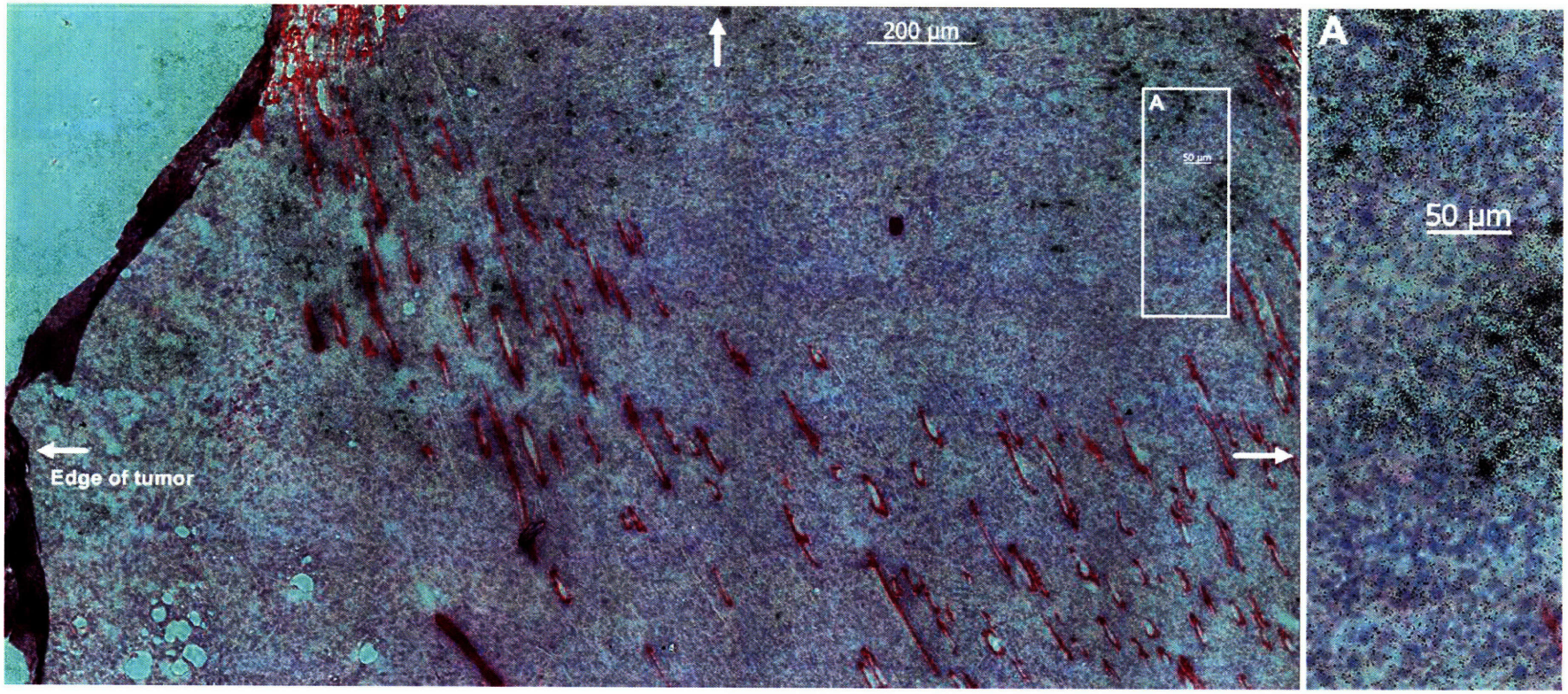

Figure 3.14. HRQAR image of the EMT-6 tumor that received a MAC+TAC injection to visualize boron-neutron capture particle tracks (black dots) superimposed on the histology. Track clusters are evident near the periphery of the tumor in the upper right and left of the low magnification image. The track density (boron concentration) also appears to decrease near the center of the tumor, as shown in the inset. Arrows indicate the edges of the tumor. Scale bar: 200 µm for the left and 50 µm for the right. (HRQAR image produced by Dr. Kent Riley.)

Figure 3.14 showed HRQAR section of an EMT-6 tumor harvested from a mouse 30 hours after injecting 0.2 ml MAC+TAC via the tail vein. Gross boron concentrations do not vary with two different i.v. injections via the tail vein and via retro-orbital sinus. Track clusters are evident near the periphery of the tumor in the upper right and left of the low magnification image. The track density (boron concentration) also appears to decrease near the center of the tumor, as shown in the inset.

3-4. Discussion

The critical qualifications of a compound for BNCT are generally a sufficient macroscopic ^{10}B uptake (20-30 μg ^{10}B/g) in the tumor and a high T/B and T/NT (tumor to normal tissues) ^{10}B concentration ratio. In this *in vivo* liposome study, the gross ^{10}B concentrations in the EMT-6 tumor from MAC-16 and BPA were comparable and produced a total absorbed dose (21 Gy: 6 Gy beam + 15 Gy boron) in the tumor that is sufficient to cause a response to tumor. MAC+TAC produced twice the ^{10}B tumor concentration of MAC-16 and BPA. However, the therapy experiments using liposomes (MAC-16 or MAC+TAC) were less effective than those with BPA or X-rays. The major reason appears to be an inhomogeneous microscopic distribution of ^{10}B delivered by liposomes in the EMT-6 tumor. These results indicate the importance of a homogenous microdistribution of ^{10}B in the study of new boron compounds for BNCT.

Liposomes with a size of 50-200 nm accumulate passively in the tumor by passing through the leaky vasculature of the tumor when they are injected intravenously (i.v.) [99, 100]. Since MAC-16 and MAC+TAC liposomes had an average diameter of 59-70 nm, these liposomes could be expected to passively pass from the tumor vasculature into the interstitial fluid within the EMT-6 tumor. However, fluorescent-labeled liposomes and HRQAR images showed boron accumulating mostly at the edge of the tumor. This condition may be caused by the configuration of the EMT-6 tumor. The EMT-6 tumor is a poorly-vascularized solid tumor. As seen in Figure 3.15, there are some hypoxic areas and necrotic regions located in the center of tumor. Due to this nature of the EMT-6 tumor, liposomes can accumulate mostly in areas which are relatively well-vascularized.

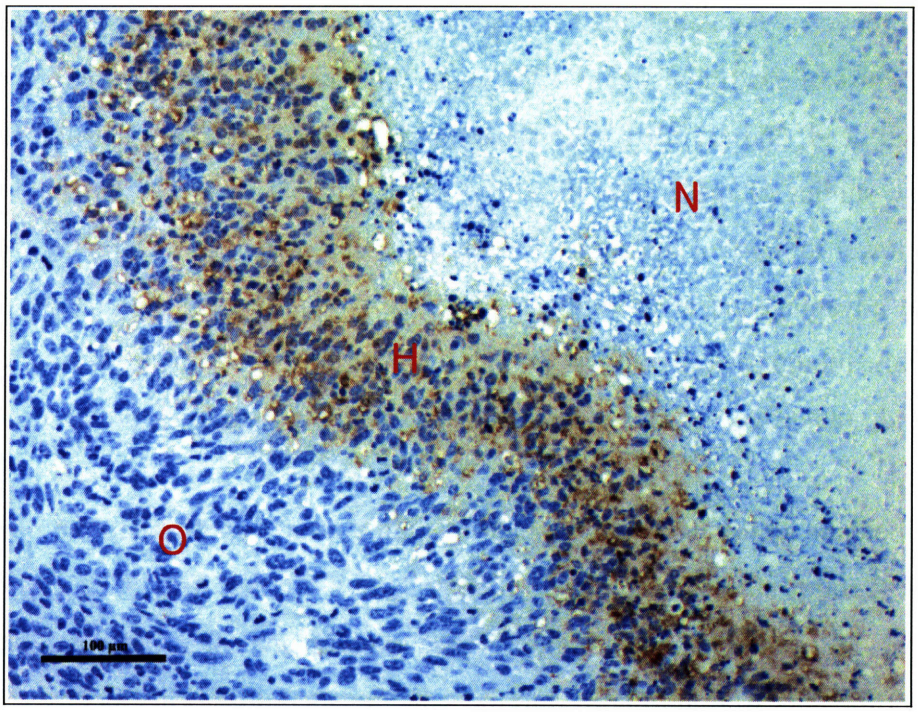

Figure 3.15. Histological section of a paraffin embedded EMT-6 tumor. Brown area indicates hypoxic (H) region with immunostaining for pimonidazole binding. To the left side of the brown region is well oxygenated (O) EMT-6 tumor, and to the right of the brown region is necrosis (N). Nuclei were stained blue. Scale bar: 100 μm. (Histology image produced by Jugal Shah.)

In general, higher T/B and T/NT ^{10}B concentration ratios suggest safer therapy with a minimized background radiation dose to surrounding normal tissue. However, in spite of lower T/B ^{10}B concentration ratios (0.6-0.9) with liposomes, there was no serious normal tissue complication observed because the mice were well shielded during irradiations. Thus, mice in the liposome-mediated BNCT group were all sacrificed due to tumor overgrowth or necrosis. Mice in the group of 6 Gy neutron beam plus liposomes did not show any normal tissue response including skin. Hair loss and reddened, scaled skin in the radiation field were observed in some mice for which tumors were controlled in the group having liposome-mediated BNCT with 8 Gy neutron beam. In BPA-mediated BNCT, hair loss and reddened skin were produced by 6 Gy neutron beam irradiation. One of these tumor-controlled mice was sacrificed due to serious skin damage, moist desquamation, about 1 month after the irradiation. Moist desquamation was also observed in all mice irradiated with 20 Gy and 30 Gy X-rays.

Moreover, 8 Gy neutron beam irradiation in the presence of BPA resulted in all mice dying because of gastrointestinal (GI) damage. At 6 days after irradiation, one of these mice was found dead, and all other mice showed a poor body condition and traces of diarrhea. Histology studies of these sick mice confirmed that there was GI damage. These results verify a lower toxicity of liposomes for normal tissues (especially, for skin and gut), which could be advantageous in the clinical use if better tumor distribution could be realized. Thus, even though a T/B ratio is an important criterion for evaluation of a new boron compound, the effect of each particular boron compound on normal tissues must be examined.

Liposome solutions were supplied in small volumes and limited the number of mice used for therapy studies. Moreover, biodistribution studies had to be carried out using different batches of liposome solution. These experiments often did not agree completely even after the data were normalized to the same injected dose. This inconsistency could be explained by the different size of liposomes in each batch (59-70 nm). For example, the size of liposomes was given as an average diameter, 71.9 nm, with the size distribution from ~55 to ~85 nm. As liposomes injected i.v. are susceptible to recognition by monophagocytes in the reticuloendothelial system, liposomes with the size <70 nm or >300 nm accumulate in liver and spleen and liposomes with the size of 100-200 nm are favorable for longer circulation in the blood [101]. Another study showed that liposomes with diameters of 90-200 nm stayed longer in the blood and accumulated more in the EMT-6 tumor than those with 40 nm or >200nm [102]. The average size of most MAC-16 and MAC+TAC liposome batches in these studies was 70 nm, which is near the size that is trapped in the liver and the pharmacokinetics may therefore be very sensitive to the actual size distribution in a batch.

For *in vivo* evaluation of a new compound especially whose characteristic in various batches would affect the study, one large quantity of compound should be used in a complete biodistribution including microdistribution and therapy studies. If a single batch production is not possible, then quality assurance on compound production needs to be considered. When a new compound sufficiently accumulates in the tumor, the homogeneity of microscopic ^{10}B distribution must be examined. Then, the therapeutic effectiveness of this compound would be studied including the normal tissue response.

3-5. Summary

Boronated liposome formulations (MAC-16 and MAC+TAC) were evaluated *in vivo* with the EMT-6 murine mammary carcinoma. Biodistribution studies showed high ^{10}B uptake in tumor (20-40 μg $^{10}B/g$) at 30 hours after an i.v. injection. Tumor control experiments were performed using the thermal neutron beam to compare the efficacy of the boron delivered by liposomes with that by BPA. Irradiations were carried out at optimized times of 30 (liposomes) and 4 hours (BPA) after injection. The MAC-16 formulation produced long-term (120 days) tumor control with the liposomes of 16 % whereas BPA controlled 63 % for similar tumor boron concentrations (approximately 20 μg $^{10}B/g$) and the same neutron beam dose. Microscopic distribution studies using fluorescent markers revealed non-uniform ^{10}B distribution in the tumor from the liposomes which were concentrated at the edge of the EMT-6 tumor. These results were independently confirmed using HRQAR that also showed uniform boron distributions with BPA. Therefore, *in vivo* evaluation characterized the uptake and retention properties of liposomes for a single injection but these appear inferior to BPA in the tumor studies performed with the EMT-6 tumors.

CHAPTER FOUR

POSSIBLE IMPROVEMENTS IN THE USE OF BORONATED LIPOSOMES

4-1. Introduction

Previous study of boronated liposomes using the EMT-6 tumor model showed no therapeutic effectiveness of BNCT, despite a sufficient gross ^{10}B uptake (20-40 μg ^{10}B/g) in EMT-6 tumor. The major reason for this unsatisfactory outcome appeared to be inhomogeneous microscopic distribution of ^{10}B in the tumor. This chapter describes studies to evaluate the effectiveness of boronated liposomes in a different tumor model and to try and improve the effectiveness by increasing the injection volume of boron.

As a different tumor model, the SCCVII mouse squamous cell carcinoma was chosen as a model for head and neck cancer. Head and neck tumors are difficult to treat successfully with conventional therapy because this tumor region is close to radiosensitive, critical organs such as central nervous system, oral mucosa, and skin. Therefore, the selective tumor targeting ability of BNCT could be beneficial for the treatment of these tumors. As a first step, a biodistribution study was carried out to measure how much boron was delivered by boronated liposomes to tumor, blood, liver and skin as a function of time after liposome injection. Since we learned its significance, the microscopic distribution of ^{10}B in the tumor was also examined.

A multiple-injection method was applied for increasing the total injected dose of liposomes because of the limited capacity (volume) for each injection. This approach has produced high tumor boron concentrations with several types of boron compounds which have the characteristics of long retention in tumor, such as porphyrins and liposomes [45, 103, 104]. Biodistribution and microscopic distribution studies following double injection of liposomes were performed using the MAC+TAC liposome solution and the EMT-6 tumor model.

4-2. Alternative tumor model – SCCVII tumor

4-2-1. Materials and methods

4-2-1-1. Tumor model

The SCCVII mouse squamous cell carcinoma was used as a tumor model of head and neck cancer. SCCVII cell line (generously provided by Brookhaven National Laboratory) was grown in Dulbecco's Modification of Eagle's Medium (DMEM, Mediatech) supplemented with 10 % fetal bovine serum (SeraCare Life Science), 1 % 200 mM L-glutamine (Mediatech), and 1 % 5,000 I.U./ml penicillin – 5,000 μg/ml streptomycin (Mediatech) at 37 °C in an atmosphere of 5 % CO_2. Cells were used for transplantation when the monolayer reached ~90 % confluence. Each female C3H mouse was anesthetized with isoflurane, and then $2x10^6$ SCCVII cells in a volume of 0.1 ml were injected subcutaneously on the lower back.

4-2-1-2. Liposome solutions

Liposome solutions were provided in batches of ~7-10 ml. Each batch had different boron concentration that varied from 425 to 600 in μg ^{10}B/ml for MAC-16 solutions and from 1160 to 1780 in μg ^{10}B/ml for MAC+TAC solutions. Liposome mean diameter varied from 59-76 nm. The injected doses are indicated in each table and graph. Thus, for some biodistribution studies, different batches of liposome solutions were used and where these data were combined results were scaled by the ratio of solution ^{10}B concentrations.

4-2-1-3. Biodistribution study

Murine biodistribution studies used female C3H mice (22-30 g) with SCCVII tumors implanted subcutaneously on the lower back about 2-3 weeks before the experiments. Each mouse received an injection of 0.2 ml into the retro-orbital sinus while under brief isoflurane anesthesia. Three to five tumor-bearing mice were euthanized at each time point by isoflurane overdose. Blood was removed directly from the heart, and tumor, liver, and skin were collected for boron analysis. Tumor mass at the time of harvesting was 100-300 mg.

Based on the experience of our earlier liposome biodistribution studies with the EMT-6 tumor, the initial liposome biodistribution study was performed at a single time of 30 hours after retro-orbital injection of ^{10}B enriched liposome solutions. After that, experiments using unenriched liposome solution were carried out for additional sacrifice times of 6 and 24 hours after injection. Finally, a complete biodistribution study for sacrifice times of 6, 24, 30, 48, 54, and 72 hours was accomplished with one large batch of unenriched liposome solution.

A BPA biodistribution study was also performed for comparison. BPA was injected intraperitoneally (i.p.) as the BPA-fructose complex (BPA-F) to improve solubility. Tumor and blood samples were taken at 1, 3, and 5 hours after administration.

4-2-1-4. Boron analysis

The initial biodistribution study used PGNAA in the MITR-II to measure macroscopic ^{10}B concentrations in blood and other tissue samples. Unlike blood and liver samples, tumor and skin samples could not be measured with PGNAA because of their low ^{10}B concentrations which were below the detection limit of PGNAA. PGNAA was also used for measuring the ^{10}B concentration of blood and tumor samples following BPA-F injection.

Since samples had low ^{10}B concentrations in both the initial study and in the studies using unenriched liposomes, total boron ($^{10}B + {}^{11}B$) concentrations were measured by using inductively coupled plasma optical emission spectroscopy (ICP-OES). ICP-OES has a lower detection limit that is practically limited to 0.1 μg B mainly because of the dilutions necessary during sample preparation with acid. Durin ICP analysis, blood was mixed with the same volume of a 2.5 % solution of the detergent Triton X-100. Then, the blood slurry was diluted to ten times the original blood volume with distilled water in order to obtain enough volume for multiple measurements. Tissues (< 200 mg) were digested in 0.6 ml of a 1:1 mixture of nitric and sulfuric acids and 2 ml of a 10 % solution of Triton X-100. The tissue samples were then diluted to 6 ml with distilled water in order to obtain a clear solution and enough volume for multiple measurements. The prompt gamma and ICP

analysis methodologies were cross calibrated and analysis of blood samples using both methods produced values that agreed to within 10 %.

4-2-2. Results

4-2-2-1. Liposome biodistribution study

Table 4.1 shows ^{10}B concentrations measured by PGNAA in tumor, blood, liver, and skin at 30 hours after ^{10}B-enriched MAC-16 and MAC+TAC solution administrations. The average boron concentration of 6.9 μg ^{10}B/g of tumor was found in the SCCVII tumor when using MAC-16. This was much less than the required boron concentration of at least 20-30 μg ^{10}B/g of tumor for a promising boron compound. MAC+TAC administration roughly raised the ^{10}B concentration to 23.4 μg ^{10}B/g of tumor; however, this amount was only half of that for the EMT-6 tumor. Boron concentrations were analyzed at other time points, 6 and 24 hours after unenriched MAC-16 and MAC+TAC solution injections (Table 4.2).

Figures 4.1 and 4.2 exhibit the combination of two experiments. To combine these two experiments that used different liposome solutions, the boron concentrations of the 6- and 24-hour time points were scaled up by the ratio of injection doses (i.d.) a factor of 1.4 for both MAC-16 and MAC+TAC. Slow tumor uptake and rapid blood clearance for MAC-16 and MAC+TAC were observed in Figures 4.1 and 4.2. However, the curves were not smooth even when the data were normalized. To check whether longer times may be better for therapy, a complete biodistribution was planned.

Table 4.1. ^{10}B concentrations measured with PGNAA for 30 hours after retro-orbital injection of MAC-16 (enriched ^{10}B, i.d. = 4.6 μg ^{10}B/gbw) and MAC+TAC (enriched ^{10}B, i.d. = 12.3 μg ^{10}B/gbw). Results are expressed as the mean ± SD for 5 mice bearing SCCVII tumors.

Liposomes	^{10}B concentration (μg ^{10}B/g)			
	Tumor	Blood	Liver	Skin
MAC-16	6.9 ± 1.5	12.0 ± 1.7	12.4 ± 0.6	3.8 ± 0.4
MAC+TAC	23.4 ± 10.5	63.0 ± 7.2	46.1 ± 5.2	10.0 ± 2.1

Table 4.2. Total boron concentrations measured with ICP-OES for 6 and 24 hours after retro-orbital injection of MAC-16 (unenriched B, i.d. = 3.3 μg B/gbw) and MAC+TAC (unenriched B, i.d. = 8.9 μg B/gbw B). Results are expressed as the mean ± SD for 5 mice bearing SCCVII tumors.

Liposomes	Time (hrs)	B concentration (μg B/g)			
		Tumor	Blood	Liver	Skin
MAC-16	6	1.7 ± 0.6	21.5 ± 1.8	22.8 ± 2.1	1.6 ± 0.2
	24	2.7 ± 1.2	8.7 ± 1.3	10.4 ± 2.2	2.3 ± 0.2
MAC+TAC	6	4.6 ± 1.4	67.6 ± 5.2	43.9 ± 2.9	3.4 ± 1.5
	24	6.1 ± 1.7	39.4 ± 5.2	39.3 ± 3.1	6.7 ± 1.8

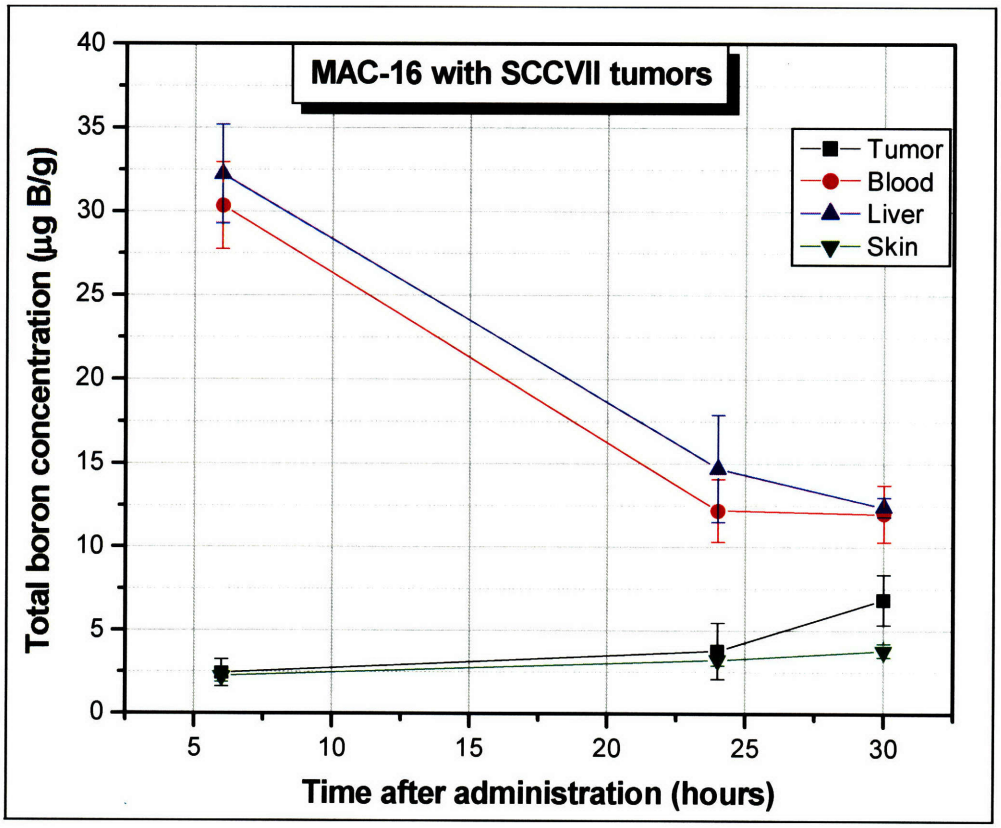

Figure 4.1. Total boron concentrations (μg B/g) versus time (hours) for MAC-16 injection into the retro-orbital sinus with a dose of 4.6 μg B/gbw. The 6-and 24-hour time points were scaled up by the ratio of injected boron dose, 1.4. Total boron concentration represents either total boron measured by ICP-OES or enriched ^{10}B measured by PGNAA. Points represent the mean ± SD for 5 mice bearing SCCVII tumors. Lines are drawn connecting the data to help guide the eye.

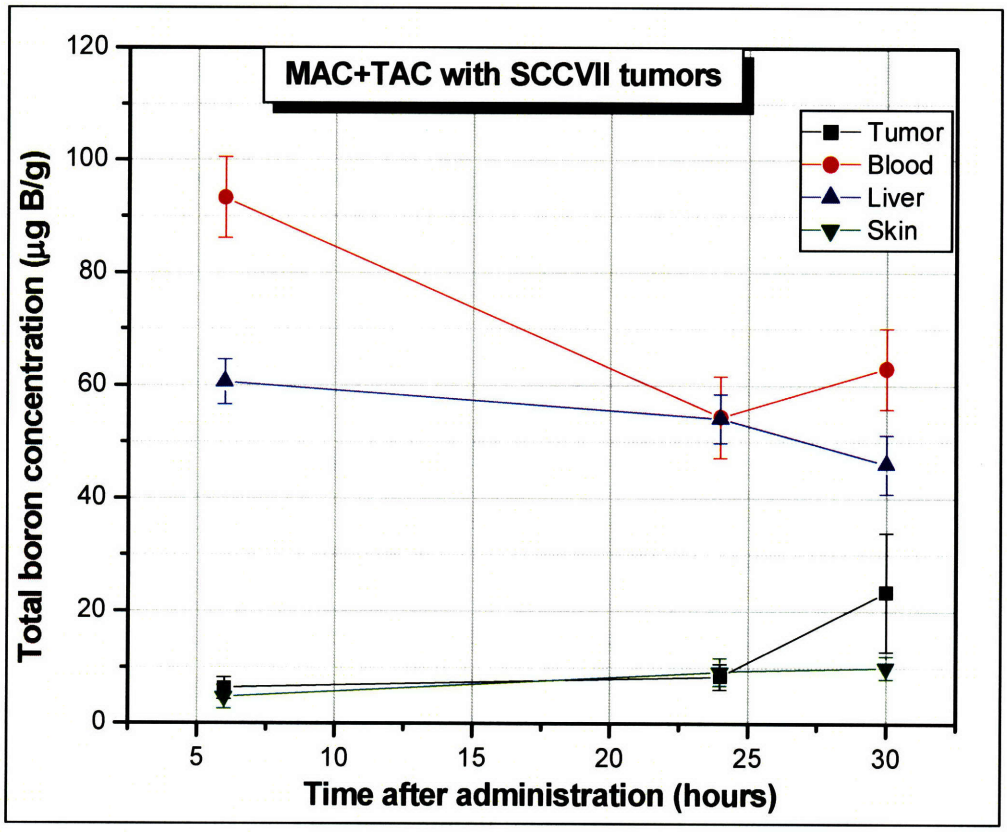

Figure 4.2. Total boron concentrations (µg B/g) versus time (hours) for MAC+TAC injection into the retro-orbital sinus at a dose of 12.3 µg B/gbw. The 6-and 24-hour time points were scaled up by the ratio of injected boron dose, 1.4. Total boron concentration represents either total boron measured by ICP-OES or enriched ^{10}B measured by PGNAA. Points represent the mean ± SD for 5 mice bearing SCCVII tumors. Lines are drawn connecting the data to help guide the eye.

A complete biodistribution study in mice bearing SCCVII tumors was carried out using an unenriched liposome solution and boron analysis by ICP-OES. Figure 4.3 and Table 4.3 show total boron concentrations measured by ICP-OES in SCCVII tumor, blood, liver, and skin as a function of time after injection of MAC-16 with a dose of 3.7 µg B/gbw. The maximum boron concentration in tumor was only 6 µg B/g at 24-30 hours after MAC-16 administration. This is far below the amount of boron needed to give enough dose in tumor during BNCT. Boron in blood and liver showed good clearance, but boron concentrations in skin were relatively high, almost the same as in tumor.

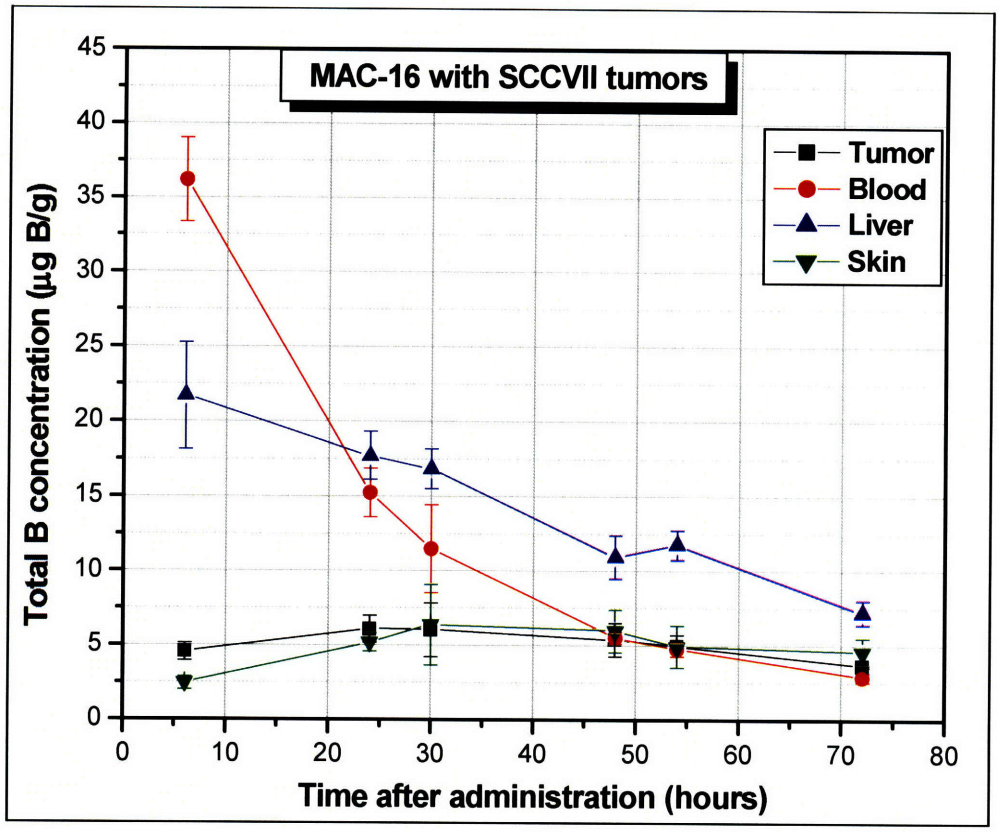

Figure 4.3. Total boron concentrations (µg B/g) versus time (hours) for MAC-16 with retro-orbital injection with a dose of 3.7 µg B/gbw. Points represent the mean ± SD for 3-4 mice bearing SCCVII tumors. Total boron concentrations were measured by ICP-OES. Lines are drawn connecting the data to help guide the eye.

Table 4.3. Total boron concentrations measured by ICP-OES for different times after MAC-16 retro-orbital injection with a dose of 3.7 µg B/gbw. Results are expressed as the mean ± SD for 3-4 mice bearing SCCVII tumors.

Time after MAC-16 administration (hrs)	B concentration (µg B/g)			
	Tumor	Blood	Liver	Skin
6	4.6 ± 0.6	36.2 ± 2.8	21.7 ± 3.6	2.5 ± 0.4
24	6.1 ± 0.9	15.2 ± 1.7	17.7 ± 1.6	5.2 ± 0.6
30	6.0 ± 1.8	11.4 ± 3.0	16.9 ± 1.3	6.4 ± 2.7
48	5.4 ± 1.1	5.5 ± 0.4	10.9 ± 1.5	6.0 ± 1.4
54	5.0 ± 0.7	4.7 ± 0.5	11.8 ± 1.0	5.0 ± 1.4
72	3.7 ± 0.1	2.9 ± 0.3	7.2 ± 0.8	4.6 ± 0.9

Figure 4.4 and Table 4.4 represent the total boron concentration in SCCVII tumor, blood, liver, and skin through the time course after administration of MAC+TAC with an injected dose of 9.6 μg B/gbw. Boron concentration in SCCVII tumor was maximized at 24 hours as only 9 μg B/g, while blood showed rapid clearance. However, tumor boron concentrations from both liposomes are too low to give successful tumor therapeutic response. Also, MAC+TAC injection produced a relatively high boron concentration in skin.

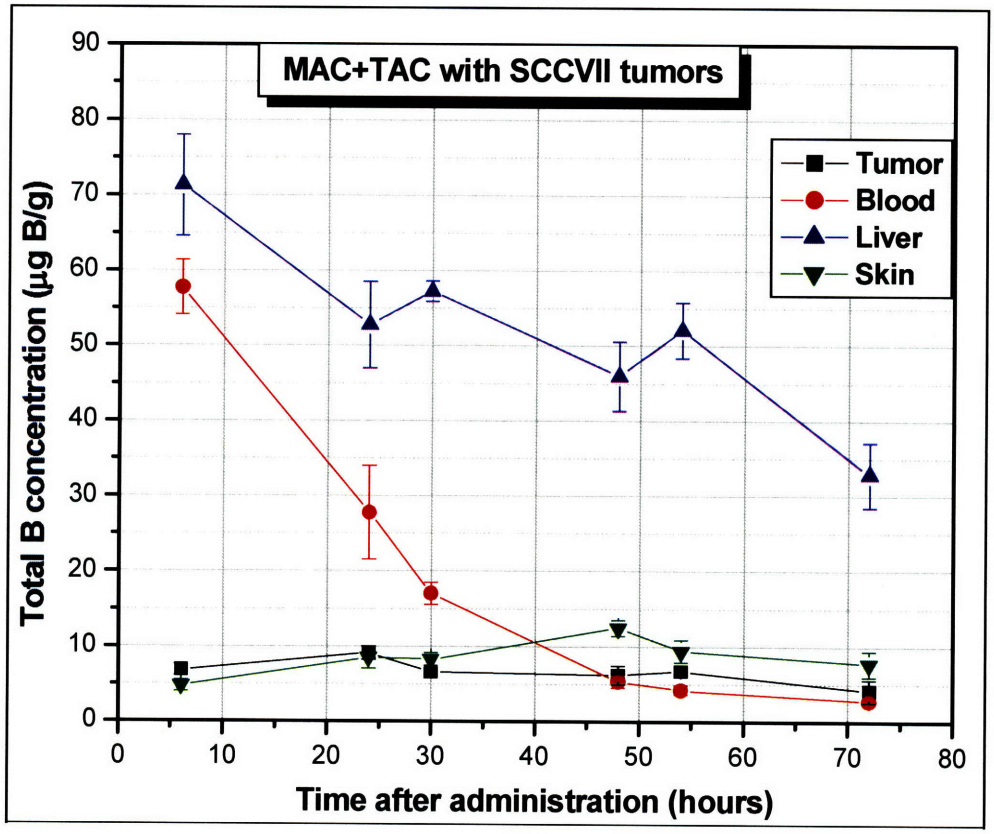

Figure 4.4. Total boron concentrations (μg B/g) versus time (hours) for MAC+TAC with retro-orbital injection dose of 9.6 μg B/gbw. Points represent the mean ± SD for 5 mice bearing SCCVII tumors. Total boron concentrations were measured by ICP-OES. Lines are drawn connecting the data to help guide the eye.

Table 4.4. Total boron concentrations measured by ICP-OES for different times after MAC+TAC retro-orbital injection with a dose of 9.6 μg B/gbw. Results are expressed as the mean ± SD for 5 mice bearing SCCVII tumors.

Time after MAC+TAC administration (hrs)	B concentration (μg B/g)			
	Tumor	Blood	Liver	Skin
6	6.8 ± 0.8	57.8 ± 4.9	71.3 ± 6.7	4.7 ± 0.8
24	9.1 ± 2.1	27.7 ± 6.2	52.8 ± 5.7	8.4 ± 1.5
30	6.6 ± 0.4	17.0 ± 1.5	57.2 ± 1.4	8.2 ± 0.9
48	6.2 ± 1.2	5.3 ± 0.8	45.9 ± 4.6	12.4 ± 1.0
54	6.7 ± 0.7	4.2 ± 0.7	52.1 ± 3.8	9.4 ± 1.5
72	4.1 ± 1.5	2.7 ± 0.3	32.8 ± 4.3	7.7 ± 1.7

4-2-2-2. BPA biodistribution study

Table 4.5 and Figure 4.5 show the ^{10}B concentrations in tumor and blood as a function of time after BPA-F injection at a dose of 43.0 μg ^{10}B /gbw. BPA which is a small molecule showed fast blood clearance and fast tumor uptake. The average ^{10}B concentration in tumor at 1 hour after BPA-F i.p. injection was 23.8 μg ^{10}B/g.

Table 4.5. ^{10}B concentrations at different times after BPA-F i.p. injection of 43.0 μg ^{10}B /gbw. Results are expressed as the mean ± SD for 5 mice bearing SCCVII tumors. ^{10}B concentrations were measured by PGNAA.

Time after BPA-F administration (hrs)	^{10}B concentration (μg ^{10}B/g)	
	Tumor	Blood
1	23.8 ± 3.0	15.3 ± 2.9
3	18.1 ± 4.3	11.3 ± 1.8
5	9.3 ± 2.3	5.5 ± 1.1

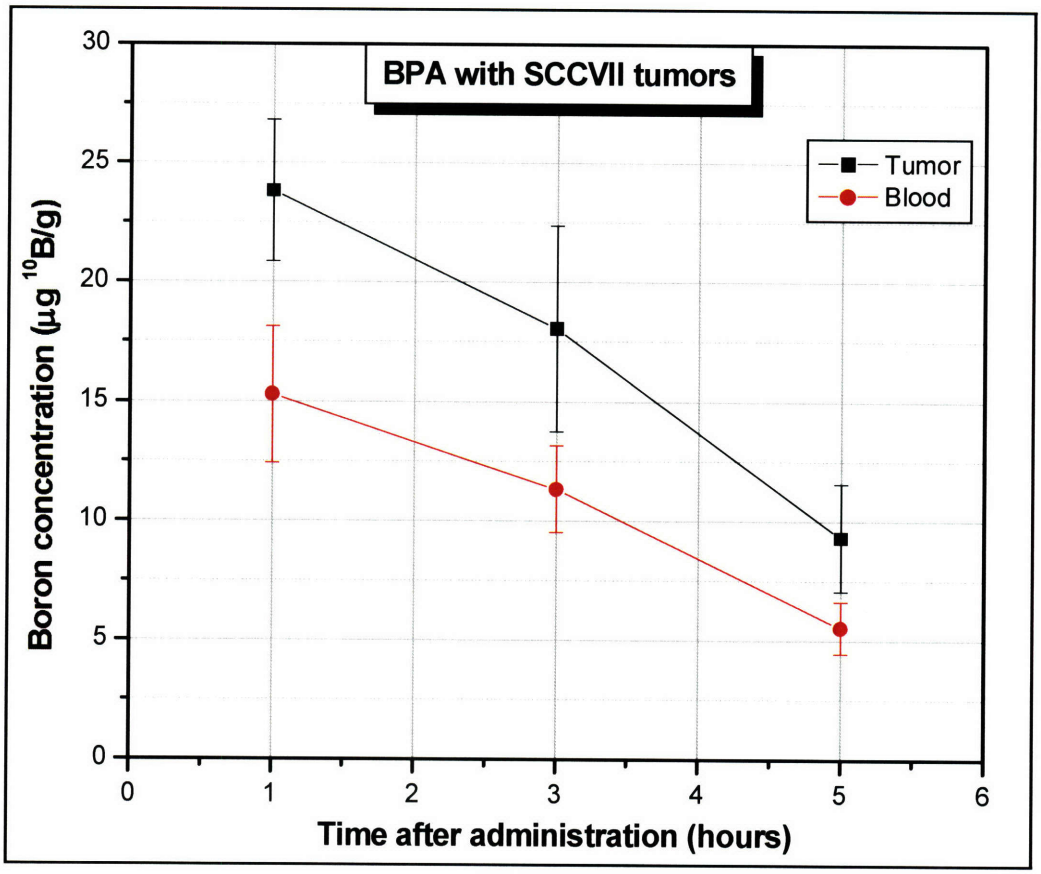

Figure 4.5. ^{10}B concentrations (μg ^{10}B/g) measured by PGNAA versus time (hours) after BPA-F i.p. injection at a dose of 43.0 μg ^{10}B /gbw. Points represent the mean ± SD for 5 mice bearing SCCVII tumors. Lines are drawn connecting the data to help guide the eye.

4-3. Multiple injections of MAC+TAC in the EMT-6 tumor model

4-3-1. Materials and methods

4-3-1-1. Tumor model

The murine mammary carcinoma EMT-6 was used as a tumor model of breast cancer. The EMT-6 cell line (kindly provided by Brookhaven National Laboratory) was grown in Dulbecco's Modification of Eagle's Medium (DMEM, Mediatech) supplemented with 10 % fetal bovine serum (SeraCare Life Science), 1 % 200 mM L-glutamine (Mediatech), and 1% 5,000 I.U./ml penicillin – 5,000 μg/ml streptomycin (Mediatech) at 37 °C in an atmosphere of 5 % CO_2. Cells were used for transplantation when the monolayer reached

~90 % confluence. Each female BALB/c mouse was briefly anesthetized with isoflurane, and then 10^6 EMT-6 cells in a volume of 0.1 ml were injected subcutaneously on the lower back.

4-3-1-2. Biodistribution study

Murine biodistribution studies used female BALB/c mice (18-20 g), with EMT-6 tumors implanted subcutaneously on the lower back at 10 days before the experiments. ^{10}B-enriched MAC+TAC solution (0.2 ml) was injected into the retro-orbital sinus of each mouse which was under brief isoflurane anesthesia. Two hours after the first injection, 0.2 ml of MAC+TAC solution was administrated into the other eye for the second injection. At the sacrifice time, which was 30 hours after the first injection, the mice were euthanized by isoflurane overdose. Blood was removed directly from the heart, and tumor, liver, and skin were collected for boron analysis. Tumor mass at the time of sacrifice was 100-250 mg. ^{10}B analysis for blood and tissues was carried out using PGNAA in the MITR-II.

4-3-1-3. Tumor therapeutic response study

Therapeutic response was evaluated in female BALB/c mice (18-21 g) bearing EMT-6 tumors implanted subcutaneously on the back at 10 days prior to the experiments. Thermal neutron beam irradiations were performed using the vertical M-011 thermal neutron beam of the MITR-II. Thermal neutron beam doses of 6 Gy were given to tumors on 8 mice at 30 hours after the first injection of the MAC+TAC double injections and to 6 mice with the beam only. Due to concerns over the high concentrations of ^{10}B in blood and liver resulting from double injections, 6 Gy was chosen as a reasonable dose in order to reduce the possibility of a severe normal tissue response or even death. To evaluate the tumor response, tumor volume was measured daily for 2 weeks after irradiations. After this 2-week period, tumor volume was measured 2-3 times per week. Tumor volume was calculated from orthogonal length and width measurements using the formula for an ellipsoid $V = (ab^2)/2$, where a is the larger of the two diameters. Mice were sacrificed if the tumor became necrotic or its volume exceeded 500 mm^3. If the tumor was controlled, mice were kept and observed to check for tumor recurrence for a period of 4-6 months.

4-3-2. Results

4-3-2-1. Biodistribution study

Boron concentrations in the EMT-6 tumor, blood, liver, and skin were measured 30 hours after the first injection (Table 4.6 and Table 4.7). Total injected doses were 25.6 μg ^{10}B/gbw for the first experiment shown in Table 5.6 and 37.5 μg ^{10}B/gbw for the second experiment shown in Table 4.7. A tumor therapeutic response study was included in the second experiment. Thus, Table 4.7 represents ^{10}B concentrations in tumor, blood, liver, and skin at the time of thermal neutron beam irradiation. Double injection of the MAC+TAC liposome solution produced ~50 μg ^{10}B/g of ^{10}B concentration in tumor, which is a sufficient amount of boron to expect tumoricidal effect. ^{10}B concentrations in blood and liver were also almost doubled compared to the single injection. Also, ^{10}B concentration in skin was significantly above the PGNAA detection limit while single injection of MAC+TAC produced a ^{10}B concentration in skin that was below the PGNAA detection limit.

Table 4.6. ^{10}B concentrations measured by PGNAA for 30 hours after the first of two retro-orbital injections of MAC+TAC (12.8 μg ^{10}B/gbw per injection). The interval between the two injections was 2 hours and the total injected dose was 25.6 μg ^{10}B/gbw. Results are expressed as the mean ± SD for 3 mice bearing EMT-6 tumor.

MAC+TAC double injection	^{10}B concentration (μg ^{10}B/g)			
	Tumor	Blood	Liver	Skin
30 hours after the first injection	51.0 ± 4.6	92.5 ± 21.8	107.6 ± 7.0	4.5 ± 0.8

Table 4.7. ^{10}B concentrations measured by PGNAA for 30 hours after the first of two retro-orbital injections of MAC+TAC (18.7 μg ^{10}B/gbw per injection). The interval between the two injections was 2 hours and the total injected dose was 37.5 μg ^{10}B/gbw. Results are expressed as the mean ± SD from 4 mice for blood, liver, and skin and from 2 mice for EMT-6 tumor.

MAC+TAC double injection	^{10}B concentration (μg ^{10}B/g)			
	Tumor	Blood	Liver	Skin
30 hours after the first injection	52.7 ± 0.1	115.4 ± 16.0	127.9 ± 7.3	6.1 ± 1.8

4-3-2-2. Tumor therapeutic response study

Table 4.8 summarizes the fraction of tumors controlled for the two treatment groups. Neutron beam irradiation alone (6 Gy) did not control any tumors. On the other hand, 6 Gy neutron beam irradiation with MAC+TAC double injection controlled 4 tumors out of 6 tumors in mice. Initially 8 mice were irradiated following MAC+TAC double injection, but 2 mice died at 7 days after irradiation. The reason of death was indeterminate, but was not from the tumor growth because the mice were found dead; there had been no signs of worsening body condition or diarrhea prior to day 7. However, because the time of death was close to the onset time of gastrointestinal (GI) injury, it could be from the GI syndrome. Neither treatment produced any evident normal tissue response. Mice in the 6 Gy beam irradiation with MAC+TAC double injection showed only a very minor hair loss over the whole body during 2 weeks after irradiation, despite the high ^{10}B concentrations in blood, liver, and skin. Some mice showed hair loss in the irradiated field. There was no redness of skin which was clearly shown during BNCT irradiation with BPA (Chapter 3).

Table 4.8. Fractions of EMT-6 tumors controlled with different treatments.

Treatment	Fraction of tumors controlled
6 Gy neutron beam	0/6 (Figure 4.6)
6 Gy neutron beam + MAC+TAC double injection	4/6* (Figure 4.7)

* 2 early deaths were censored.

Figure 4.6 and 4.7 represent measured tumor volumes of each mouse following 6 Gy neutron beam irradiation with and without double injections of MAC+TAC beginning 30 hours prior. Both groups show tumor growth delay post-irradiation but with different recovery rates. In the 6 Gy neutron beam alone group, growth suppression was initially maintained for ~6-7 days post-irradiation, but the tumors were quick to recover there after. This result is consistent with earlier 6 Gy neutron beam only irradiations described in Chapter 3. A much longer growth suppression period of ~26-28 days post-irradiation was observed in the 6 Gy neutron beam irradiations following double injection of MAC+TAC.

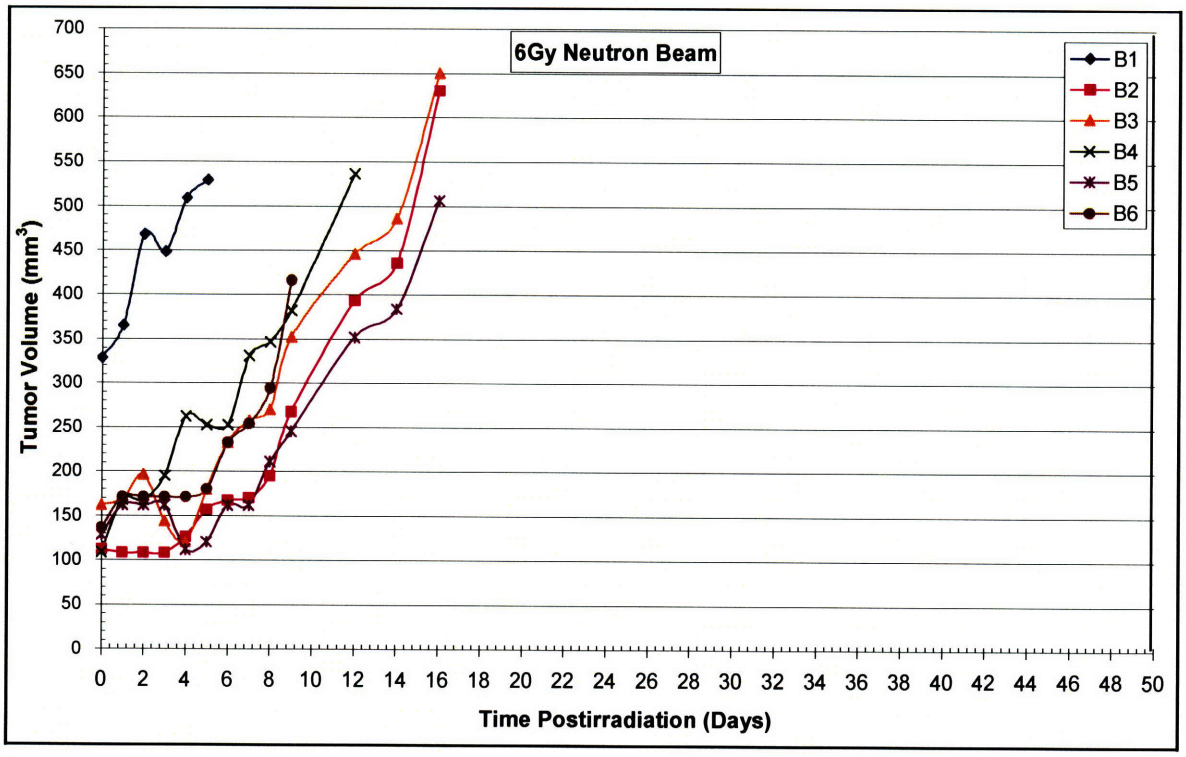

Figure 4.6. EMT-6 tumor volume (mm^3) versus time (days) after 6 Gy neutron beam irradiation. Each line indicates the tumor volume for an individual mouse.

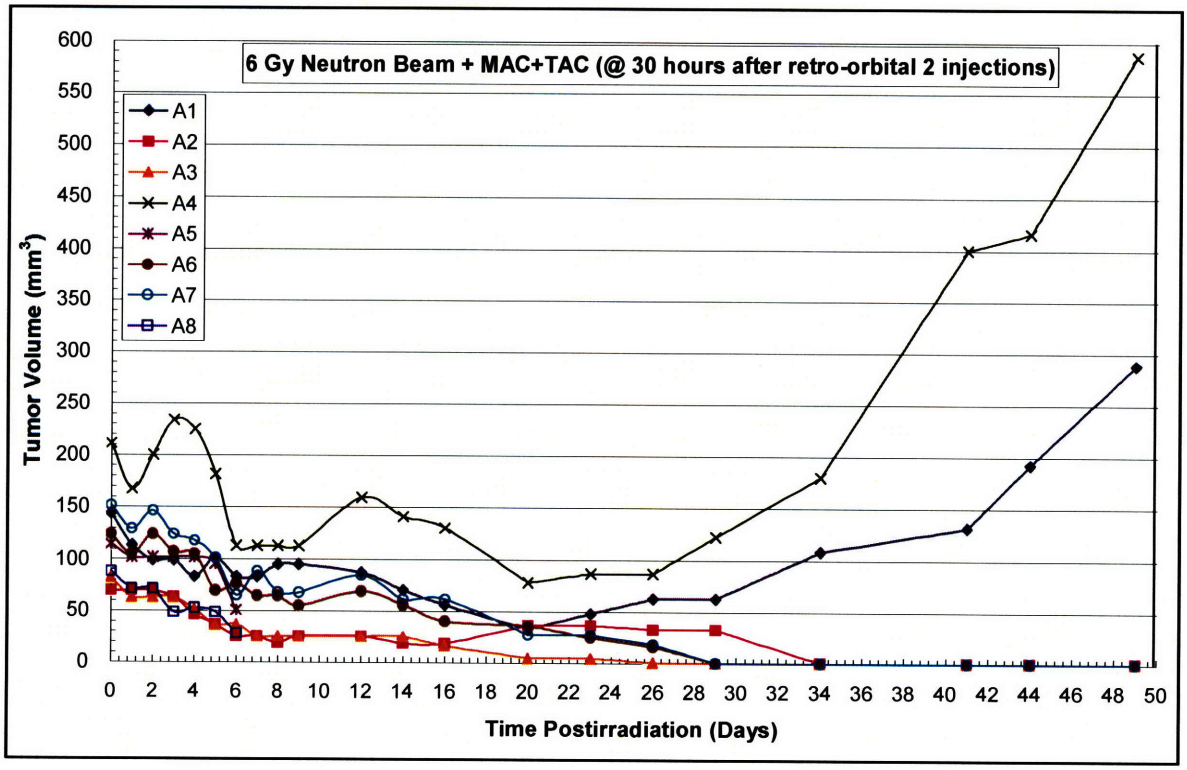

Figure 4.7. EMT-6 tumor volume (mm^3) versus time (days) after 6 Gy neutron beam irradiation at 30 hours after 1st injection of MAC+TAC double injections. Each line indicates the tumor volume for an individual mouse.

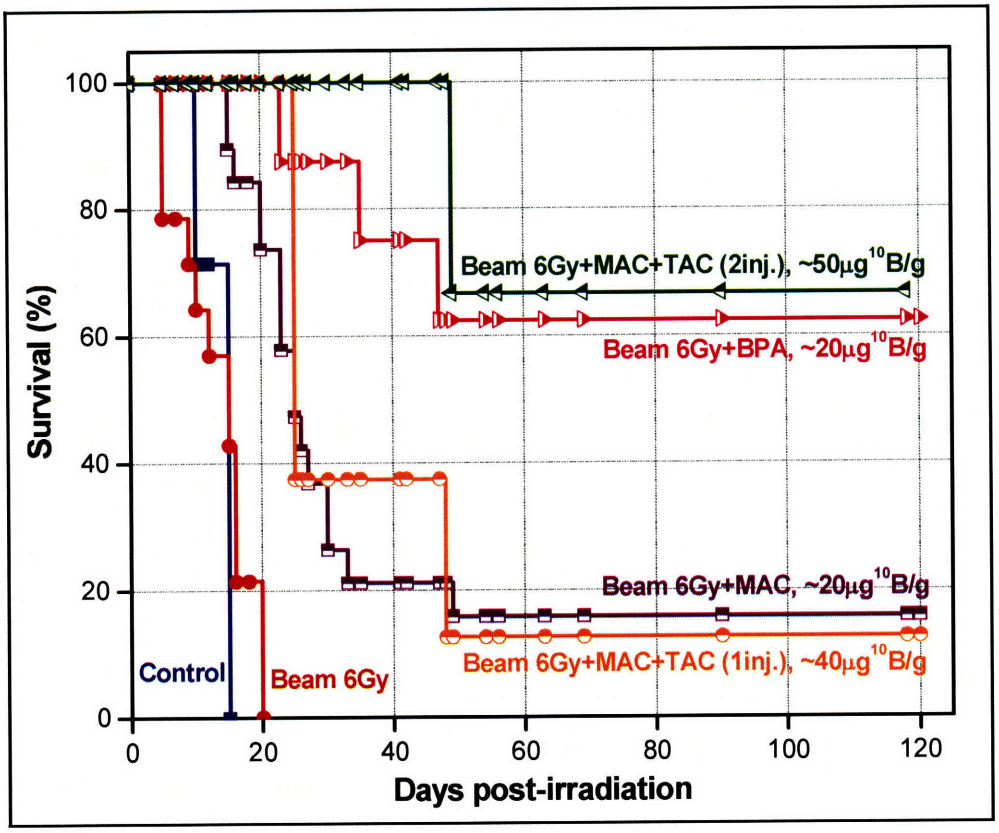

Figure 4.8. Mouse survival (%) as a function of time after EMT-6 tumor irradiation with 6 Gy thermal neutron beam alone (n=14), 6 Gy thermal neutron beam in the presence of MAC (n=19), MAC+TAC (single (n=8) and double (n=6) injections), and BPA (n=8). A control group of mice bearing EMT-6 tumors (n=7) received no irradiation. Approximate ^{10}B concentrations in the tumor at the time of BNCT are indicated in the Figure.

Figure 4.8 illustrates the mouse survival percentage as a function of time after irradiation with 6 Gy thermal neutron beam alone, 6 Gy thermal neutron beam in the presence of MAC, MAC+TAC (single and double injections), and BPA. Approximate ^{10}B concentrations in the tumor at the time of BNCT were 20 μg ^{10}B/g from MAC and BPA, 40 μg ^{10}B/g from a single injection of MAC+TAC, and 50 μg ^{10}B/g from a double injection of MAC+TAC. The survival following 6 Gy neutron beam alone was obtained by combining the results of this experiment (Figure 4.6; n = 6) and the first experiment (Figure 3.6; n = 8). With the same 6 Gy neutron beam dose, double injections of MAC+TAC showed a superior mouse survival (66.7 %). Here, two mice in the 6 Gy with MAC+TAC two injections that died of unknown cause at day 7 were excluded as they possibly died from side effects related to the experiment.

4-4. Discussion

As described in Chapter 3, liposome-based BNCT in the EMT-6 tumor model had little effect. The primary reason was believed to be the poor microscopic distribution of ^{10}B in the tumor at the time of therapy. Two approaches were taken to further explore the potential usefulness of liposomes for BNCT: 1) To determine if the poor microscopic boron distribution was unique to the EMT-6 model, a biodistribution study was carried out in another tumor model; the SCCVII mouse squamous cell carcinoma. 2) A modified injection protocol was used in an attempt to increase the ^{10}B concentration and uniformity of uptake in the EMT-6 tumor model.

As an alternative, the SCCVII mouse squamous cell carcinoma was used, which is a well-established tumor model for head and neck cancer. Variable results were obtained from the different uptake studies that used different batches of liposomes. In the complete time study, boron uptake was measured at between 6-72 hours after injection. The maximum boron concentration in tumor achieved with MAC+TAC was only 9.1 μg B/g after 24 hours. This maximum tumor boron concentration is a third of the blood boron concentration and this trend is consistent in another study using ^{10}B-enriched liposomes. MAC-16 or MAC+TAC liposomes did not produce enough ^{10}B uptake in the SCCVII tumor, which was less than the requisite boron amount for BNCT (20-30 μg B/g) and especially less than in the EMT-6 tumor. Therefore, further study was not warranted in this tumor model.

The EMT-6 and SCCVII tumors showed different uptake of liposomes. Since liposomes accumulate in the tumor via tumor leaky vasculature, a higher boron uptake can be observed in the well-vascularized tumors. These two tumors are poorly-vascularized, solid animal tumors, which commonly consist of hypoxic cells [105]. The EMT-6 tumors generally contain larger necrotic area and hypoxic cells than the SCCVII tumors [106]. The histology sections showed an apparent necrotic region in the EMT-6 tumors even with a small diameter of approximately 5 mm. The hypoxic fraction of tumor increases with increasing tumor size. With the tumor size of 5-10 mm, which is the range for our studies, the EMT-6 tumor has relatively higher hypoxic fraction (5-20 %) than the SCCVII tumor (1-10 %) since the EMT-6 tumor grows faster than SCCVII tumor [107]. This histology information suggests that the SCCVII tumor would be a better tumor model in the use of

liposomes. However, the SCCVII tumor showed much less boron uptake than the EMT-6 tumor, so there must be other explanations. The vasculature permeability of these two tumors could be different, which could affect passage of the liposomes and consequently result in different boron uptake in the tumor. Blood and liver showed relatively faster clearance in C3H mice bearing SCCVII tumors, which could indicate less ^{10}B is available to accumulate in the tumor. ^{10}B accumulation in the skin for the SCCVII tumor model, which used C3H female mice, was much higher (maximum [^{10}B] = ~13 μg ^{10}B/g from MAC+TAC) than for the EMT-6 tumor model using BALB/c female mice whose skin showed undetectable boron uptake by PGNAA.

The EMT-6 tumor showed sufficient boron uptake but had poor microscopic boron distribution. Since each injection volume was limited to 0.2 ml, a multiple-injection method, which increased the total injection dose, was applied in an effort to improve microscopic distribution. As a pilot study, a simple protocol, a double injection with a 2-hour interval between injections with the EMT-6 tumor, was evaluated in a single experiment. This produced approximately 50 μg ^{10}B/g in the EMT-6 tumors, which was almost twice the desired boron concentration. ^{10}B concentrations in blood and liver were also relatively high; over 100 μg ^{10}B/g.

Initially 8 mice bearing EMT-6 tumors were irradiated after two injections of MAC+TAC, but 2 mice died at 7 days after irradiation. This death was not from the tumor overgrowth. However, there was no obvious evidence of death such as diarrhea by GI damage, and it was not possible to perform histology study in gut, bone marrow, or liver to determine the reason for death because mice were found dead in their cage. All mice which received a double injection lost from 2 to 4 g of their body weight (10-20 % of total body weight) within 6 days after the irradiation. Both dead mice lost 4 g of body weight a day before dying. The fact that the time of death (7 days after irradiation) would imply the death could be from GI damage since the GI syndrome generally occurs at 5-6 days after the irradiation. Another explanation might be liver toxicity, because part of liver was in the irradiation field and ^{10}B concentration in liver was around 130 μg ^{10}B/g. Even though the neutron flux is attenuated at the depth of liver, boron dose may nevertheless be significant and cause some damage. Irradiations following a single injection of MAC+TAC did not

cause deaths other than tumor overgrowth with boron concentrations in blood and liver of 51 and 76 μg ^{10}B/g, respectively.

Minor hair loss over the whole body was observed from mice irradiated with 6 Gy of neutron beam following a double injection of MAC+TAC, but it recovered in 2 weeks after irradiation. The irradiated area of each mouse was shaved at the time of implanting tumor cells, but hair on some mice did not regrow after irradiation for several weeks. All mice in which tumors were controlled had fully regrown hair on their back in about 4 weeks. There was no other apparent skin damage such as redening. In BPA-mediated BNCT from Chapter 3, one of these mice showed severe moist desquamation at 3-4 weeks after irradiation [108]. On the other hand, in all liposome-mediated BNCT using MAC-16 and MAC+TAC even with a double injection, there was no obvious skin damage. This could be an advantage of using liposomes.

The tumor response study controlled 4 EMT-6 tumors out of 6 (66.7 % tumor control). Here, two mice that died on day 7 probably from GI damage were not included in the survival graph. An improved tumor response from the double liposome injection could be from increased overall boron concentration in the tumor. Since sufficient amounts of boron accumulated at the edge parts of the tumor, this could kill all the tumor cells at the edge and could lead to an absolute lack of blood and oxygen supply to the middle part of tumor which already consists of many necrotic cells. This condition could control tumor, especially for a small size of tumor. Another possible explanation for improved tumor response could be the synergetic effect of damages on tumor cells and tumor vasculature. High boron accumulation in blood can cause a significant damage on tumor vasculature along with the direct damage on tumor cells from boron present in tumor. A more uniform distribution of boron in the tumor was anticipated, but the HRQAR image (Figure 4.9) from a double injection of liposomes shows that although more boron is taken up in the EMT-6 tumor (as measured by PGNAA) the overall distribution is still highly non-uniform. Further investigation is suggested for understanding the mechanism of improved therapy response.

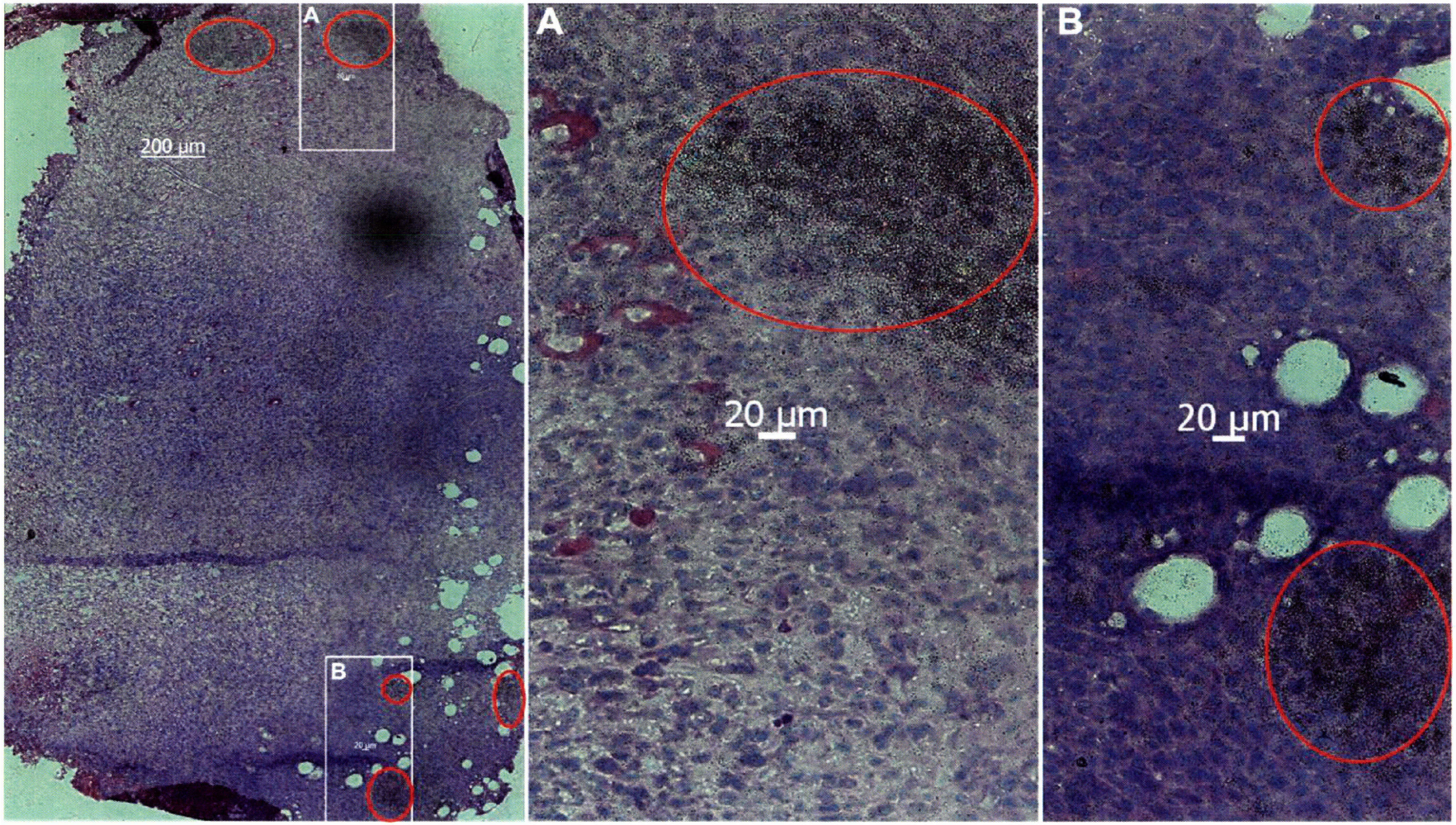

Figure 4.9. HRQAR image of the EMT-6 tumor that received a double MAC+TAC injection to visualize boron-neutron capture particle tracks (black dots) superimposed on the histology. Red circles highlight areas of concentrated tracks. More boron is taken up in the EMT-6 tumor, but the overall distribution is still highly non-uniform. Scale bar: 200 µm for the left and 20 µm for the middle and right panels that are magnified portion of the identified insets A and B. (HRQAR image produced by Dr. Kent Riley.)

Concerning the safety of this high ^{10}B concentration in blood, the responses of central nervous system (CNS) to BSH using a rat spinal cord model were reviewed due to the similar behavior in the CNS of liposomes and BSH because of their large size [108, 109]. The model for the CNS was the rat spinal cord irradiated at BMRR with a boron concentration in blood, approximately 100 μg ^{10}B/g. The endpoint was limb paralysis within 7 months. Effective doses for 50 % paralysis (ED_{50}) were 24.9 Gy of boron dose and 5.4 Gy of beam dose in the neutron beam with BSH group [109]. Since the quality of beam was different between the MITR-II and the BMRR, the RBE values of the beam were different: 1.2 at the MITR-II for rat lung irradiation [89] and 1.4 at the BMRR for rat spinal cord irradiation [109]. The same CBE value, 0.46, for CNS response could be applied to both BSH and liposomes due to their similar behavior in the CNS. Using these data and ED_{50} (boron dose = 25.7 Gy) determined for the MITR-II thermal neutron beam, the maximum boron concentration in blood before the onset of serious CNS response would be 35 μg ^{10}B/g at the beam dose of 6 Gy. Therefore, if this double injection protocol was applied to tumor which contained spinal cord in the irradiation field, it would cause severe CNS response.

The same type of analysis for liposomes can be applied to the skin response by comparing with BSH. Using the information of the RBE of the BMRR beam (3.5), ED_{50} for moist desquamation in the skin response (47.86 Gy BMRR beam), and the CBE for skin response (0.55) [108], the maximum boron concentration in skin to avoid serious skin response would be 87 μg ^{10}B/g with 6 Gy of the MITR-II thermal neutron beam dose. When BSH was injected in rats, boron concentrations in blood and skin (~80 μg ^{10}B/g) were comparable between 30 minutes and 2 hours after injection [108]. However, boron concentrations in skin delivered by liposomes remained below 10 μg ^{10}B/g at all time points with a double injection. This is a major difference between liposomes and BHS and indicates that liposomes can be much safer than BSH in the skin.

This double injection experiment was a single pilot study using only a few animals. Considering the promising result of this experiment, the administration for multiple injections could be modified for further improvement of the use of liposomes. Several injections of liposome solution delivered after the blood has cleared would achieve even higher ^{10}B concentration in the tumor due to a long retention there and low boron

concentrations in the blood and liver. Since the EMT-6 tumor grows relatively rapidly, loaded boron from multiple injections might be diluted by an enlarged tumor size over the period of several days. A simple estimation can be used to simulate the boron concentration in tissues after the multiple-injection. The boron concentration profile from a single injection can be shifted with the interval of the injection time and then the boron concentration of each time point can be added. This estimation for a double injection with 2-hour-interval agreed well for boron concentration of tumor and liver but not for blood. Blood boron concentration was measured as ~50 % higher than the estimation, which suggests that high boron concentration in blood or liver may affect boron clearance from blood. This estimation using a single injection profile of MAC-16 liposome solution with the EMT-6 tumor showed low boron concentration in the blood and liver (< 50 μg ^{10}B/g) and high boron concentration in the tumor (~90 μg ^{10}B/g) at 70 hours after 1st injection when MAC-16 solution was injected 6 times every 4 hours over 2 days. Even though blood boron concentration may be underestimated, this can be a safer and more effective protocol for multiple injection experiments.

CHAPTER FIVE

CONCLUSIONS

5-1. Summary

This project developed a radiobiological assay for testing new boron compounds with the aim of identifying promising new compounds to help optimize and improve the effectiveness of BNCT. An *in vitro* evaluation methodology was developed to enable the efficacy of a boron compound to be determined during the early stages of its development and which is consequently available in only limited quantities (less than a milligram of ^{10}B). A colorimetric assay and 96-well plates were applied to minimize the quantity of compound required for testing and was optimized for the murine SCCVII, squamous cell carcinoma to determine the chemical toxicity and relative cellular uptake by comparison with reference compounds, boric acid and BPA. Chemical toxicity testing revealed a test compound, BOPP, was toxic over concentrations of 10 μg ^{10}B/ml that was considered an upper limit of acceptability during testing so as not to mask radiation induced damage. Cell irradiations were performed using the thermal neutron beam at MITR-II and survival curves for different compounds were compared at concentrations of approximately 5 μg ^{10}B/ml for each compound. Using less than 300 μg of BOPP, and 250 kVp X-rays as control irradiations, a compound biological effectiveness (CBE) of 3.3 ± 0.7 was determined for BOPP. A comparable result (3.5 ± 0.5) was obtained for boric acid whereas BPA was significantly higher (6.1 ± 0.7). These CBEs reflect the relative intracellular accumulation of ^{10}B: similarly low for BOPP and boric acid, higher for BPA. A comprehensive uncertainty analysis for the CBE value yielded an uncertainty of 10-20 %. Thus, when general CBE factor is applied to another study for the same endpoint using a different biological system (i.e. humans), this large uncertainty must be recognized as a major source of experimental error especially for a study in which the dose-response relationship is steep and a slightly different dose could cause a large change in outcome.

Boronated liposomes have shown a sufficient boron uptake for therapeutic BNCT in the EMT-6 murine mammary carcinoma model that warranted further evaluation with a therapy study. This had not been performed before. In this thesis, boronated liposomes were evaluated for the first time with tumor therapy experiments using the EMT-6 tumor model. Results of earlier biodistribution studies were confirmed and similar boron uptake in the tumor (approximately 20 μg ^{10}B/g) was observed with MAC-16 liposomes and BPA, one of the two boron compounds approved for clinical trials of BNCT in the USA. However, the tumor control in mice for the EMT-6 tumor from BPA was superior (62.5 %) to that from MAC-16 liposomes (15.8 %). Microscopic distribution studies using fluorescent-labeled liposomes and HRQAR exhibited a non-uniform microscopic distribution of boron delivered from liposomes in the tumor at the time of therapy and explains the lack of therapeutic effect. This underlines the importance of a boron distribution at a microscopic level. Further exploration of the potential usefulness of liposomes was attempted by using another tumor model, the SCCVII mouse squamous cell carcinoma. Insufficient boron uptake in the SCCVII tumor was shown in the biodistribution study with liposomes and no further investigation was performed. Animal irradiations following a double injection of MAC+TAC liposomes were performed as a pilot study. Double injection of MAC+TAC liposomes did not improve the observed homogeneity of ^{10}B within the tumor, but an enhanced therapeutic effect (comparable to BPA-based BNCT) was obtained that is mainly attributed to higher ^{10}B concentration from the increased injected dose of the compound.

5-2. General concepts for evaluating boron compounds

The best method for evaluating new boron compounds depends upon their stage of development as well as their mechanism for selective tumor uptake. Since boron compounds are often synthesized in small quantities at early stages of development, applying an *in vitro* screening method is often advantageous. If the boron compound has to be tested in a specific cell line that for example express a particular enzyme, the protocol for the colorimetric assay must first be optimized especially for initially plated cell density and growth time. These results can then be used in the clonogenic assay to get more precise CBE factors. A boron compound that has already demonstrated promising *in vitro* results

can be evaluated in a small animal model to demonstrate sufficient tumor uptake, followed by therapy experiments to test its radiobiological effectiveness for BNCT. The tumor model has to be chosen after considering the targeting properties of the compound and the possible clinical application for BNCT. *In vivo* evaluation is best performed by using one large compound batch.

1) *In vitro* compound screening at an early stage of compound development

i. Identification of chemical toxicity: The pharmacological toxicity is determined by incubating cells with boron compound at increasing concentrations using the colorimetric assay.
ii. Optimization of protocol for the colorimetric assay: The protocol of the colorimetric assay must be optimized for each cell line. Important parameters are the number of cells initially plated in each well and the growth time.
iii. Determination of efficacy: The presence of an effect from boron is determined with the colorimetric assay by comparing cell irradiations of a test compound with those of boric acid and BPA at the same boron concentration of 5-10 μg ^{10}B/ml.
iv. Optimization of experimental conditions for the clonogenic assay: When a test compound appears superior to boric acid with the colorimetric assay, experimental conditions for the clonogenic assay are optimized. Important parameters are the number of cells plated in the Petri dish at each absorbed dose point and the total quantity of boron required.
v. Verification of a test compound: Using the clonogenic assay, the efficacy of a test compound is verified as a promising boron compound for further *in vivo* study.

2) *In vivo* evaluation after *in vitro* testing or where *in vitro* models are not adequate

i. Biodistribution study: A biodistribution experiment is performed to measure boron uptake in the tumor and other tissues, such as blood, liver, skin, and other vital organs, as a function of time after injection. Then, the time for BNCT is determined when the boron concentration in tumor is highest relative to normal tissue.
ii. Microdistribution study: The microscopic distribution of boron in the tumor is analyzed using HRQAR with the tissues harvested from the biodistribution study.

iii. Tumor therapy response study: A boron compound that delivers sufficient ^{10}B to tumor warrants a tumor therapeutic response study to evaluate the effectiveness BNCT at the time determined in the biodistribution study. The efficacy of a testing compound may be compared to that of BPA, which is preferentially taken up in many tumors.

iv. Normal tissue response study: The response of normal tissues is characterized under the same conditions used for the tumor therapy. Normal tissues include CNS, skin, and the oral mucosa, as well as other critical organs that may have exhibited uptake in the biodistribution study.

5-3. Considerations for future work

As an attempt to construct a more systematic *in vitro* compound evaluation for new compounds which do not need a specific cell line to be tested, the protocol for the colorimetric assay can be optimized in advance for several tumor cell lines which can be considered as possible candidates for BNCT. Thus, when promising compounds, determined by *in vitro* testing, are evaluated further in a small animal model, the tumor model for *in vivo* evaluation can be rationally selected based on tumor cell line results from *in vitro* screening.

Tumor therapy response from a pilot study with a double injection of liposomes was comparable to that from BPA. However, with a double injection of liposomes, two mice (25 % of total irradiated mice) died for unknown reasons after irradiation. These appear to be a risk with high blood and liver boron concentrations. The microscopic analysis using HRQAR indicates that a double injection of liposomes increased the total amount of boron throughout the tumor rather than improved uniformity of boron uptake, which caused improved therapy response. Further quantitative analysis with HRQAR at a microscopic level could be carried out in order to distinguish which part of the EMT-6 tumor would accumulate more boron from a multiple injection of liposomes. Since the mechanism for the improved therapy response was not well understood, further investigation to elucidate the mechanism would be useful, which can be performed simultaneously with therapy using for example the *in vivo/in vitro* assay, micronucleus assay, or apoptosis detection [110, 111].

REFERENCES

1. G.L. Locher, *Biological effects and therapeutic possibilities of neutrons.* Am J Roentgenol, 1936. **36**: p. 1 - 13.

2. J.A. Coderre, J.C. Turcotte, K.J. Riley, P.J. Binns, O.K. Harling, and W.S. Kiger III, *Boron Neutron Capture Therapy: Cellular targeting of high linear energy transfer radiation.* Technology in Cancer Research and Treatment, 2003. **2**: p. 355-375.

3. R.F. Barth, A.H. Soloway, and R.G. Fairchild, *Boron Neutron Capture Therapy of Cancer.* Cancer Res, 1990. **50**: p. 1061 - 1070.

4. J.A. Coderre and G.M. Morris, *The radiation biology of boron neutron capture therapy.* Radiat Res, 1999. **151**(1): p. 1-18.

5. D.N. Slatkin, *A history of boron neutron capture therapy of brain tumours. Postulation of a brain radiation dose tolerance limit.* Brain, 1991. **114**(Pt 4): p. 1609-29.

6. W.H. Sweet, *Early history of development of boron neutron capture therapy of tumors.* J Neurooncol, 1997. **33**(1-2): p. 19-26.

7. J.T. Godwin, L.E. Farr, W.H. Sweet, and J.S. Robertson, *Pathological study of eight patients with glioblastoma multiforme treated by neutron capture therapy using boron 10.* Cancer, 1955. **8**: p. 601 - 615.

8. A.H. Soloway, H. Hatanaka, and M.A. Davis, *Penetration of brain and brain tumor. VII. Tumor-binding sulfhydryl boron compounds.* J Med Chem, 1967. **10**: p. 714 - 717.

9. Y. Nakagawa, K. Pooh, T. Kobayashi, T. Kageji, S. Uyama, A. Matsumura, and H. Kumada, *Clinical review of the Japanese experience with boron neutron capture therapy and a proposed strategy using epithermal neutron beams.* J Neurooncol, 2003. **62**(1-2): p. 87-99.

10. J.A. Coderre, T.M. Button, P.L. Micca, C.D. Fisher, M.M. Nawrocky, and H.B. Liu, *Neutron capture therapy of the 9L rat gliosarcoma using the p-boronophenylalanine-fructose complex.* Int J Radiat Oncol Biol Phys, 1994. **30**(3): p. 643-52.

11. O.K. Harling, K.J. Riley, T.H. Newton, B.A. Wilson, J.A. Bernard, L.-W. Hu, E.J. Fonteneau, P.T. Menadier, S.J. Ali, B. Sutharshan, G.E. Khose, Y. Ostrovsky, P.W. Stahle, P.J. Binns, W.S. Kiger III, and P.M. Busse, *The fission converter-based epithermal neutron irradiation facility at the Massachusetts Institute of Technology reactor.* Nuc Sci Eng, 2002. **140**: p. 223-240.

12. K.J. Riley, P.J. Binns, and O.K. Harling, *A state-of-the-art epithermal neutron irradiation facility for neutron capture therapy.* Phys Med Biol, 2004. **49**(16): p. 3725-35.

13. A.Z. Diaz, *Assessment of the results from the phase I/II boron neutron capture therapy trials at the Brookhaven National Laboratory from a clinician's point of view.* J Neurooncol, 2003. **62**(1-2): p. 101-9.

14. M. Chadha, J. Capala, J.A. Coderre, E.H. Elowitz, J. Iwai, D.D. Joel, H.B. Liu, L. Wielopolski, and A.D. Chanana, *Boron neutron-capture therapy (BNCT) for glioblastoma multiforme (GBM) using the epithermal neutron beam at the Brookhaven National Laboratory.* Int J Radiat Oncol Biol Phys, 1998. **40**(4): p. 829-34.

15. A.D. Chanana, J. Capala, M. Chadha, J.A. Coderre, A.Z. Diaz, E.H. Elowitz, J. Iwai, D.D. Joel, H.B. Liu, R. Ma, N. Pendzick, N.S. Peress, M.S. Shady, D.N. Slatkin, G.W. Tyson, and L. Wielopolski, *Boron neutron capture therapy for glioblastoma multiforme: interim results from the phase I/II dose-escalation studies.* Neurosurgery, 1999. **44**(6): p. 1182-1193.

16. P.M. Busse, O.K. Harling, M.R. Palmer, W.S. Kiger III, J. Kaplan, I. Kaplan, C.F. Chuang, J.T. Goorley, K.J. Riley, T.H. Newton, G.A. Santa Cruz, X.Q. Lu, and R.G. Zamenhof, *A critical examination of the results from the Harvard-MIT NCT program phase I clinical trial of neutron capture therapy for intracranial disease.* J Neurooncol, 2003. **62**(1-2): p. 111-21.

17. S.J. Liberman, A. Dagrosa, R.A. Jimenez Rebagliati, M.R. Bonomi, B.M. Roth, L. Turjanski, S.I. Castiglia, S.J. Gonzalez, P.R. Menendez, R. Cabrini, M.J. Roberti, and D.A. Batistoni, *Biodistribution studies of boronophenylalanine-fructose in melanoma and brain tumor patients in Argentina.* Appl Radiat Isot, 2004. **61**(5): p. 1095-100.

18. S.J. Gonzalez, M.R. Bonomi, G.A. Santa Cruz, H.R. Blaumann, O.A. Calzetta Larrieu, P. Menendez, R. Jimenez Rebagliati, J. Longhino, D.B. Feld, M.A. Dagrosa, C. Argerich, S.G. Castiglia, D.A. Batistoni, S.J. Liberman, and B.M. Roth, *First BNCT treatment of a skin melanoma in Argentina: dosimetric analysis and clinical outcome.* Appl Radiat Isot, 2004. **61**(5): p. 1101-5.

19. H. Joensuu, L. Kankaanranta, T. Seppala, I. Auterinen, M. Kallio, M. Kulvik, J. Laakso, J. Vahatalo, M. Kortesniemi, P. Kotiluoto, T. Seren, J. Karila, A. Brander, E. Jarviluoma, P. Ryynanen, A. Paetau, I. Ruokonen, H. Minn, M. Tenhunen, J. Jaaskelainen, M. Farkkila, and S. Savolainen, *Boron neutron capture therapy of brain tumors: clinical trials at the Finnish facility using boronophenylalanine.* J Neurooncol, 2003. **62**(1-2): p. 123-34.

20. K. Hideghety, W. Sauerwein, K. Haselsberger, F. Grochulla, H. Fankhauser, R. Moss, R. Huiskamp, D. Gabel, and M. de Vries, *Postoperative treatment of glioblastoma with BNCT at the petten irradiation facility (EORTC protocol 11,961).* Strahlenther Onkol, 1999. **175 Suppl 2**: p. 111-4.

21. Y. Nakagawa and H. Hatanaka, *Boron neutron capture therapy. Clinical brain tumor studies.* J Neurooncol, 1997. **33**(1-2): p. 105-15.

22. Y. Nakagawa, K. Pooh, T. Kobayashi, T. Kageji, S. Uyama, A. Matsumura, and H. Kumada, *Clinical review of the Japanese experience with boron neutron capture therapy and a proposed strategy using epithermal neutron beams.* J Neurooncol, 2003. **62**(1-2): p. 87-99.

23. T. Yamamoto, A. Matsumura, K. Nakai, Y. Shibata, K. Endo, F. Sakurai, T. Kishi, H. Kumada, K. Yamamoto, and Y. Torii, *Current clinical results of the Tsukuba BNCT trial.* Appl Radiat Isot, 2004. **61**(5): p. 1089-93.

24. I. Kato, K. Ono, Y. Sakurai, M. Ohmae, A. Maruhashi, Y. Imahori, M. Kirihata, M. Nakazawa, and Y. Yura, *Effectiveness of BNCT for recurrent head and neck malignancies.* Appl Radiat Isot, 2004. **61**(5): p. 1069-73.

25. L. Kankaanranta, T. Seppala, H. Koivunoro, K. Saarilahti, T. Atula, J. Collan, E. Salli, M. Kortesniemi, J. Uusi-Simola, A. Makitie, M. Seppanen, H. Minn, P. Kotiluoto, I. Auterinen, S. Savolainen, M. Kouri, and H. Joensuu, *Boron Neutron Capture Therapy in the Treatment of Locally Recurred Head and Neck Cancer.* Int J Radiat Oncol Biol Phys, 2007.

26. O.K. Harling, K.J. Riley, P.J. Binns, H. Patel, and J.A. Coderre, *The MIT User Center for neutron capture therapy research.* Radiat Res, 2005. **164**(2): p. 221-9.

27. R.F. Barth, J.A. Coderre, M.G. Vicente, and T.E. Blue, *Boron neutron capture therapy of cancer: current status and future prospects.* Clin Cancer Res, 2005. **11**(11): p. 3987-4002.

28. A. Wittig, W.A. Sauerwein, and J.A. Coderre, *Mechanisms of transport of p-borono-phenylalanine through the cell membrane in vitro.* Radiat Res, 2000. **153**(2): p. 173-80.

29. C.M. van Rij, A.J. Wilhelm, W.A. Sauerwein, and A.C. van Loenen, *Boron neutron capture therapy for glioblastoma multiforme.* Pharm World Sci, 2005. **27**(2): p. 92-5.

30. G.M. Morris, P.L. Micca, M.M. Nawrocky, L.E. Weissfloch, and J.A. Coderre, *Long-term infusions of p-boronophenylalanine for boron neutron capture therapy: evaluation using rat brain tumor and spinal cord models.* Radiat Res, 2002. **158**(6): p. 743-52.

31. Y. Nakagawa and H. Hatanaka, *Boron Neutron Capture Therapy: Clinical Brain Tumor Studies.* J Neuro-Oncol, 1997. **33**: p. 105-115.

32. T. Kageji, Y. Nakagawa, K. Kitamura, K. Matsumoto, and H. Hatanaka, *Pharmacokinetics and boron uptake of BSH (Na2B12H11SH) in patients with intracranial tumors.* J Neurooncol, 1997. **33**(1-2): p. 117-30.

33. T. Kageji, S. Nagahiro, Y. Mizobuchi, H. Toi, Y. Nakagawa, and H. Kumada, *Radiation injury of boron neutron capture therapy using mixed epithermal- and thermal neutron beams in patients with malignant glioma.* Appl Radiat Isot, 2004. **61**(5): p. 1063-7.

34. M.F. Hawthorne, *The role of chemistry in the development of boron neutron capture therapy of cancer.* Angew Chem Int Ed, 1993. **32**: p. 950 - 984.

35. A.H. Soloway, W. Tjarks, B.A. Barnum, F.G. Rong, R.F. Barth, I.M. Codogni, and J.G. Wilson, *The Chemistry of Neutron Capture Therapy.* Chem Rev, 1998. **98**(4): p. 1515-1562.

36. E. Crossley, E. Ziolkowski, J. Coderre, and L. Rendina, *Boronated DNA-Binding Compounds as Potential Agents for Boron Neutron Capture Therapy.* Mini Rev Med Chem, 2007. **7**(3): p. 303-13.

37. R.F. Barth and H. Joensuu, *Boron neutron capture therapy for the treatment of glioblastomas and extracranial tumours: as effective, more effective or less effective than photon irradiation?* Radiother Oncol, 2007. **82**(2): p. 119-22.

38. W. Yang, R.F. Barth, G. Wu, S. Kawabata, T.J. Sferra, A.K. Bandyopadhyaya, W. Tjarks, A.K. Ferketich, M.L. Moeschberger, P.J. Binns, K.J. Riley, J.A. Coderre, M.J. Ciesielski, R.A. Fenstermaker, and C.J. Wikstrand, *Molecular targeting and treatment of EGFRvIII-positive gliomas using boronated monoclonal antibody L8A4.* Clin Cancer Res, 2006. **12**(12): p. 3792-802.

39. G. Wu, W. Yang, R.F. Barth, S. Kawabata, M. Swindall, A.K. Bandyopadhyaya, W. Tjarks, B. Khorsandi, T.E. Blue, A.K. Ferketich, M. Yang, G.A. Christoforidis, T.J. Sferra, P.J. Binns, K.J. Riley, M.J. Ciesielski, and R.A. Fenstermaker, *Molecular targeting and treatment of an epidermal growth factor receptor-positive glioma using boronated cetuximab.* Clin Cancer Res, 2007. **13**(4): p. 1260-8.

40. M. Miura, D.D. Joel, H.M. Smilowitz, M.M. Nawrocky, P.L. Micca, D.A. Hoch, J.A. Coderre, and D.N. Slatkin, *Biodistribution of copper carboranyltetraphenylporphyrins in rodents bearing an isogeneic or human neoplasm.* J Neurooncol, 2001. **52**(2): p. 111-7.

41. J.S. Hill, S.B. Kahl, S.S. Stylli, Y. Nakamura, M.S. Koo, and A.H. Kaye, *Selective tumor kill of cerebral glioma by photodynamic therapy using a boronated porphyrin photosensitizer.* Proc Natl Acad Sci USA, 1995. **92**: p. 12126 - 12130.

42. M. Miura, P.L. Micca, C.D. Fisher, C.R. Gordon, J.C. Heinrichs, and D.N. Slatkin, *Evaluation of carborane-containing porphyrins as tumour targeting agents for boron neutron capture therapy.* British Journal of Radiology, 1998. **71**: p. 773-781.

43. E.L. Kreimann, M. Miura, M.E. Itoiz, E. Heber, R.N. Garavaglia, D. Batistoni, R.J. Rebagliati, M.J. Roberti, P.L. Micca, J.A. Coderre, and A.E. Schwint, *Biodistribution of a carborane-containing porphyrin as a targeting agent for Boron Neutron Capture Therapy of oral cancer in the hamster cheek pouch.* Arch Oral Biol, 2003. **48**(3): p. 223-32.

44. H. Wu, P.L. Micca, M.S. Makar, and M. Miura, *Total syntheses of three copper (II) tetracarboranylphenylporphyrins containing 40 or 80 boron atoms and their biological properties in EMT-6 tumor-bearing mice.* Bioorg Med Chem, 2006. **14**(15): p. 5083-92.

45. M. Miura, G.M. Morris, P.L. Micca, D.T. Lombardo, K.M. Youngs, J.A. Kalef-Ezra, D.A. Hoch, D.N. Slatkin, R. Ma, and J.A. Coderre, *Boron Neutron Capture Therapy of a Murine Mammary Carcinoma using a Lipophilic Carboranyltetraphenylporphyrin.* Radiat Res, 2001. **155**(4): p. 603-610.

46. G.M. Morris, J.A. Coderre, P.L. Micca, M. Nawrocky, J.W. Hopewell, and M. Miura, *Porphyrin-mediated boron neutron capture therapy: a preclinical evaluation of the response of the oral mucosa.* Radiat Res, 2005. **163**(1): p. 72-78.

47. G.W. Kabalka and M.L. Yao, *The synthesis and use of boronated amino acids for boron neutron capture therapy.* Anticancer Agents Med Chem, 2006. **6**(2): p. 111-25.

48. P. Dozzo, M.S. Koo, S. Berger, T.M. Forte, and S.B. Kahl, *Synthesis, characterization, and plasma lipoprotein association of a nucleus-targeted boronated porphyrin.* J Med Chem, 2005. **48**(2): p. 357-9.

49. S. Narayanasamy, B.T. Thirumamagal, J. Johnsamuel, Y. Byun, A.S. Al-Madhoun, E. Usova, G.Y. Cosquer, J. Yan, A.K. Bandyopadhyaya, R. Tiwari, S. Eriksson, and W. Tjarks, *Hydrophilically enhanced 3-carboranyl thymidine analogues (3CTAs) for boron neutron capture therapy (BNCT) of cancer.* Bioorg Med Chem, 2006. **14**(20): p. 6886-99.

50. X. Pan, G. Wu, W. Yang, R.F. Barth, W. Tjarks, and R.J. Lee, *Synthesis of cetuximab-immunoliposomes via a cholesterol-based membrane anchor for targeting of EGFR.* Bioconjug Chem, 2007. **18**(1): p. 101-8.

51. V.J. Reddy, M.M. Roforth, C. Tan, and M.V. Reddy, *Synthesis of functionalized carboranes as potential anticancer and BNCT agents.* Inorg Chem, 2007. **46**(2): p. 381-3.

52. N. Tilly, P. Olsson, T. Hartman, J. Coderre, M. Makar, J. Malmquist, S. Sjoberg, J. Pettersson, J. Carlsson, and B. Glimelius, *In vitro determination of toxicity, binding, retention, subcellular distribution and biological efficacy of the boron neutron capture agent DAC-1.* Radiother Oncol, 1996. **38**(1): p. 41-50.

53. V. Gottumukkala, R. Luguya, F.R. Fronczek, and M.G. Vicente, *Synthesis and cellular studies of an octa-anionic 5,10,15,20-tetra[3,5-(nido-carboranylmethyl)phenyl]porphyrin (H(2)OCP) for application in BNCT.* Bioorg Med Chem, 2005. **13**(5): p. 1633-40.

54. R. Luguya, T.J. Jensen, K.M. Smith, and M.G. Vicente, *Synthesis and cellular studies of a carboranylchlorin for the PDT and BNCT of tumors.* Bioorg Med Chem, 2006. **14**(17): p. 5890-7.

55. E. Justus, D. Awad, M. Hohnholt, T. Schaffran, K. Edwards, G. Karlsson, L. Damian, and D. Gabel, *Synthesis, Liposomal Preparation, and in Vitro Toxicity of Two Novel Dodecaborate Cluster Lipids for Boron Neutron Capture Therapy.* Bioconjug Chem, 2007.

56. S. Masunaga, H. Nagasawa, M. Hiraoka, Y. Sakurai, Y. Uto, H. Hori, K. Nagata, M. Suzuki, A. Maruhashi, Y. Kinashi, and K. Ono, *Applicability of the 2-nitroimidazole-sodium borocaptate-10B conjugate, TX-2060, as a 10B-carrier in boron neutron capture therapy.* Anticancer Res, 2004. **24**(5A): p. 2975-83.

57. S. Masunaga, H. Nagasawa, K. Gotoh, Y. Sakurai, Y. Uto, H. Hori, K. Nagata, M. Suzuki, A. Maruhashi, Y. Kinashi, and K. Ono, *Evaluation of hypoxia-specific cytotoxic bioreductive agent-sodium borocaptate-10B conjugates as 10B-carriers in boron neutron capture therapy.* Radiat Med, 2006. **24**(2): p. 98-107.

58. R.F. Barth, W. Yang, D.M. Adams, J.H. Rotaru, S. Shukla, M. Sekido, W. Tjarks, R.A. Fenstermaker, M. Ciesielski, M.M. Nawrocky, and J.A. Coderre, *Molecular Targeting of the Epidermal Growth Factor Receptor for Neutron Capture Therapy of Gliomas.* Cancer Res, 2002. **62**(11): p. 3159-3166.

59. R.F. Barth, W. Yang, A.S. Al-Madhoun, J. Johnsamuel, Y. Byun, S. Chandra, D.R. Smith, W. Tjarks, and S. Eriksson, *Boron-containing nucleosides as potential delivery agents for neutron capture therapy of brain tumors.* Cancer Res, 2004. **64**(17): p. 6287-95.

60. S. Masunaga, H. Nagasawa, M. Hiraoka, Y. Sakurai, Y. Uto, H. Hori, K. Nagata, M. Suzuki, A. Maruhashi, Y. Kinashi, and K. Ono, *The usefulness of 2-nitroimidazole-sodium borocaptate-10B conjugates as 10B-carriers in boron neutron capture therapy.* Appl Radiat Isot, 2004. **61**(5): p. 953-8.

61. R.G. Fairchild, S.B. Kahl, B.H. Laster, J. Kalefezra, and E.A. Popenoe, *In vitro determination of uptake, retention, distribution, biological efficacy, and toxicity of boronated compounds for neutron capture therapy - A comparison of porphyrins with sulfhydryl boron hydrides.* Cancer Res, 1990. **50**: p. 4860-4865.

62. J.A. Coderre, M.S. Makar, P.L. Micca, M.M. Nawrocky, H.B. Liu, D.D. Joel, D.N. Slatkin, and H.I. Amols, *Derivations of relative biological effectiveness for the high-LET radiations produced during boron neutron capture irradiations of the 9L rat gliosarcoma in vitro and in vivo.* Int J Radiat Oncol Biol Phys, 1993. **27**: p. 1121 - 1129.

63. J.R. Choi, S.D. Clement, O.K. Harling, and R.G. Zamenhof, *Neutron capture therapy beams at the MIT research reactor*, in *Neutron Beam Design, Development, and Performance for Neutron Capture Therapy*, O.K. Harling, J.A. Bernard, and R.G. Zamenhof, Editors. 1990, Plenum Press: New York. p. 201 - 218.

64. R. Sankaranarayanan, E. Masuyer, R. Swaminathan, J. Ferlay, and S. Whelan, *Head and neck cancer: a global perspective on epidemiology and prognosis.* Anticancer Res, 1998. **18**(6B): p. 4779-86.

65. J.S. Cooper, T.F. Pajak, A.A. Forastiere, J. Jacobs, B.H. Campbell, S.B. Saxman, J.A. Kish, H.E. Kim, A.J. Cmelak, M. Rotman, M. Machtay, J.F. Ensley, K.S. Chao, C.J. Schultz, N. Lee, and K.K. Fu, *Postoperative concurrent radiotherapy and chemotherapy for high-risk squamous-cell carcinoma of the head and neck.* N Engl J Med, 2004. **350**(19): p. 1937-44.

66. D.J. Haraf, R.R. Weichselbaum, and E.E. Vokes, *Re-irradiation with concomitant chemotherapy of unresectable recurrent head and neck cancer: a potentially curable disease.* Ann Oncol, 1996. **7**(9): p. 913-8.

67. E.J. Hall, *Radiobiology for the Radiologist.* 5th ed. 2000, Philadelphia: Lippincott Williams & Wilkins.

68. S. Rockwell, *Tumor-Cell Survival*, in *Tumor Models in Cancer Research*, B.A. Teicher, Editor. 2002, Humana Press Inc.: Totowa, NJ. p. 617-631.

69. B. Pauwels, A.E. Korst, C.M. de Pooter, G.G. Pattyn, H.A. Lambrechts, M.F. Baay, F. Lardon, and J.B. Vermorken, *Comparison of the sulforhodamine B assay and the clonogenic assay for in vitro chemoradiation studies.* Cancer Chemother Pharmacol, 2003. **51**(3): p. 221-6.

70. T. Mosmann, *Rapid colorimetric assay for cellular growth and survival: application to proliferation and cytotoxicity assays.* J Immunol Methods, 1983. **65**(1-2): p. 55-63.

71. J. Capala, M.S. Makar, and J.A. Coderre, *Accumulation of boron in malignant and normal cells incubated in vitro with boronophenylalanine, mercaptoborane or boric acid.* Radiat Res, 1996. **146**(5): p. 554-60.

72. J.A. Coderre, J. Capala, M. Makar, and A.Z. Diaz, *Application of BNCT to other types of tumors*, in *Advances in Neutron Capture Therapy: Volume II, Chemistry and Biology*, J.C. B. Larsson, and R. Weinreich, Editor. 1997, Elsevier Science B.V: Amsterdam. p. 649-653.

73. R.D. Rogus, O.K. Harling, and J.C. Yanch, *Mixed field dosimetry of epithermal neutron beams for boron neutron capture therapy at the MITR-II research reactor.* Med Phys, 1994. **21**(10): p. 1611-1625.

74. K.J. Riley, P.J. Binns, and O.K. Harling, *Performance characteristics of the MIT fission converter based epithermal neutron beam.* Phys Med Biol, 2003. **48**(7): p. 943-58.

75. M.A. Dagrosa, M. Viaggi, R.J. Rebagliati, D. Batistoni, S.B. Kahl, G.J. Juvenal, and M.A. Pisarev, *Biodistribution of boron compounds in an animal model of human undifferentiated thyroid cancer for boron neutron capture therapy.* Mol Pharm, 2005. **2**(2): p. 151-6.

76. K. Riley and O. Harling, *An improved prompt gamma neutron activation analysis facility using a focused diffracted neutron beam.* Nucl Instrum Meth Phys Res B, 1998. **143**: p. 414-421.

77. P. Armitage, G. Berry, and J.N.S. Matthews, *Statistical Methods in Medical Research*, ed. 4th. 2002, Oxford: Blackwell Science.

78. G.F. Knoll, *Radiation detection and measurement.* 3rd ed, ed. R. Factor. 2000, New York: John Wiley & Sons, Inc.

79. N. Takamatsu, *[The new colorimetric assay (WST-1) for cellular growth with normal aging and Alzheimer's disease].* Nippon Ronen Igakkai Zasshi, 1998. **35**(7): p. 535-42.

80. A. Wittig, W. Sauerwein, F. Poller, C. Fuhrmann, K. Hideghety, and C. Streffer, *Evaluation of boron neutron capture effects in cell culture using sulforhodamine-B assay and a colony assay.* Int J Radiat Biol, 1998. **73**(6): p. 679-90.

81. J. Carmichael, W.G. DeGraff, A.F. Gazdar, J.D. Minna, and J.B. Mitchell, *Evaluation of a tetrazolium-based semiautomated colorimetric assay: assessment of chemosensitivity testing.* Cancer Res, 1987. **47**(4): p. 936-42.

82. J. Carmichael, J.B. Mitchell, W.G. DeGraff, J. Gamson, A.F. Gazdar, B.E. Johnson, E. Glatstein, and J.D. Minna, *Chemosensitivity testing of human lung cancer cell lines using the MTT assay.* Br J Cancer, 1988. **57**(6): p. 540-7.

83. K. Kawada, T. Yonei, H. Ueoka, K. Kiura, M. Tabata, N. Takigawa, M. Harada, and M. Tanimoto, *Comparison of chemosensitivity tests: clonogenic assay versus MTT assay.* Acta Med Okayama, 2002. **56**(3): p. 129-34.

84. J. Carmichael, W.G. DeGraff, A.F. Gazdar, J.D. Minna, and J.B. Mitchell, *Evaluation of a tetrazolium-based semiautomated colorimetric assay: assessment of radiosensitivity.* Cancer Res, 1987. **47**(4): p. 943-6.

85. M.J. Eble, F.W. Hensley, M. Flentje, A. Schlotz, and M. Wannenmacher, *A modified computer-assisted colorimetric microtitre assay (MTT) to assess in vitro radiosensitivity of V79, CaSki, HeLa and WiDr cells.* Int J Radiat Biol, 1994. **65**(2): p. 193-201.

86. D.J. Brenner and D.E. Herbert, *The use of the linear-quadratic model in clinical radiation oncology can be defended on the basis of empirical evidence and theoretical argument.* Med Phys, 1997. **24**(8): p. 1245-8.

87. D.E. Callahan, T.M. Forte, S.M. Afzal, D.F. Deen, S.B. Kahl, K.A. Bjornstad, W.F. Bauer, and E.A. Blakely, *Boronated protoporphyrin (BOPP): localization in lysosomes of the human glioma cell line SF-767 with uptake modulated by lipoprotein levels.* Int J Radiat Oncol Biol Phys, 1999. **45**(3): p. 761-71.

88. J.S. Hill, S.B. Kahl, S.S. Stylli, Y. Nakamura, M.S. Koo, and A.H. Kaye, *Selective tumor kill of cerebral glioma by photodynamic therapy using a boronated porphyrin photosensitizer.* Proc Natl Acad Sci U S A, 1995. **92**(26): p. 12126-30.

89. J.L. Kiger, *Radiobiology of normal rat lung in boron neutron capture therapy*, in *Nuclear Science and Engineering Department*. 2006, Massachusetts Institute of Technology: Cambridge, MA.

90. N. Oku and Y. Namba, *Long-circulating liposomes.* Crit Rev Ther Drug Carrier Syst, 1994. **11**(4): p. 231-70.

91. R.K. Jain, *Delivery of molecular and cellular medicine to solid tumors.* Adv Drug Deliv Rev, 1997. **26**(2-3): p. 71-90.

92. M.F. Hawthorne and K. Shelly, *Liposomes as drug delivery vehicles for boron agents.* J Neurooncol, 1997. **33**(1-2): p. 53-8.

93. D. Feakes, K. Shelly, C. Knobler, and M. Hawthorne, *Na3[B20H17NH3]: Synthesis and Liposomal Delivery to Murine Tumors.* Proc Natl Acad Sci USA, 1994. **91**(8): p. 3029-3033.

94. D.A. Feakes, K. Shelly, and M.F. Hawthorne, *Selective boron delivery to murine tumors by lipophilic species incorporated in the membranes of unilamellar liposomes.* Proc Nat Acad Sci, USA, 1995. **92**: p. 1367 - 1370.

95. K. Shelly, Georgiev, E.M., Watson-Clark, R., Hawthorne, M.F., *Boron delivery to tumors for BNCT: recent murine results with liposomes.*, in *Advances in Neutron Capture Therapy Volume II, Chemistry and Biology*, B. Larsson, Crawford, J., Weinreich, R., Editor. 1997, Elsevier Science B.V.: Lausanne. p. 357-361.

96. W.S. Kiger III, P.L. Micca, G.M. Morris, and J.A. Coderre, *Boron microquantification in oral muscosa and skin following administration of a neutron capture therapy agent.* Radiat Prot Dosimetry, 2002. **99**(1-4): p. 409-12.

97. W.S. Kiger III, *Development in Micro- and Macrodosimetry of Boron Neutron Capture Therapy*, in *Nuclear Engineering Department*. 2000, Massachusetts Institute of Technology: Cambridge, MA.

98. T.C. Harris, *High resolution quantitative auto-radiography to determine microscopic distributions of B-10 in neutron capture therapy*, in *Nuclear Science and Engineering Department*. 2006, Massachusetts Institute of Technology: Cambridge, MA.

99. S.M. Moghimi, A.C. Hunter, and J.C. Murray, *Nanomedicine: current status and future prospects.* Faseb J, 2005. **19**(3): p. 311-30.

100. M.N. Khalid, P. Simard, D. Hoarau, A. Dragomir, and J.C. Leroux, *Long circulating poly(ethylene glycol)-decorated lipid nanocapsules deliver docetaxel to solid tumors.* Pharm Res, 2006. **23**(4): p. 752-8.

101. D.C. Litzinger, A.M. Buiting, N. van Rooijen, and L. Huang, *Effect of liposome size on the circulation time and intraorgan distribution of amphipathic poly(ethylene glycol)-containing liposomes.* Biochim Biophys Acta, 1994. **1190**(1): p. 99-107.

102. D. Liu, A. Mori, and L. Huang, *Role of liposome size and RES blockade in controlling biodistribution and tumor uptake of GM1-containing liposomes.* Biochim Biophys Acta, 1992. **1104**(1): p. 95-101.

103. E.L. Kreimann, M. Miura, M.E. Itoiz, E. Heber, R.N. Garavaglia, D. Batistoni, R.J. Rebagliati, M.J. Roberti, P.L. Micca, J.A. Coderre, and A.E. Schwint, *Biodistribution of a carborane-containing porphyrin as a targeting agent for Boron Neutron Capture Therapy of oral cancer in the hamster cheek pouch.* Arch Oral Biol, 2003. **48**(3): p. 223-32.

104. H. Yanagie, K. Maruyama, T. Takizawa, O. Ishida, K. Ogura, T. Matsumoto, Y. Sakurai, T. Kobayashi, A. Shinohara, J. Rant, J. Skvarc, R. Ilic, G. Kuhne, M. Chiba, Y. Furuya, H. Sugiyama, T. Hisa, K. Ono, H. Kobayashi, and M. Eriguchi, *Application of boron-entrapped stealth liposomes to inhibition of growth of tumour cells in the in vivo boron neutron-capture therapy model.* Biomed Pharmacother, 2006. **60**(1): p. 43-50.

105. J.E. Moulder and S. Rockwell, *Hypoxic fractions of solid tumors: experimental techniques, methods of analysis, and a survey of existing data.* Int J Radiat Oncol Biol Phys, 1984. **10**(5): p. 695-712.

106. Y. Shibamoto, Y. Yukawa, K. Tsutsui, M. Takahashi, and M. Abe, *Variation in the hypoxic fraction among mouse tumors of different types, sizes, and sites.* Jpn J Cancer Res, 1986. **77**(9): p. 908-15.

107. S. Rockwell and J.E. Moulder, *Hypoxic fractions of human tumors xenografted into mice: a review.* Int J Radiat Oncol Biol Phys, 1990. **19**(1): p. 197-202.

108. G.M. Morris, J.A. Coderre, J.W. Hopewell, P.L. Micca, and M. Rezvani, *Response of rat skin to boron neutron capture therapy with p-boronophenylalanine or borocaptate sodium.* Radiother Oncol, 1994. **32**: p. 144 - 153.

109. G.M. Morris, J.A. Coderre, J.W. Hopewell, P.L. Micca, M.M. Nawrocky, H.B. Liu, and A. Bywaters, *Response of the central nervous system to boron neutron capture irradiation: Evaluation using rat spinal cord model.* Radiother Oncol, 1994. **32**: p. 249 - 255.

110. G.Z. Guo, K. Sasai, N. Oya, T. Takagi, K. Shibuya, and M. Hiraoka, *Simultaneous evaluation of radiation-induced apoptosis and micronuclei in five cell lines.* Int J Radiat Biol, 1998. **73**(3): p. 297-302.

111. S. Masunaga, K. Ono, M. Suzuki, Y. Kinashi, and M. Takagaki, *Radiobiologic significance of apoptosis and micronucleation in quiescent cells within solid tumors following gamma-ray irradiation.* Int J Radiat Oncol Biol Phys, 2001. **49**(5): p. 1361-8.